CANADIAN THESES ON MICROFICHE

I.S.B.N.

THESES CANADIENNES SUR MICROFICHE

National Library of Canada
Collections Development Branch

Canadian Theses on
Microfiche Service

Ottawa, Canada
K1A 0N4

Bibliothèque nationale du Canada
Direction du développement des collections

Service des thèses canadiennes
sur microfiche

NOTICE

The quality of this microfiche is heavily dependent upon the quality of the original thesis submitted for microfilming. Every effort has been made to ensure the highest quality of reproduction possible.

If pages are missing, contact the university which granted the degree.

Some pages may have indistinct print especially if the original pages were typed with a poor typewriter ribbon or if the university sent us a poor photocopy.

Previously copyrighted materials (journal articles, published tests, etc.) are not filmed.

Reproduction in full or in part of this film is governed by the Canadian Copyright Act, R.S.C. 1970, c. C-30. Please read the authorization forms which accompany this thesis.

THIS DISSERTATION
HAS BEEN MICROFILMED
EXACTLY AS RECEIVED

AVIS

La qualité de cette microfiche dépend grandement de la qualité de la thèse soumise au microfilmage. Nous avons tout fait pour assurer une qualité supérieure de reproduction.

S'il manque des pages, veuillez communiquer avec l'université qui a conféré le grade.

La qualité d'impression de certaines pages peut laisser à désirer, surtout si les pages originales ont été dactylographiées à l'aide d'un ruban usé ou si l'université nous a fait parvenir une photocopie de mauvaise qualité.

Les documents qui font déjà l'objet d'un droit d'auteur (articles de revue, examens publiés, etc.) ne sont pas microfilmés.

La reproduction, même partielle, de ce microfilm est soumise à la Loi canadienne sur le droit d'auteur, SRC 1970, c. C-30. Veuillez prendre connaissance des formules d'autorisation qui accompagnent cette thèse.

LA THÈSE A ÉTÉ
MICROFILMÉE TELLE QUE
NOUS L'AVONS REÇUE

NL-339 (r. 82/08)

Canada

PREFACE

In recent years, there has been considerable interest in the properties of thorium and uranium, because of their many-fold applications as well as their fundamental interest in Inorganic Chemistry. These two metals exhibit properties that are essential for their application in the chemical and nuclear industries and primarily because of the large size of their atoms, their behaviour in relation to other elements is of particular interest.

This thesis describes the isolation and characterization of some heteroligand organoperoxo complexes of thorium and uranium and their possible use in oxygen transfer reactions. Peroxo complexes are the model compounds of natural oxygen carriers, e.g., the hemoglobins and hemocyanins. The chemistry of the complex metal peroxides serves as a first step towards an insight into this area of biochemistry. The present work also describes some fundamental thermochemical aspects of thorium and uranium that are very important in understanding their behaviour.

Some of the work described in this thesis has been published, and the remainder is in the process of publication:

1. Novel Peroxo Complexes of Thorium Containing Organic Ligands, A.D. Westland and M.T.H. Tarafder, Inorg. Chem: 21, 3228 (1982).

2. Novel Peroxo Complexes of Uranium Containing Organic Ligands, A.D. Westland and M.T.H. Tarafder, Inorg. Chem., 20, 3992 (1981).
3. The Nature of Bonding in Hexahalothorates and Hexahalouranates (IV), A.D. Westland and M.T.H. Tarafder, manuscript submitted to Canadian Journal of Chemistry for publication.

ACKNOWLEDGEMENTS

I wish to express my sincere appreciation, great admiration and gratitude to Professor A.D. Westland, my research supervisor, for his unfailing help, continuous encouragement and guidance throughout the course of this work. I am especially indebted to him for his readiness to help with experimental work and to discuss various aspects of the problems whenever it was necessary.

I wish to express my gratitude to Professor J.C. Woolley, Department of Physics, University of Ottawa, for providing me with the X-ray facilities. I am also thankful to him for his invaluable discussions in interpreting the X-ray work.

I am also thankful to Drs. J.B. Milne and B.A. Morrow for providing me with the Raman facilities. I am grateful to Mr. P. Lahie (formerly a graduate student of this Department) and R. McFerline for their assistance in running the solid-state Raman spectra. Helpful discussions with Professor H. Alper are also greatly appreciated.

Special thanks are also due to Mr. Raj Kapoor for recording the ^{13}C and some ^{1}H NMR spectra, Dr. J. Krause for running the mass spectra of some organic samples and Mr. E. Kristoff for his help in glass blowing.

Thanks are also due to Mrs. S. Ryan for typing this thesis and Mrs. E. Szabo for the preparation of the diagrams.

I gratefully acknowledge the Canadian Commonwealth Committee for offering me a scholarship.

Finally, I would like to extend my deep gratitude to my wife, Zakia, and daughter, Tina, for their unbound patience, continuous encouragement and understanding throughout the course of this work.

CONTENTS

LIST OF FIGURES

LIST OF TABLES

ABSTRACT

This work deals with the coordination chemistry of thorium and uranium including peroxo complexes of these metals and their oxygen transfer reactions towards some organic substrates. In addition, some thermochemical aspects of the chemistry of halogen compounds of these metals in the quadrivalent state are examined.

Complexes were isolated from the reaction of $ThCl_4$ or UCl_4 with stoichiometric amounts of organic ligands (pyridine-N-oxide, triphenylphosphine oxide, triphenylarsine oxide, pyridine-2-carboxylic acid, aniline-2-carboxylic acid, 2-aminophenol, pyridine-2,6-dicarboxylic acid and the Schiff bases, N-(2-Hydroxyphenyl)salicylidenimine and N-(2-Carboxyphenyl)salicylidenimine) in a suitable solvent. These complexes are called the intermediate (precursor) compounds of Th(IV) and U(IV). The thorium intermediate complexes had the compositions, ThL_2Cl_2 and ThL'_2 and the uranium compounds were $UCl_4 2L'''$, UL_2Cl_2LH, $UL_2Cl_2H_2O$ and UL'_2 where L''' , L and L' refer to neutral monodentate, bidentate, uninegative and tridentate, dinegative ligands, respectively. Peroxo complexes were prepared by treating these intermediate complexes of thorium and uranium with aqueous H_2O_2 solution. The thorium peroxo complexes had

the compositions $ThL_2(O_2)$ and $ThL'(O_2)H_2O$ where uranium complexes were $U(O)(O_2)_2 2L'''$, $[U(O)_2(O_2)L(H_2O)]^-H^+$ and $U(O)(O_2)L'H_2O$.

The multidentate heteroligands probably stabilize the coordinated peroxo group as evident from the finding that $ThCl_4 \cdot 2OAsPh_3$ or $ThCl_4 \cdot 2OPPh_3$ complexes do not give rise to the organo-peroxo complexes on treatment with H_2O_2, but instead form ThO_2. Besides, the uranium peroxo complexes containing monodentate ligands were only prepared in the solid phase by moistening their precursors with H_2O_2. In solution uranyl peroxide was the product.

The complexes were characterized by elemental analyses, conductivity measurements, I.R., Raman, ^{13}C NMR, and electronic spectroscopic measurements. Some uranium compounds were further analyzed by alkalimetric and Ce(IV)-titrations.

Infrared and ^{13}C NMR spectra reveal the monodentate, bidentate and tridentate character of the organic ligands used. The Th(IV)- intermediate and the peroxo complexes are all hexacoordinate. The U(IV)-analogues are also hexacoordinate with the exception of $U(C_6H_4NH_2O)_2H_2OCl_2$, which is heptacoordinate. The peroxo uranium compounds are all seven- or eight-coordinate.

The frequency of the ν_1 mode of the $M(O_2)$ (M=Th and U) grouping, which is essentially an O-O stretch, is observed

only in the Raman spectra, the group appears to be behaving as it does in alkali peroxides where it has essentially linear symmetry and is ionic. Thorium peroxo complexes display ν_1(0-0) stretches at 820-840 cm^{-1}, i.e., lower in frequency than the corresponding band of other lighter metals in group 4B. The $\nu_1(UO_2)$ bands appear at 803-860 cm^{-1}, much lower in frequency than corresponding bands of the lighter elements of group 6B. The present ν_1(0-0) values thereby demonstrate that with the increase of atomic number in a group, peroxo stretches decrease. Moreover, the ν_1 mode varies somewhat with the choice of ancillary ligands used, e.g., the ν_1 mode in $U(O)(O_2)_2OAsPh_3H_2O$ appears at a lower frequency than it does in $U(O)(O_2)_2OPPh_3H_2O$. This has been rationalized on the basis that Ph_3AsO is more negative than Ph_3PO.

Thorium peroxo complexes are somewhat more reactive than their uranium analogues. Thorium peroxo complexes, on treatment with aqueous iodide, give a discernible liberation of I_2 within 3-4 minutes whereas for uranium compounds 3-4 h elapsed before any brown coloration appeared in the solution.

Two of the thorium peroxo complexes were found to oxidize olefinic compounds, viz., trans-stilbene and allyl alcohol, to the corresponding epoxides in an anhydrous medium. They also catalyzed the oxidation of these same compounds with hydrogen peroxide to form benzoin and glycerol, respectively.

Two of the uranium peroxo complexes were also employed to oxidize trans-stilbene and allyl alcohol to the epoxides, but at a lower yield (based on percent conversion) compared to the above cases. The reaction of a uranium peroxo complex with trans-stilbene (1:1 molar ratio) in the presence of excess H_2O_2 in dioxane produced benzoin. Here, catalytic reactions could not be achieved, because, in the course of the reaction, the peroxo complexes decompose to give UO_3 and the free organic ligand and the subsequent reaction of UO_3 with H_2O_2 to regenerate peroxo-uranium species is not feasible. Three of the uranium peroxo complexes were found to be unreactive towards the simple olefins, cyclohexene and cyclooctene.

Thermochemical studies were made on A_2MX_6 (A=alkali metal, Na and K; M=Th and U; X=Cl and Br) prepared by heating stoichiometric quantities of the component halides in a quartz tube under vacuum. The study involved the calorimetric determination of the enthalpy of reactions of the type:

$$2AX(c) + ThX_4(c) = A_2ThX_6(c)$$

The enthalpy of this reaction, ΔH_c, is a measure of the comparative stability of the ternary complexes. Consideration of ΔH_c for different A_2ThX_6 complexes indicates that Cs_2ThX_6 complexes are more stable than the potassium analogues and thorium has a preference for chloro complexation compared

to bromo-complexation unlike U(IV) which shows a greater affinity for bromide.

Measurements of ΔH_c afforded values of the standard enthalpies of formation of $A_2MX_6(c)$ and $MX_6^{2-}(g)$.

Calculated lattice energies of A_2MX_6 complexes, the standard enthalpy of formation of $A_2MX_6(c)$ and $MX_6^{2-}(g)$ and other ancillary data, were used to obtain the enthalpy of the reaction,

$$MX_4(g) + 2X^-(g) \xrightarrow{\overline{\Delta H}_x(g)} MX_6^{2-}(g)$$

$\overline{\Delta H}_x(g)$ represents the double-halide ion affinity in the gas phase. The results indicate that chlorothorate is more stable than chlorouranate whereas bromouranate is much more stable than bromothorate. This illustrates class a and class b behaviour of thorium and uranium respectively. The results were rationalized on the basis of halogen to metal $p_\pi \rightarrow d_\pi$ bonding.

Thermochemical bond energies of M-X systems were obtained following the approach of Jenkins and Pratt. M-X bonds were classified into two categories, (i) homolytic, and (ii) heterolytic (coordinate) bond energies. Bond energy data indicate that

$$E(Th\text{-}Cl)_{hom/het} > E(U\text{-}Cl)_{hom/het}$$

However, the heterolytic (coordinate) bond energy data demonstrate that

$$E(U\text{-}Br)_{het} > E(Th\text{-}Br)_{het}$$

The Raman spectra of the solid samples show a trend similar to the trend in bond energy values.

SYMBOLS AND ABBREVIATIONS

O_2^- = superoxide

O_2^{2-} = peroxide

O^{2-} = oxide

DMSO = dimethylsulfoxide

HMPT = hexamethylphosphorictriamide

ATP = adenosine triphosphate

$C_5H_3N(COOH)_2$ = pyridine-2,6-dicarboxylic acid

$C_6H_4NH_2OH$ = 2-aminophenol

C_5H_4NCOOH = picolinic acid

$C_6H_4NH_2COOH$ = aniline-2-carboxylic acid

Schiff base L = $C_{13}H_{11}NO_2$ = N-(2-Hydroxyphenyl)salicylidenimine

Schiff base L' = $C_{14}H_{11}NO_3$ = N-(2-Carboxyphenyl)salicylidenimine

HMPA = same as HMPT

Intermediate complexes of Th(IV) and U(IV) = precursors of their peroxo complexes

$C_{36}H_{44}N_4$ = octaethyl porphirin

$Ti(Oi\text{-}Pr)_4$ = titanium tetraisopropoxide

TMS = tetramethylsilane

THE CHEMISTRY OF THORIUM AND URANIUM

PART 1. PEROXO COMPLEXES

CHAPTER 1

1. GENERAL INTRODUCTION

In recent years, the actinide elements thorium and uranium have been of increasing interest for their usefulness in both chemical and nuclear industries. The development of atomic energy has resulted in a world-wide interest in the chemistry of these elements.

Thorium was discovered in 1828 by the Swedish chemist, J.J. Berzelius. The element was isolated from thorite, $ThSiO_4$, from Southern Norway (1). The radioactivity of thorium was discovered independently by Madame Curie and C.G. Schmidt in 1898 (1). The element is used in the manufacture of incandescent gas mantles and in the metallurgy of magnesium and tungsten, but it has great potential importance in the field of atomic energy as an alternate reactor fuel. The natural isotope of thorium, Th^{232}, can be converted by neutron bombardment to thorium isotope, Th^{233}, which yields an isotope of uranium, U^{233}, that is fissionable (1). Linus Pauling claimed that thorium will save the entire world from the energy crisis after 1000 years (2).

The principal ore of thorium is monazite, $(Ce,La,Y,Th)PO_4$, and most of the world's supply of this mineral comes from Brazil, Canada, Sri Lanka, New Mexico, Nigeria, Southern Norway,

Travancore (India) and U.S.A. (1,3-4). In Canada, uranothorite, $(U,Th)O_2.SiO_2$ occurs abundantly in Hybla (Ontario) and Quebec (1,3). Deposits of monazite and uranothorite are also mined in the Elliot Lake-Blind River and Agnew Lake areas (5,6-7). These ores commonly contain 0.03 to 0.04 percent ThO_2 (7).

The main uranium minerals include uraninite, pitchblende, monazite and brannerite. The first two are varieties of the same mineral; uraninite is the crystallized variety and pitchblende the massive variety, generally a mixture of U(IV) and U(VI) oxides (7).

In 1789, the German chemist and mineralogist, M.H. Klaproth, prepared a yellow oxide (UO_3) from pitchblende. When this was heated with carbon, a dark, metallic-looking powder was obtained which was thought to be uranium until 1841 when the French chemist, E. Peligot, showed that it was in fact the oxide, UO_2 (1). He obtained the metal by reducing UCl_4 with potassium (1).

The radioactivity of uranium was discovered by Henri Bequerel in 1896 (1). Until the discovery of uranium fission by Hahn and Strassman in 1939, uranium had little commercial importance. Uranium or its compounds are used in the ceramic and textile industries, as an alloy constituent in steel, in the preparation of fluorescent materials, as a catalyst in ammonia synthesis, and in photography and X-ray anticathodes (1).

Four countries, Canada, South Africa, the United States and France, control 85 to 90 percent of the world's known low-cost uranium reserves (8-10). In Canada, uranium deposits as uranothorite and monazite are mined in the Elliot Lake-Blind River and Agnew Lake region (7). Deposits of pitchblende are found in the Beaverlodge, Gunnar, Rayrock, Rabbit Lake, Makkovik, Lake Athabasca and Bancroft areas (7). Most Canadian ores (7,11-12) occur as a mixture of oxides of thorium and uranium. In many places (for example, the Agnew Lake area), the ratio of ThO_2 to U_3O_8 is as high as 3:1 (7).

The expanded production of thorium and uranium have been occasioned by their increased use in modern technology. In view of the great importance of these elements, continued investigation of their properties is desirable.

The present study can be loosely divided into two sections:

(A) Coordination chemistry of thorium and uranium including peroxo complexes of these metals and their oxygen transfer reactions towards some organic substrates,

(B) Thermochemical studies of some simple and complex halides of these metals.

2. SECTION A - INTRODUCTION

Dioxygen complexes of the transition metals are the focus of active current research arising from their involvement in the activation and transfer of molecular oxygen to organic substrates (13-27). Dioxygen itself is a reactive entity but since it has a triplet ground state, its direct combination with organic molecules is a spin-forbidden process (24). Transition metals having multiple spin and oxidation states can readily interact with dioxygen, and in some cases, they form isolable oxygen adducts. In these associations, the metal acts as a reducing agent by filling the antibonding π_g^* orbitals of dioxygen. It increases the O-O distance and facilitates its cleavage. The oxygen molecule is thereby activated and the chemist may make use of this activated oxygen for scientifically or technically interesting oxidation reactions.

Investigations into the fixation and activation of molecular oxygen by transition metals were largely initiated because of an interest in model compounds that are used in studying reversible oxygenation mechanisms involved in the very complex natural oxygen carriers, e.g., the hemoglobins and hemocyanins, viz.,

$$ML_i + O_2 \rightleftharpoons O_2ML_i \qquad [1]$$

M = Fe ; L_i = porphyrin ligand.

The respiratory pigments are able to fix oxygen molecules from the atmosphere, to transport them to their sites of reaction and there to release them. This, in a sense, is a catalytic process and is reversible. The respiratory chain used to produce energy in the form of ATP (adenosine triphosphate) in aerobic metabolism is based on the reduction of oxygen to water and is extremely efficient. A common feature of these reactions is the involvement of metal atoms in complexing and activating oxygen. Although it appears well established that transition metals (particularly iron) play an important role, our knowledge about the structure of the natural metal complexes involved, the bonding of the dioxygen, and the valency state of the metal is still not clearly understood. Investigation of the natural products is complicated by their macromolecular protein component. Therefore, there is considerable interest in low-molecular weight model substances containing a transition metal center that is able to combine reversibly with oxygen.

Dioxygen complexes of transition metals, besides having an intrinsic interest of their own, are of considerable and growing importance for their ability to catalyze oxygen insertion reactions and oxidation of organic substrates (13-27, 28-29). In this respect, they may be compared in some ways to "oxygenases" and "oxidases" respectively.

The heaviest metals have not so far been investigated in this regard. Therefore, the importance of these model systems containing thorium and uranium and their novel chemistry should be of general interest.

A great number of transition metal complexes with oxygen as a ligand are known. As early as 1852, Fremy (30) reported that "ammonia-cobalt salts", and particularly the nitrate, absorb oxygen from the air, and release it again when dissolved in water. In 1933, Pfeiffer et al. (31) reported that the red-brown crystals of bis-salicylaldehyde-ethylene-diiminecobalt(II) complex darkened on exposure to air. However, it was not until five years later that Tsumaki (32) proved that the colour change was due to reversible sorption of molecular oxygen. But it was a long way from there to the more sophisticated cobalt(II) chelates, which are considered today as suitable model substances for the natural oxygen carrier systems, and to the catalytically active transition metal-oxygen complexes. These have been extensively reviewed (13,15,18,29,33-34).

Oxygen carrier complexes have many uses. One of the novel applications was their use by the U.S. Navy during World War II, to supply oxygen for welding and cutting purposes (13,35).

3. OXYGENATED COMPLEXES OF TRANSITION METALS

The dioxygen-metal adduct, MO_2, can have either the "Superoxo" structure (O_2^-) when the metal is a potential one-

electron donor, or the "peroxo" structure (O_2^{2-}) when the metal is a potential two-electron donor. These dioxygen adducts may further react with a second metal to produce the "μ-peroxo" species, MO_2M, which can be transformed either by cleavage of the O-O bond into the "oxo" species M=O, or by loss of one oxygen atom into the "μ-oxo" species M-O-M. The hydroxo species M-OH can be further obtained by hydrolysis of the oxo complex. The oxygenated complexes of transition metals are shown in Fig. 1.

All these six different types of oxygenated complexes can be considered as potential sources of oxygen atoms liable to be given to reactive substrates (24,36).

(i) Superoxo complexes are the primary reversible dioxygen adducts occurring naturally in the oxygen-carrying iron-porphyrin respiratory pigments such as myoglobin. They also intervene as precursors of active peroxidic species in enzymatic monooxygenases containing the cytochrome P_{450} as prosthetic group (24).

(ii) Peroxo and μ-peroxo complexes contain dioxygen bonded to the metal in a peroxidic form. They are responsible for various selective oxidations such as epoxidation, ketonization, oxidative cleavage of olefins and Bayer-Villiger lactonization of ketones, etc.

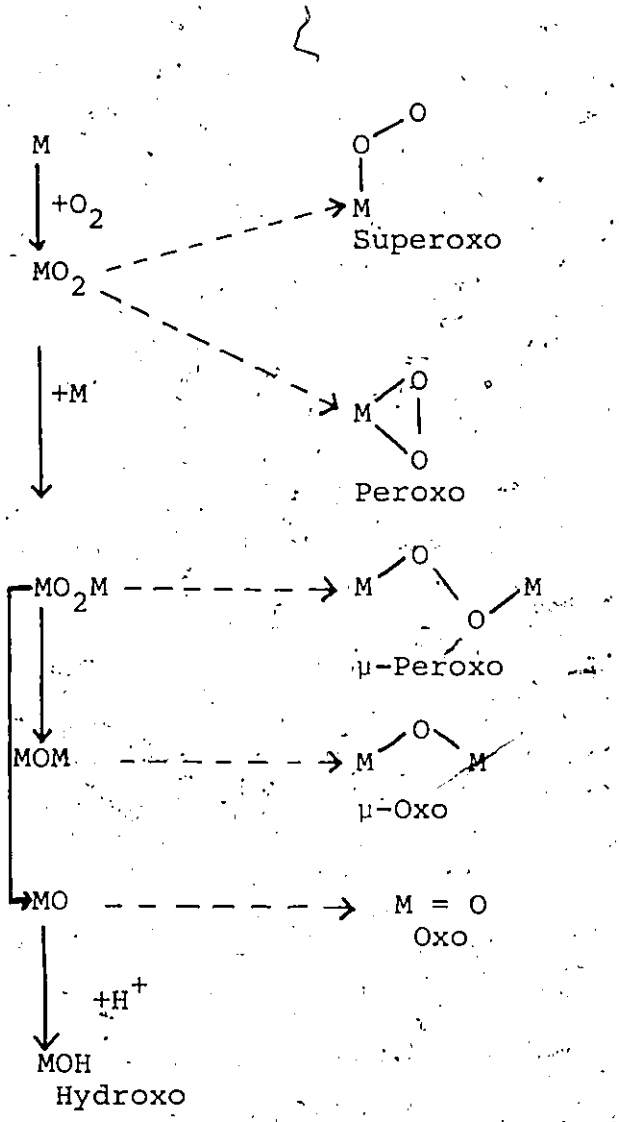

Fig. 1. Oxygenated complexes of transition metals.

The present work describes the isolation of peroxo complexes of thorium and uranium containing different organic moieties and some use of these compounds as oxidants towards simple olefinic compounds.

(iii) μ-Oxo complexes have been recently shown to be the active species in copper-catalyzed oxidation of alcohols to ketones, and oxidative cleavage of pyrocatechol (24).

(iv) Oxo complexes often behave as carbenic reagents and are responsible for various oxidation reactions, e.g., epoxidation of olefins, oxidative cleavage, etc.

(v) Hydroxo complexes intervene in Wacker-type oxidations involving hydroxypalladation of olefins giving carbonyl compounds.

The reactivity of different oxygenated metal complexes other than the peroxo complexes will not be considered here.

4. THE BONDING OF OXYGEN TO METAL

(i) The Electronic Structure of Dioxygen Compounds

The bonding in molecular oxygen is best described by molecular orbital theory (37). According to this theory, the valence orbitals of the two oxygen atoms ($2s^2 2p^4$) combine to

give molecular orbitals whose relative energies are shown in Fig. 2. The ground state of molecular oxygen is a triplet state ($^3\Sigma$) with two unpaired electrons occupying a pair of π^*-antibonding orbitals. The two lowest excited states are formed by redistributing the two electrons in these $2p\pi^*$ orbitals. The configurations and energies for the ground state and the first two excited states are shown in Fig. 3.

The molecular orbital diagram given in Fig. 2 is valid for a free oxygen molecule but for O_2 under the influence of the electrostatic field of a transition metal ion in a complex, the situation will be somewhat different. It was first postulated by Griffith (38) that this influence might remove the degeneracy of the $2p\pi^*$ level, and that in certain cases, the energy difference between the two orbitals may become larger than the energy of pairing, i.e., the two electrons will then be located in the more stabilized of the two orbitals with their spins paired (Fig. 4). Griffith has also indicated that in this situation the oxygen molecule has an electronic configuration comparable with that of ethylene in its ground state. We may therefore visualize the electron distribution in terms of a trigonal sp^2 hybridization at the two oxygen atoms. One of the sp^2 hybrid orbitals of each oxygen atom is used for mutual σ-bonding and the other two are each doubly occupied; in other words, they form a set of four lone pair orbitals (n_o) oriented in the same way as the four hydrogen atoms in ethylene

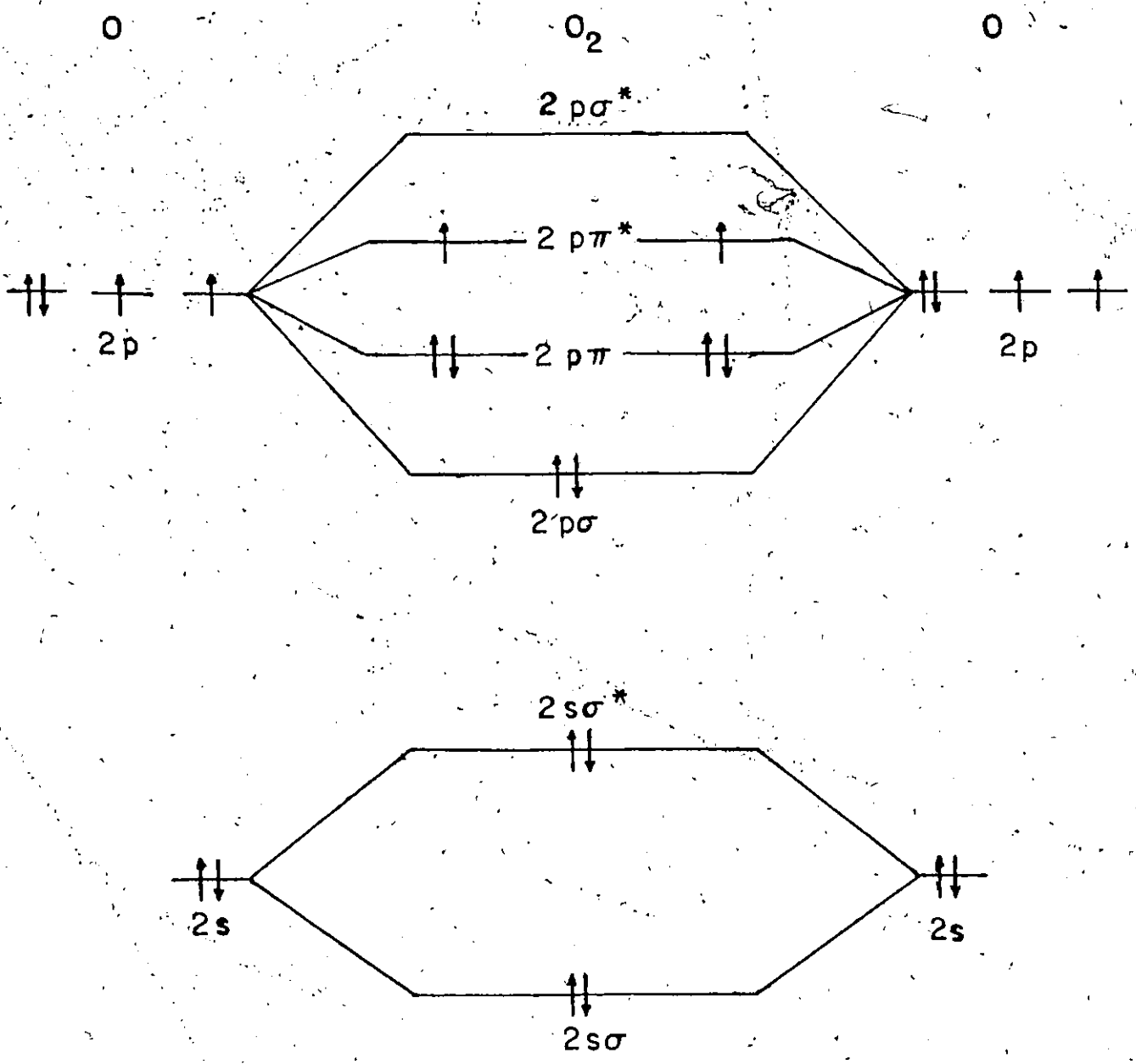

Fig. 2. Molecular orbital diagram for O_2.

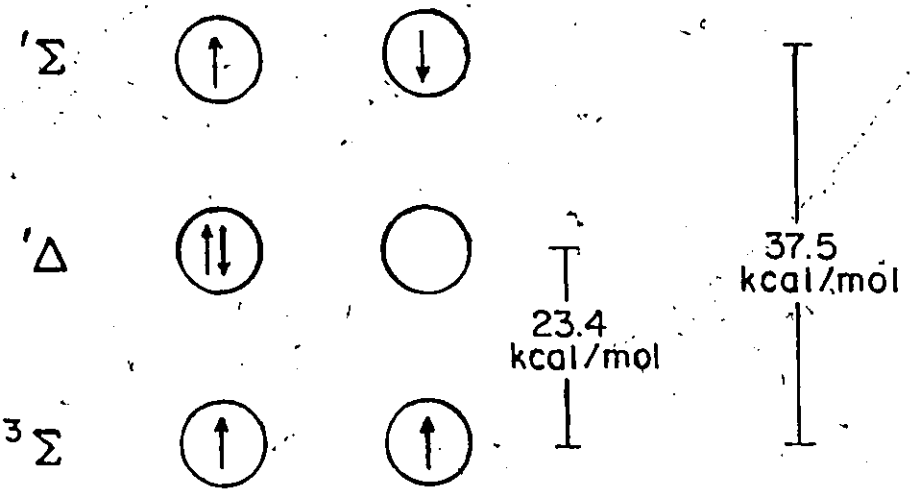

(a)

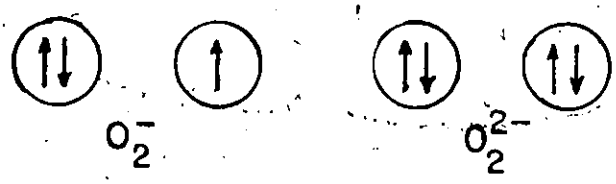

(b)

Fig. 3. (a) π^* orbital occupancy and energies of the first two electronically excited states of O_2.
(b) π^* occupancy of superoxide and peroxide.

(Fig. 5). There is also one effective π-bond in the molecule; the lowest energy, empty antibonding orbital is $2p\pi^*(p_x)$.

(ii) Bonding in Metal Dioxygen Complexes

Two basic classes of metal dioxygen complexes have been proposed as model systems; those incorporating dioxygen in a side-on linkage (the Vaska-type complexes, Fig. 6) (14,38-39), and those involving a single metal dioxygen σ-bond, proposed by Pauling and others (40-42) (Fig. 7). The former class, discovered and intensively studied by Vaska (20,43) and others (18,23-27,44-46), were said to have covalent linkages between the metal and the peroxide group in an isosceles triangular fashion.

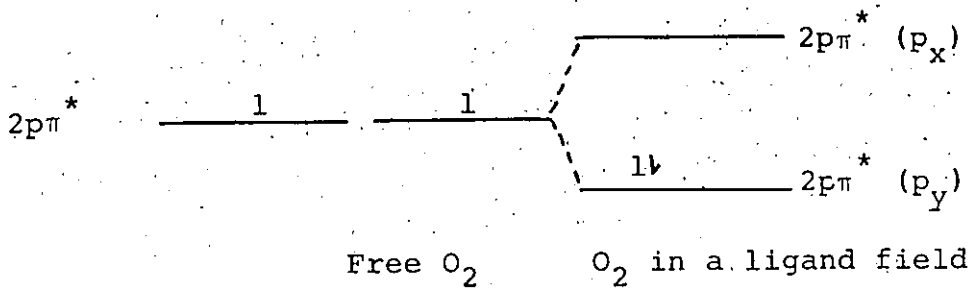

Fig. 4. Influence of a ligand field on the electron distribution in the oxygen molecule.

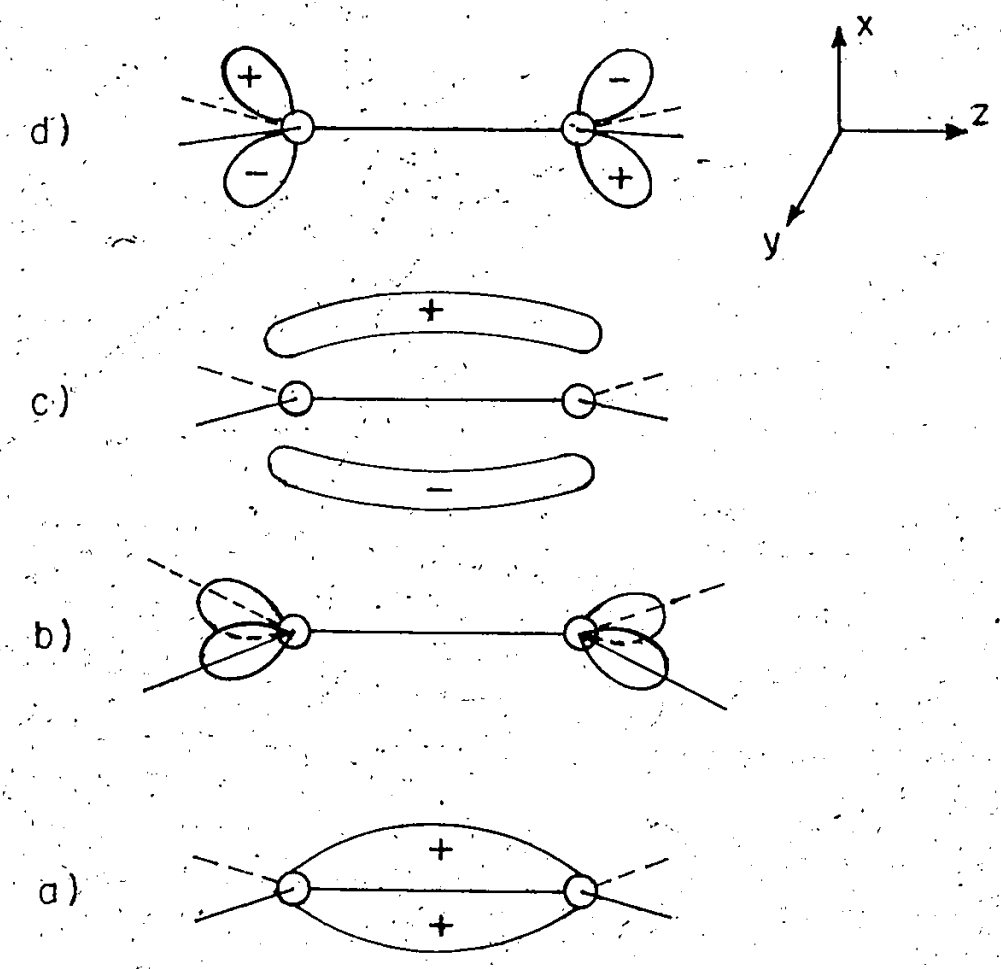

Fig. 5. The "valence state" molecular orbitals of the oxygen molecule: a) σ-bonding MO; b) sp^2 lone pair orbitals (n_o); c) π-bonding MO; d) π^*-antibonding MO (according to (38)).

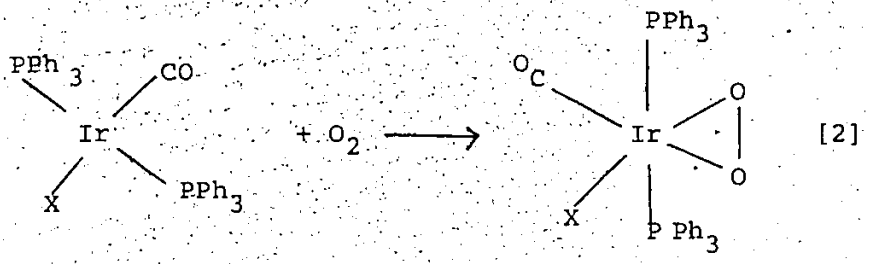

[2]

Fig. 6. Vaska's peroxo complex.

Fig. 7. Diagrammatic representation of the possible modes of O_2 binding to metal ions.

Perhaps the simplest way to understand the metal-peroxide interaction would be through the comparison of O_2^{2-} and C_2H_4 as ligands (14). In the ethylene complexes, the olefin is usually considered as donating electrons from the π-bonding orbital to the metal, while the metal donates electrons from an appropriate, filled d orbital to the empty, antibonding π^* orbital of the olefin. In the peroxide ion, the π^* orbital is already filled, so that no back-bonding is possible. At the same time, there may be donation to the metal both from the π- and π^* orbitals of the peroxide group, at least when the metal is in a sufficiently high oxidation state. The effect of coordination on the O-O bond would then depend on the relative strengths of the two interactions - in other words, on whether donation was principally from π- or from π^* orbitals of the peroxide group (Fig. 8).

It has already been mentioned that removal and addition of electrons to the π^*-orbital of dioxygen brings about many changes as summarized in Table 1 (18,20).

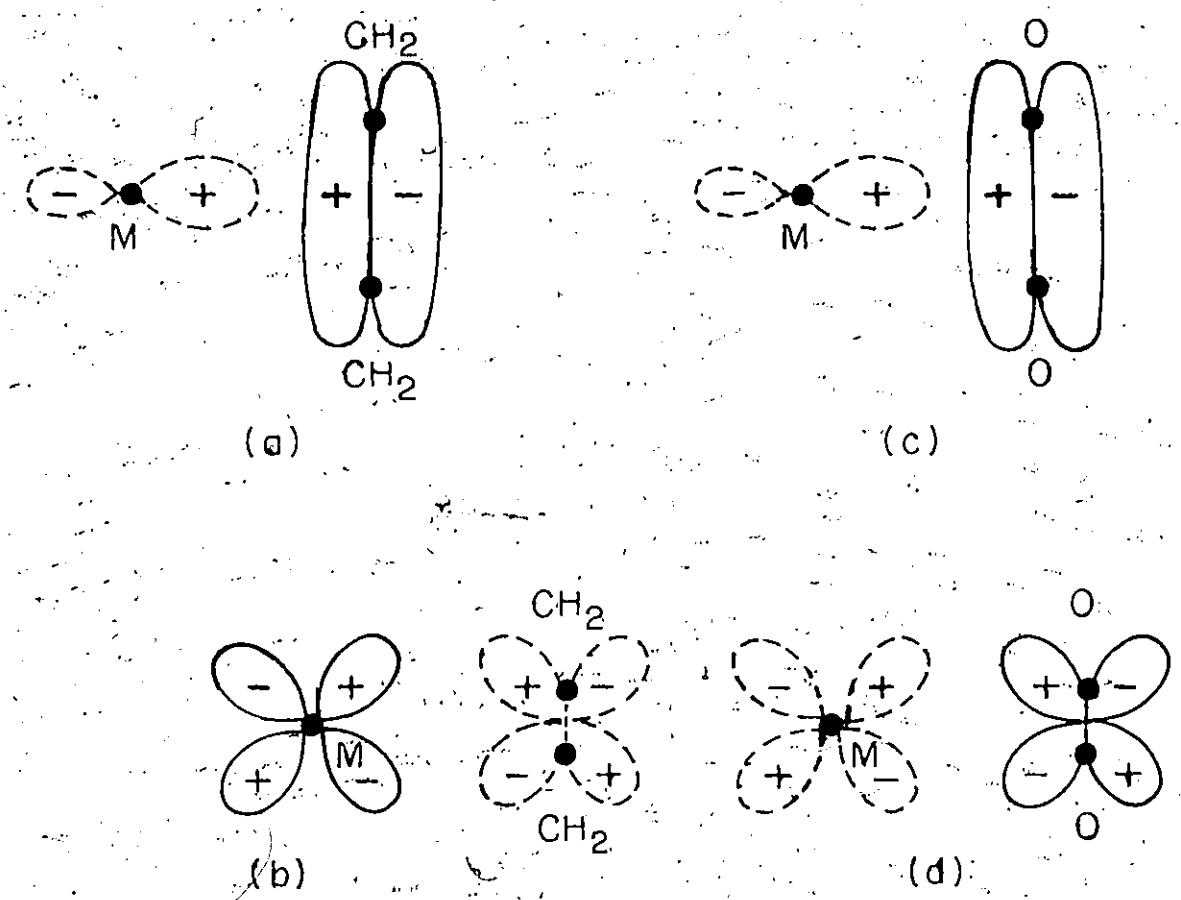

Fig. 8. Possible scheme for representing the interaction between a transition metal atom and ethylene or peroxide as ligands. (a) Donation to the metal from a π-bonding orbital of ethylene; (b) donation from the metal to a π-antibonding orbital of ethylene; (c) donation to the metal from a π-bonding orbital of peroxide; (d) donation to the metal from a π-antibonding orbital of peroxide. An orbital indicated by full lines contains an electron-pair; those indicated by broken lines are empty. For simplicity, the metal orbital interacting with the π-bonding ligand orbitals have been drawn as sp hybrids, although they will probably have d-character (14).

Table 1. Properties of dioxygen and its ions.

	Bond Order	O-O A°	Bond Energy kcal mol^{-1}	ν(O-O) cm^{-1}
O_2^+	2.5	1.12		1905
↑				
O_2	2	1.21	118	1580
↓				
O_2^- (Superoxide)	1.5	1.33		1097
↓				
O_2^{2-} (Peroxide)	1.0	1.49	35	802
↓				
$2O^{2-}$	0			

5. MODE OF FORMATIONS OF TRANSITION METAL PEROXIDES

The dioxygen complexes which are referred to as side-bonded or π-bonded dioxygen complexes are diamagnetic and can be obtained by two principal methods (23-24,45,47).

(i) Ligand exchange by reaction of O_2^{2-} and a high-valent metal complex; an acid-base interaction

Specifically, this consists of reaction of hydrogen peroxide with a complex containing a metal in a higher oxidation state,

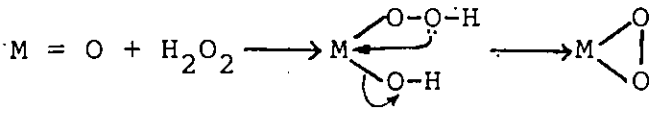

[3]

Examples:

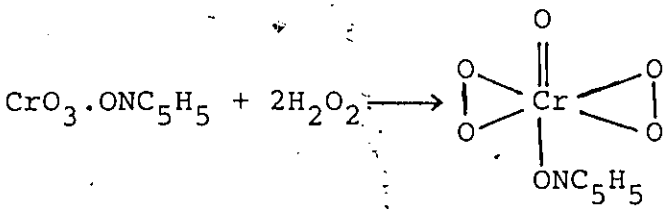

[4]

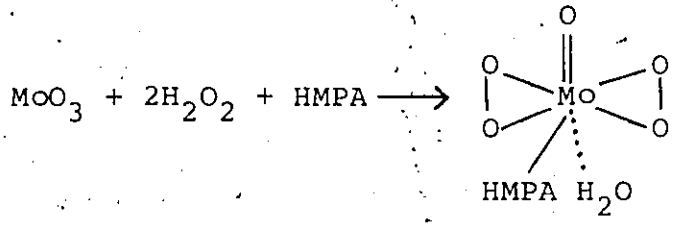

[5]

or

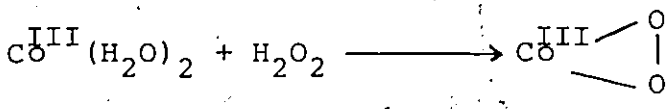

[6]

In these examples, the dioxygen is provided in an already reduced (peroxide) state. The metals in their higher oxidationtion states do not enter into back-bonding to dioxygen. Complexation occurs from the (Lewis) acid-base interaction between the metal ion and the peroxide ion.

A great number of peroxo complexes of Groups 4B, 5B and 6B have been prepared by this method and shown by x-ray crystallographic structure determination to exhibit the triangular model of bonding of peroxide to metal (14,26,45-46,48). For most of these complexes, there is very little variation in

the O-O bond distance despite differences in metal, ancillary ligands, valence state, and structure (24).

(ii) Oxidative addition of dioxygen to a complex of a low-valent metal

The second method of obtaining peroxo complexes is the direct interaction of dioxygen with reduced, two electron-donor metal complexes,

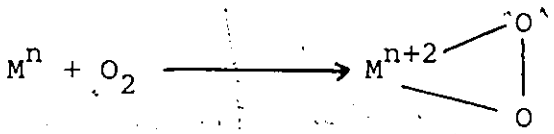

[7]

Examples:

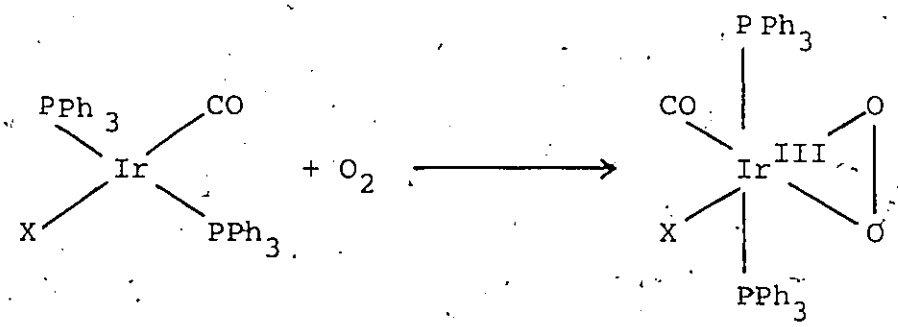

[2]

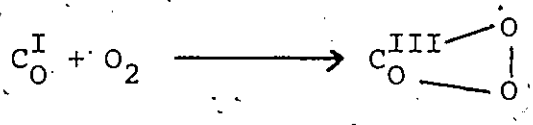

[8]

The peroxidic nature of dioxygen adducts such as $M(PPh_3)_2O_2$ (M=Pd,Pt) has been demonstrated by obtaining hydrogen peroxide upon hydrolysis of the complexes with strong acids (49).

6. TRANSFER OF COORDINATED OXYGEN FROM TRANSITION METAL PEROXIDES TO ORGANIC SUBSTRATES

The peroxo complexes can be considered as potential donors of oxygen to reactive substrates. The primary oxygen source for the preparation of these peroxidic complexes can be either molecular oxygen itself or peroxidic compounds such as hydrogen peroxide or alkyl hydroperoxide. Hence, the way in which transition metal peroxides release oxygen to substrates is particularly relevant to the catalytic properties of transition metal complexes in selective oxidations involving O_2, ROOH or H_2O_2 as the oxygen source.

In order to understand better the reactions of peroxo complexes, it is instructive to consider the general reaction of olefin with M-X groups. The key step in most of the transition-metal catalyzed transformations of olefins consists of the π-σ rearrangement of the olefin on the metal (50), shown by the equation [9]

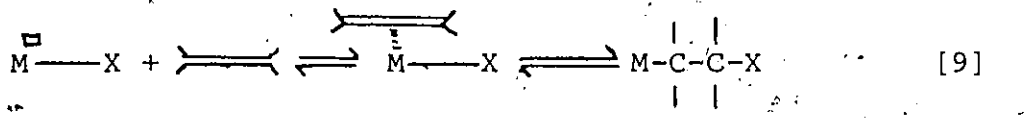

[9]

This transformation can be described as the insertion of the coordinated olefin into the metal-nucleophile bond M-X.

In the case of the metal-bearing oxygen atoms, the application of this general principle leads to a peroxymet-

allation process if the metal is bonded to a peroxidic group, or to an oxymetallation process if the metal is bonded to an oxygen atom as in oxo complexes or hydroxo complexes.

Peroxymetallation

The insertion of substrates such as olefins or ketones into the metal-peroxide bond gives rise to the formation of a five-membered peroxometallocyclic adduct, e.g., for olefins,

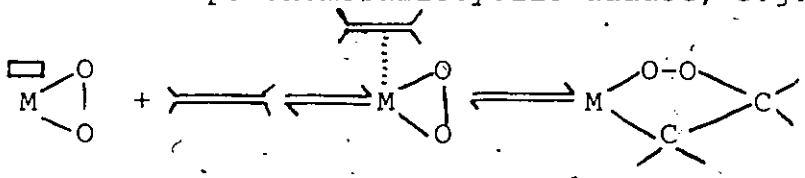

[10]

For ketones,

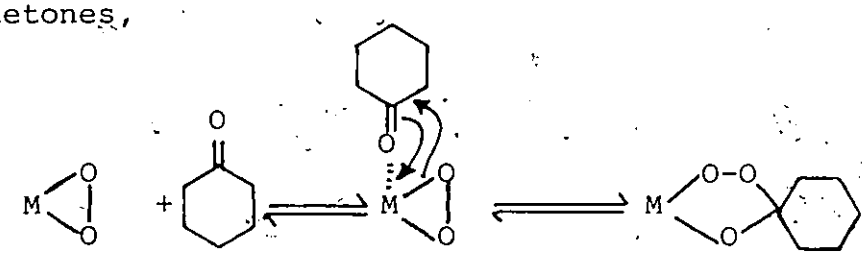

[11]

The coordination of the substrate to the metal prior to insertion is only necessary for nucleophilic substrates (24,51). For electrophilic substrates such as cyano olefins or hexafluoroacetone, this preliminary coordination is not necessary, and the peroxo metallocyclic adduct results from the bimolecular 1,3-dipolar addition of the substrate to the peroxo group, as shown in Eqns. [12] (52) and [13] (53).

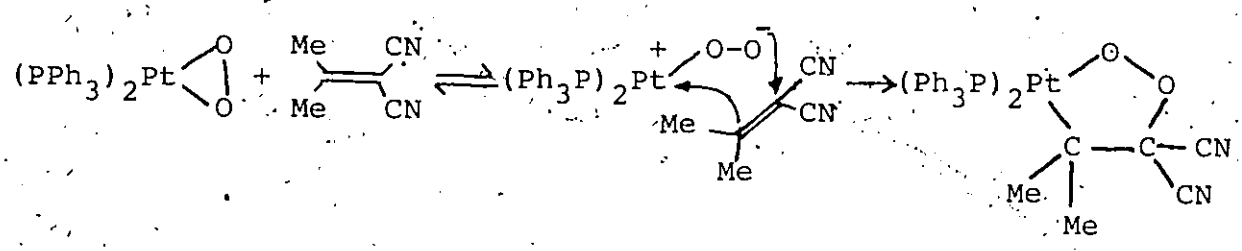

[12]

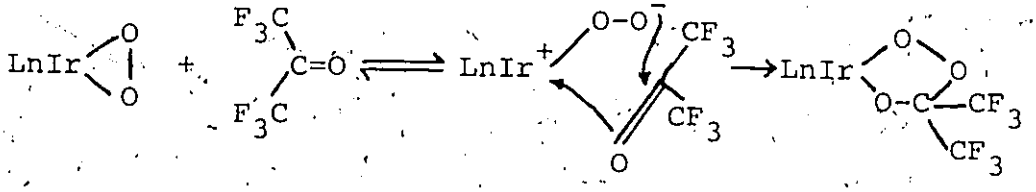

[13]

Oxymetallation

(a) In the case of oxo-metal complexes, the insertion of the olefin into the M=O bond would lead to the formation of a four-membered metallocycle,

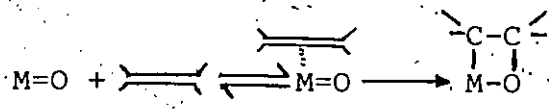

[14]

This may occur with non-metals also. For example, the addition of SO_3 to olefins gives rise to the formation of β sultones (Eqn. [15], (54)).

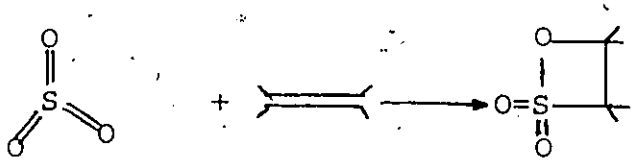

[15]

(b) In the case of metal-hydroxo complexes, the insertion of the olefin into the M-OH bond gives rise to the formation of an organometallic hydroxylic adduct

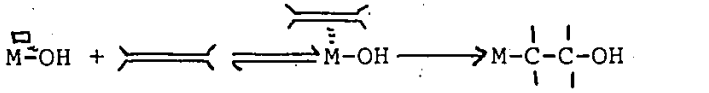

[16]

Such hydroxylic adducts have been obtained from the reaction of mercuric salts with olefins in the presence of water (Eqn. [17], (55)),

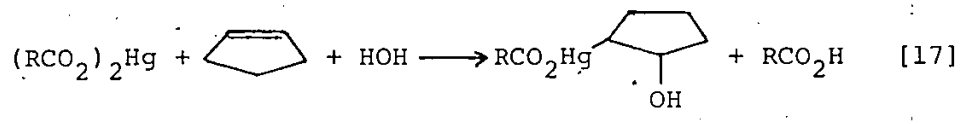

[17]

The hydroxypalladation of olefins and the ensuing β hydride elimination are the key steps in the Wacker-type oxidation of olefins to carbonyl compounds (Eqn. [18], (56)).

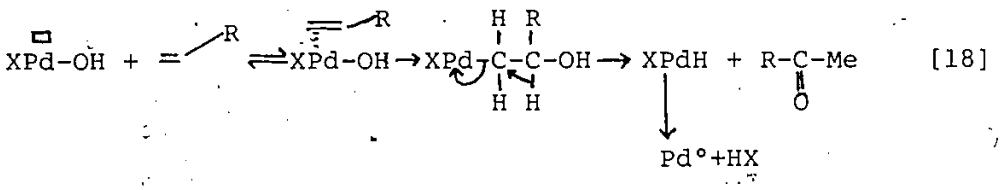

[18]

7. OXYGEN TRANSFER FROM PEROXO COMPLEXES TO SUBSTRATES

Oxidations by Group 6 metal peroxo complexes: chromium, molybdenum and tungsten oxodiperoxo complexes with the general formula $M(O)(O\text{-}O)_2L_2$ have been obtained by reaction of a ligand, L (e.g. amide, phosphoramide, amine, phosphine oxide,

arsine oxide, aromatic amines and their oxides), with a solution of MoO_3 or WO_3, H_2O in hydrogen peroxide (23,57). These complexes, which are soluble in organic solvents, are able to react with various reactive substrates. Mimoun et al.(16,24) have studied epoxidation of olefins by $MoO(O_2)_2$. HMPA.H_2O and showed that the reaction proceeds via two steps: reversible coordination of olefin to the metal displacing the ligand, followed by irreversible oxygen transfer to the olefin.

Displacement of the ligand, L, by the olefin has been shown to occur using NMR measurements and kinetic studies. Further, a strong inhibitory effect of the presence of σ donor ligands on the rate of epoxidation has been observed (24).

Since coordination of olefin to the metal is the rate determining step, epoxidation occurs more readily when the olefin possesses substituents which make it more nucleophilic (24).

The scheme [19] represents the proposed mechanism for the oxygen transfer from the peroxo complex to the olefin. After displacement of the ligand, L(HMPA), by the olefin, the latter inserts into the Mo-O bond, forming a five-membered peroxometallocycle which decomposes to give epoxide and the molybdenum dioxo complex (16,24).

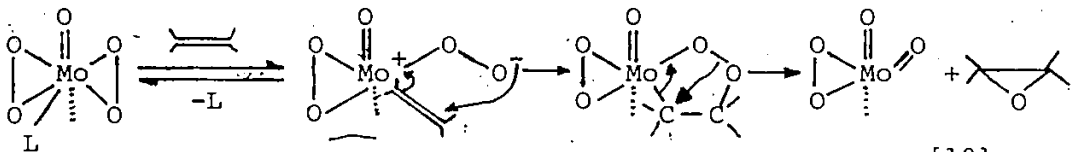

[19]

Epxodiation of olefins by molybdenum peroxo complexes is highly stereospecific and occurs with complete retention of configuration (24,58).

Recently, Olah et al. (22) carried out the epoxidation of many organic olefinic compounds with uranyl peroxide, $U(O)_2(O_2).4H_2O$. They also proposed a mechanistic path for epoxide formation similar to Mimoun's.

Jacobson et al.(46) have reported oxo di- and mono-peroxo complexes of Mo and W containing picolinato and pyridine-2, 6-dicarboxylato ligands of general formulae $[M(O)(O_2)_2C_5H_4NCOO]^-H_3O^+$ and $[M(O)(O_2)C_5H_3N(COO)_2]H_2O$. They also reported characterization of peroxo complexes of Mo and W having outer sphere uncoordinated ligand, e.g.,

$$[M(O)(O_2)_2C_5H_4NCOO]^-.2C_5H_4NCOOH.H_3O^+ \quad (M=Mo \text{ and } W).$$

The molybdenum peroxo complexes, $[Mo(O)(O_2)_2C_5H_4NCOO]^-H_3O^+$ and $[Mo(O)(O_2)C_5H_3N(COO)_2]H_2O$ have been used as catalysts for the Bayer-Villiger oxidation of cyclic ketones by H_2O_2 (90%) to lactones and their derivatives. Using the peroxo complex $[Mo(O)(O_2)C_5H_3N(COO)_2]H_2O$ as oxidant and cyclopentanone as substrate, Jacobson et al. (59) obtained δ-valerolactone (45%) and 5-hydroxypentanoic acid (15%) [20],

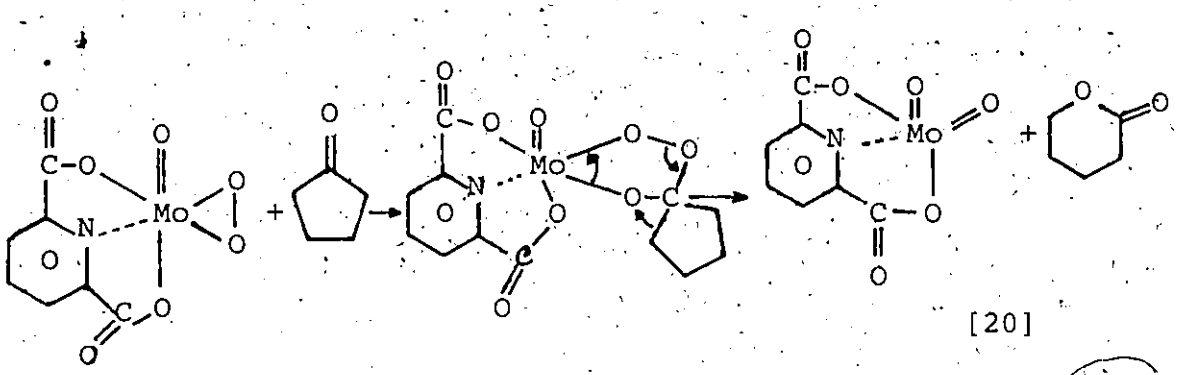

[20]

The suggested mechanism involved the formation of the peroxo-metallocycle via the insertion of the carbonyl bond between the M-O bond, just as the proposed mechanism for the epoxidation of olefins [19]. It has been reported that peroxo complexes containing monodentate ligands such as $Mo(O)(O_2)_2 \cdot HMPA:H_2O$ decompose readily and are not suitable as catalysts for oxidation of cyclic ketones (57,59); however, peroxo complexes stabilized by polydentate ligands are being used as successful oxidants. Besides, the complexes $[M(O)(O_2)_2C_5H_4NCOO]^-H_3O^+$ (M=Mo,W) oxidize secondary alcohols to ketones (60).

Similarly, peroxo complexes of group 4B elements are becoming increasingly important for their potential use in oxidation reactions. The ability of titanium to transfer oxygen has recently been elegantly exemplified by Sharpless et al. (61-62) in the asymmetric transformation of allylic alcohols into epoxy alcohols by t-BuOOH in the presence of titanium tetraisopropoxide as a catalyst [21].

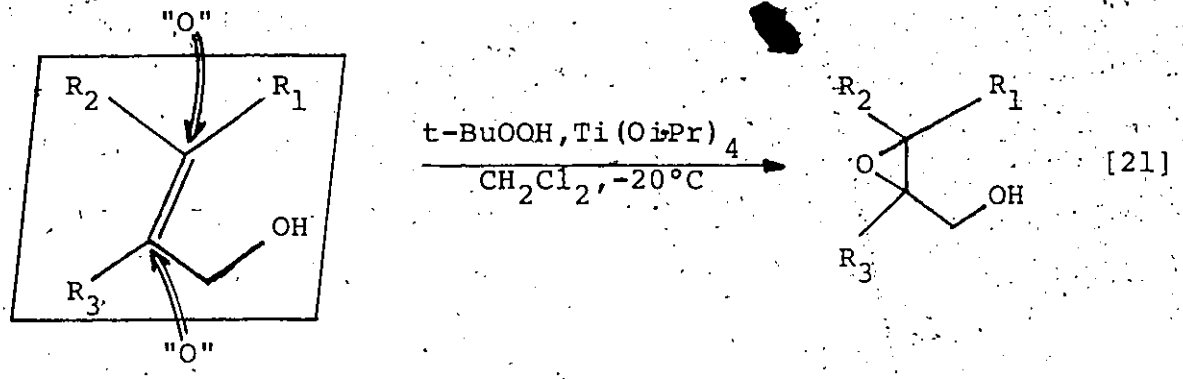

[21]

Very recently, Mimoun et al. (26) have reported the synthesis, structure and properties, with respect to oxygen transfer to various substrates, of peroxotitanium (IV) derivatives of general structure (Fig. 9).

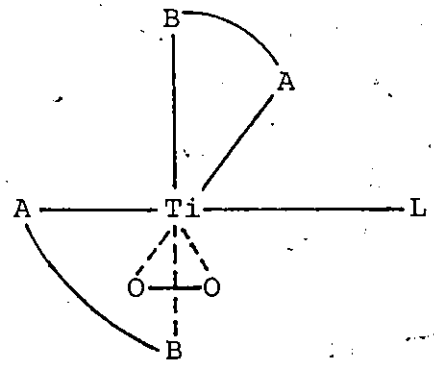

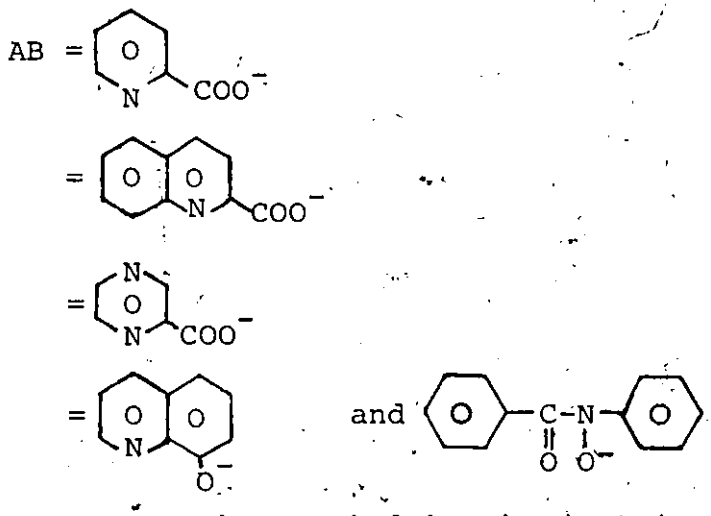

and L = HMPT = hexamethylphosphoric triamide.

Fig. 9. Structure of peroxo complexes of titanium containing different organic ligands.

Mimoun et al. have reported that strong stabilization of the peroxotitanium moiety by picolinato, hydroxyquinolino or hydroximato ligands precluded oxygen transfer from the titanium compounds to olefins, allylic alcohols, cyclic ketones or sulfides. However, triphenylphosphine was slowly converted (complete transformation required 12h at room temperature) to the phosphine oxide by a stoichiometric amount of titanium peroxo complex in CH_2Cl_2 under anaerobic conditions (26).

8. AIM OF THE PRESENT WORK

In view of the great importance of the peroxo complexes of Group 4B and 6B elements, a program was undertaken to synthesize new peroxo complexes of thorium and uranium, the last members of the above two groups respectively. Synthesis of the peroxo complexes of thorium and uranium consists of two steps:

1. isolation of coordination compounds resulting from the reaction of $ThCl_4$ or UCl_4 with stoichiometric amounts of organic ligands (ONC_5H_5, $OPPh_3$, $OAsPh_3$, $C_5H_3N(COOH)_2$, $C_6H_4NH_2OH$, C_5H_4NCOOH, $C_6H_4NH_2COOH$, $C_{13}H_{11}NO_2$, and $C_{14}H_{11}NO_3$) in a suitable solvent,
2. reaction of these precursor compounds with aqueous H_2O_2 solution.

The oxidizing properties of the peroxo complexes of thorium and uranium towards trans-stilbene and allyl alcohol were investigated. The results have been rationalized.

The coordination chemistry of the precursor compounds resulting from the reaction of $ThCl_4$ or UCl_4 with different organic ligands has been of interest also.

Description of the peroxo complexes will follow a description of their precursors.

CHAPTER 2

1. COMPLEXES OF THORIUM AND URANIUM

As thorium and uranium resemble the Group 4B and 6B elements respectively, it was of interest to discover whether they would form analogous peroxo complexes which contain organic moieties. As indicated earlier , isolation of peroxo complexes of thorium and uranium follows two reaction steps. The first step, the reaction of MCl_4 (M=Th,U) with a stoichiometric amount of a chosen ligand in a suitable solvent, yields the so-called intermediate complexes. In the second step, treatment of the intermediate compounds, either in the solid-state or solution, with aqueous hydrogen peroxide solution, yielded peroxo complexes. The detailed methods for the preparation of all these complexes will be given in Chapter 4.

The complexes isolated were characterized by elemental analyses, conductometric, alkalimetric and ceric sulfate titrations of some uranium compounds, I.R., Raman, NMR and electron spectroscopic studies.

2. COMPLEXES OF THORIUM

The intermediate thorium compounds have the general structure,

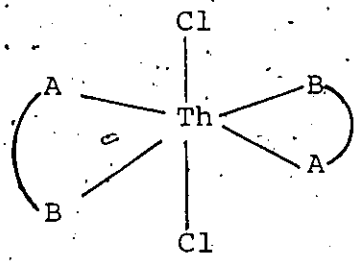

and

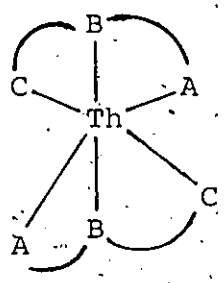

where

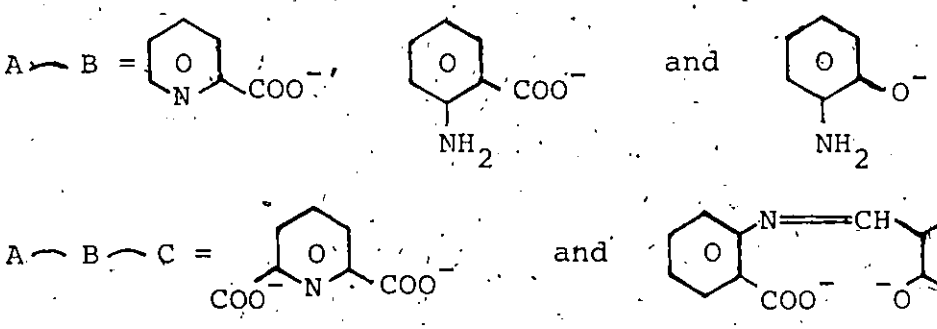

Fig. 10. Intermediate complexes of thorium.

The peroxo complexes of thorium have the structure

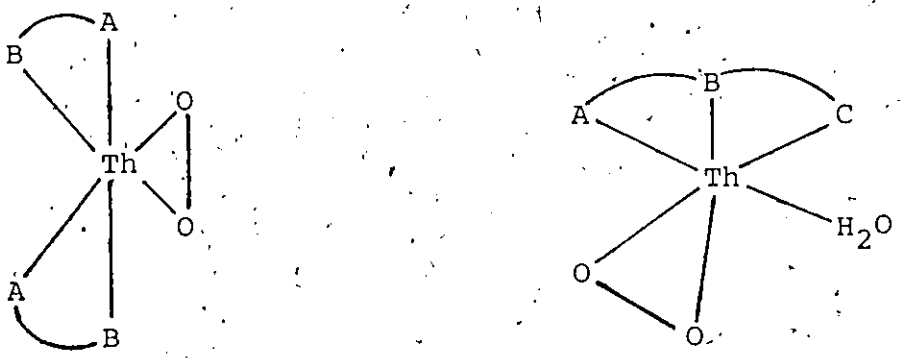

Fig. 11. Peroxo complexes of thorium.

In the context of the two methods for preparation of peroxo complexes of transition metals, the thorium peroxo complexes were prepared by method (i), i.e.,

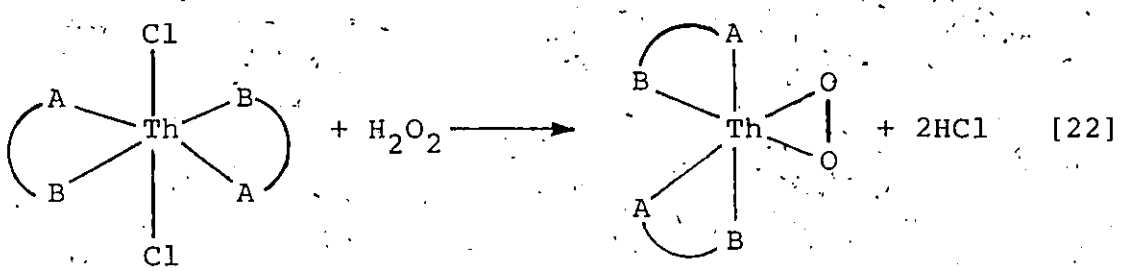

[22]

and

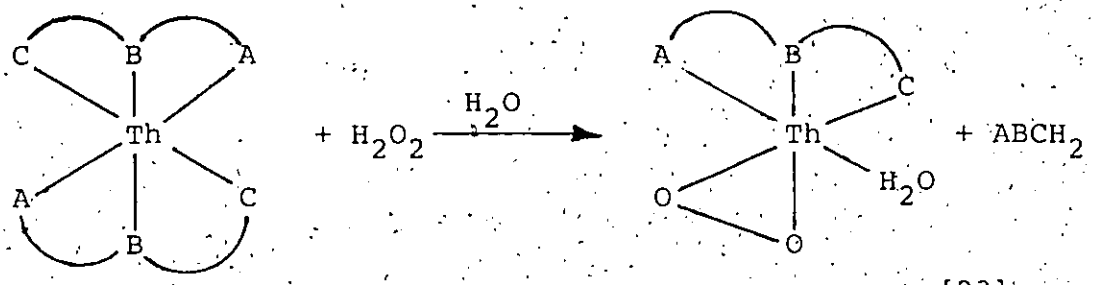

[23]

3. COMPLEXES OF URANIUM

The intermediate complexes of uranium have the following structures,

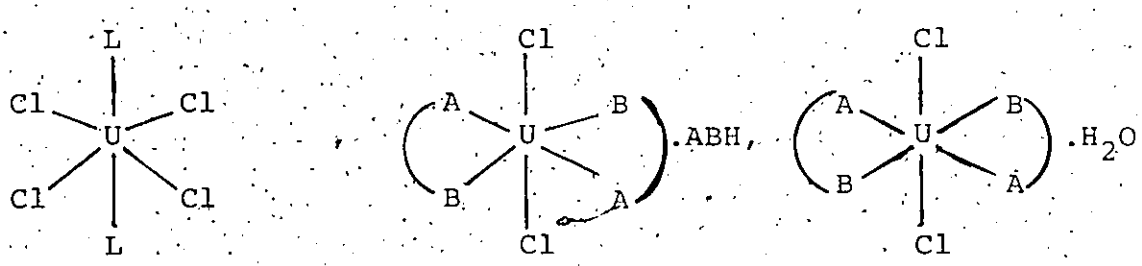

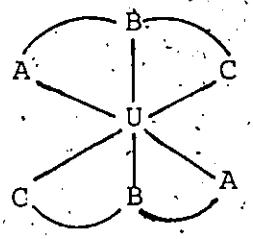

L refers to neutral monodentate ligands, ONC_5H_5, $OPPh_3$, and $OAsPh_3$.

Fig. 12. Structure of intermediate complexes of uranium.

The peroxo complexes of uranium have the structure,

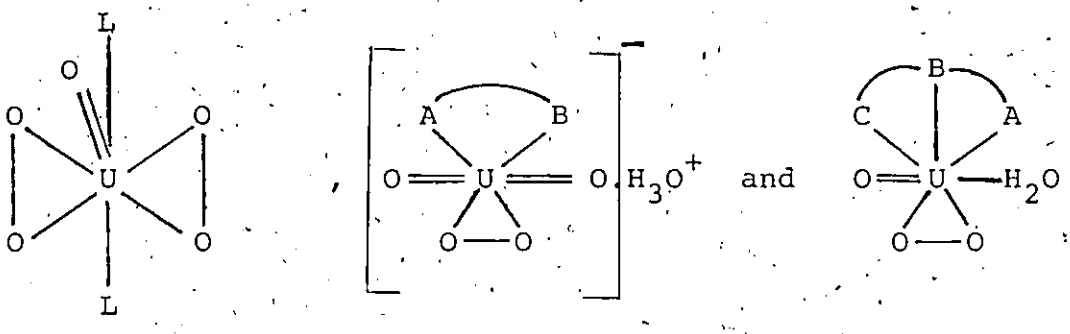

Fig. 13. Peroxo complexes of uranium.

The description of peroxo complexes of uranium from their precursors is conceptually identical with the combination of two processes, i.e., ligand exchange and oxidation, perhaps by the mechanism shown,

(i)

(a)

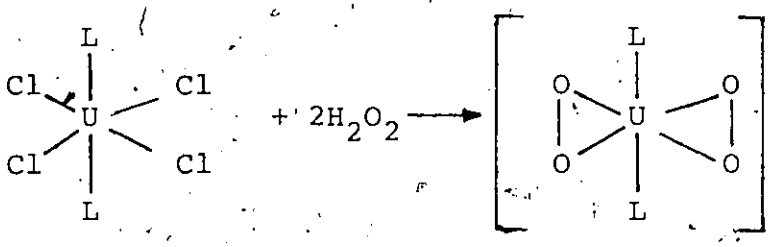

[24]

(b)

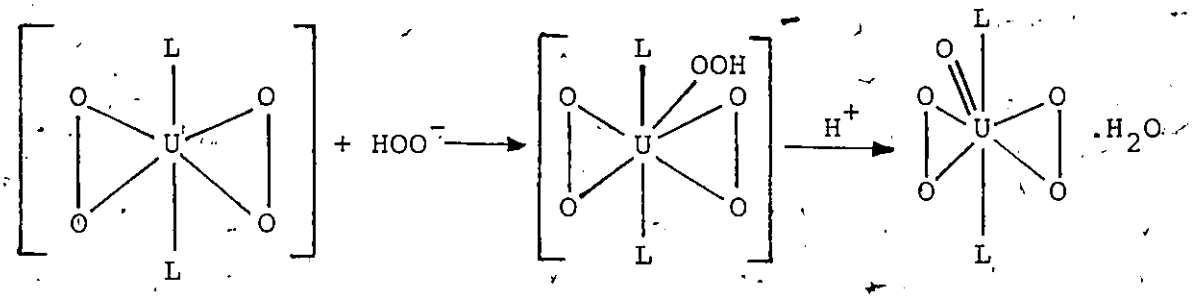

[25]

(ii)

(a)

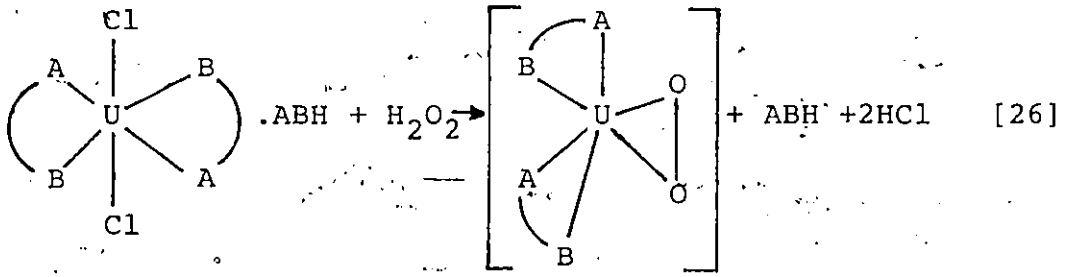

[26]

(b)

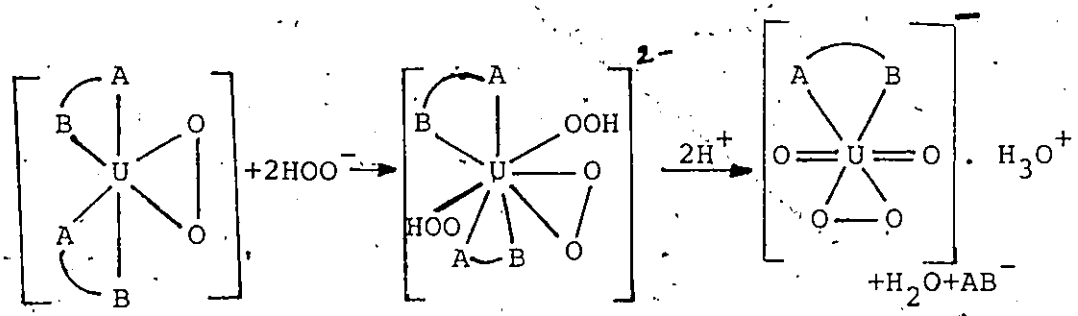

[27]

(iii)

(a)

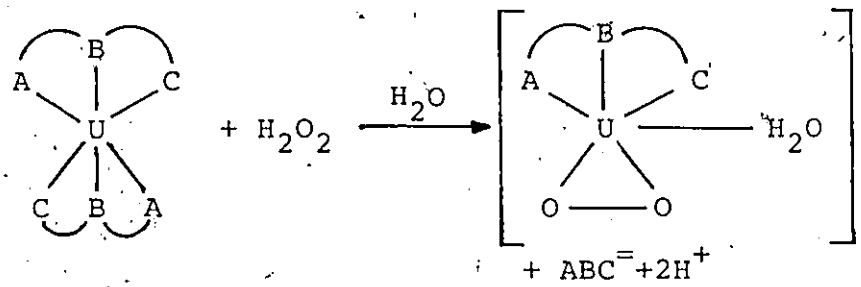

[28]

(b)

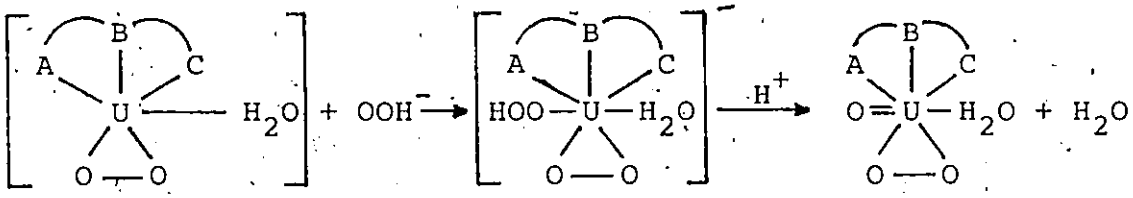

[29]

Other plausible mechanisms are:

i) a route where oxidation occurs first followed by ligand exchange

ii) a concerted mechanism, one in which the ligand replacement reaction by the peroxo group and oxidation of U(IV) to U(VI) could occur simultaneously in a single step.

CHAPTER 3

EXPERIMENTAL TECHNIQUES

In this chapter, experimental techniques other than methods of preparing specific compounds will be discussed. These include:

1. the purification and handling of materials
2. details of making various physical measurements
3. analytical methods.

Preparative work will be discussed in Chapter 4.

1. PURIFICATION AND HANDLING OF MATERIALS

Unless otherwise specified, all the preparations, except for the peroxo complexes of thorium and uranium, were done in an atmosphere of dry, oxygen-free nitrogen.

Routine glassware cleaning

Glassware was cleaned in an acid bath, a hot mixture of sulfuric acid and nitric acid (~20:1) (65-70°C). The filtration apparatus (Fig. 14) could not be put in the bath. Instead, the acid was passed through the glass frit. The acid was removed with tap water and the apparatus cleaned with dilute ammonium hydroxide and finally with water. The glassware was dried at 180°C for 2-3 h.

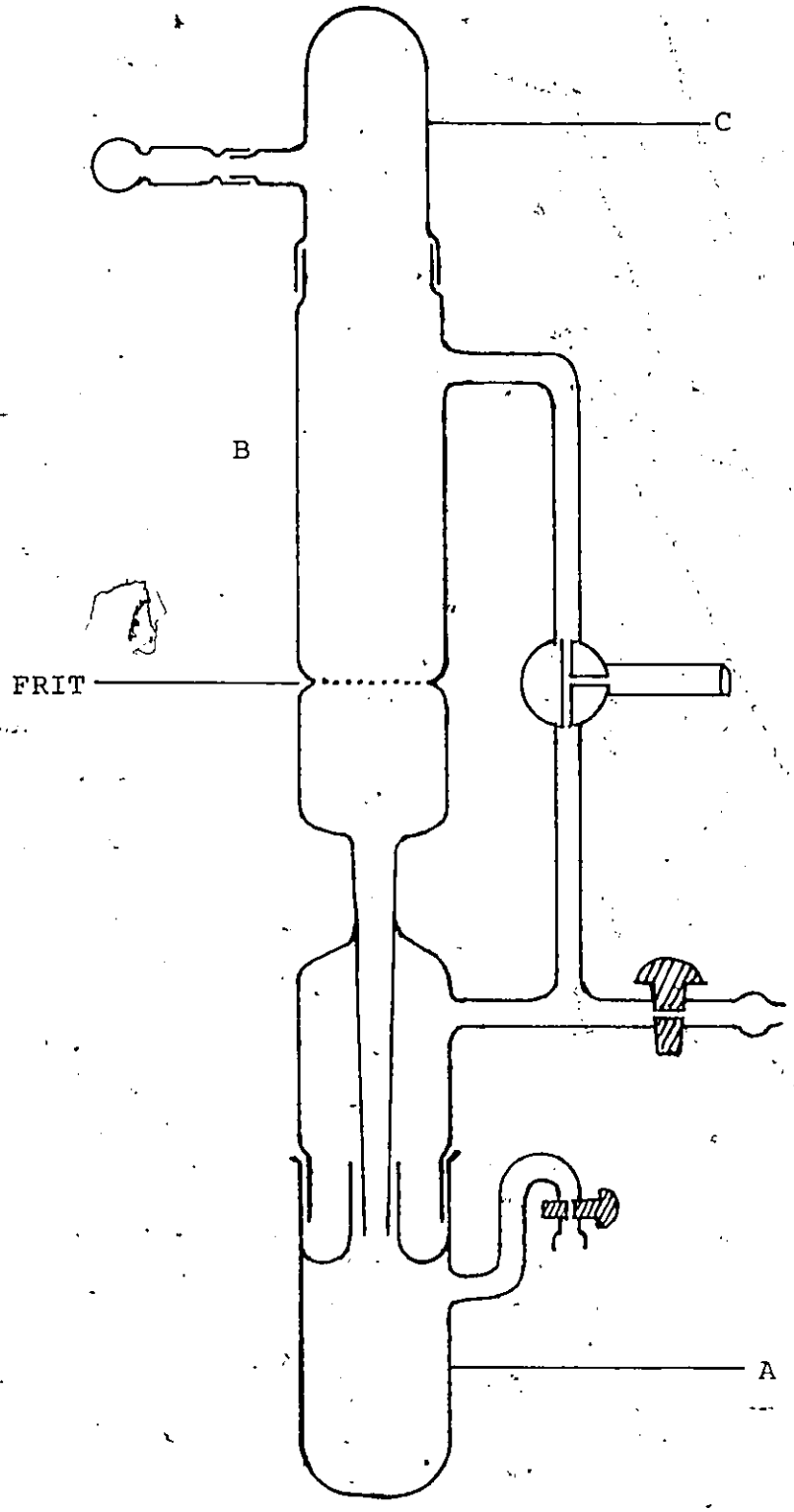

Fig. 14. Apparatus for filtration under N_2 atmosphere.

Materials

(i) Thorium and uranium compounds

Thorium nitrate, 4-hydrate and uranyl nitrate, 6-hydrate were obtained from J.T. Baker Chemical Co., Phillipsburg, N.J. and were used to obtain ThO_2 and U_3O_8 by strong heating.

(ii) Ligands

Pyridine-1-oxide, C_5H_5NO; triphenylphosphine oxide, $OPPh_3$; triphenylarsine oxide, $OAsPh_3$; all from Eastman, picolinic acid, C_5H_4NCOOH; 2-aminobenzoic acid, $C_6H_4NH_2COOH$; 2-aminophenol, $C_6H_4NH_2OH$; 2,6-pyridinedicarboxylic acid, $C_5H_3N(COOH)_2$, all from Aldrich Chemical Co. were used as supplied. Salicylaldehyde, HOC_6H_4CHO, used to prepare Schiff bases, was used as received from Aldrich Chemical Company.

(iii) Acetone

Spectrograde acetone (Baker Analyzed Reagent) was dried by cooling in the presence of NaI to form crystals of $(CH_3)_2CONaI$. The acetone was recovered by warming the crystals to 30°C and then distilling. The distillate was collected in a flask that had been dried at 180°C and cooled by flushing with dry, oxygen-free nitrogen. The solvent was stored in contact with Linde Molecular Sieves Type 4A, which had been heated to 350-400°C and cooled in a desiccator.

Unless otherwise stated, all other solvents were stored in the same way as described for acetone.

(iv) Acetonitrile

Spectrograde acetonitrile (Baker Analyzed Reagent) was refluxed over P_2O_5 and distilled.

(v) Tetrahydrofuran

Spectrograde tetrahydrofuran (Fisher) was refluxed with lithium aluminum hydride and distilled under nitrogen.

(vi) Ethanol

99% ethanol was refluxed with iodine and magnesium turnings and distilled.

(vii) Miscellaneous Reagents

Spectrograde nitromethane (Aldrich), nitrobenzene (B.D.H.), 1,4-dioxane (Fisher), methanol (Baker Analyzed Reagent), dimethylsulfoxide (Baker Analyzed Reagent) and carbon tetrachloride (Baker Analyzed Reagent) were distilled.

Aqueous ammonia was distilled and stored in a polyethylene bottle.

(viii) Dry Oxygen-Free Nitrogen

Nitrogen supplied in cylinders contained sufficient oxygen to oxidize most of the complexes of uranium(IV). The oxygen was removed from the nitrogen by passing the gas through a copper furance held at 250-300°C (Fig. 15). It was subsequently bubbled through concentrated sulfuric acid and passed finally through two columns containing phosphorous pentoxide.

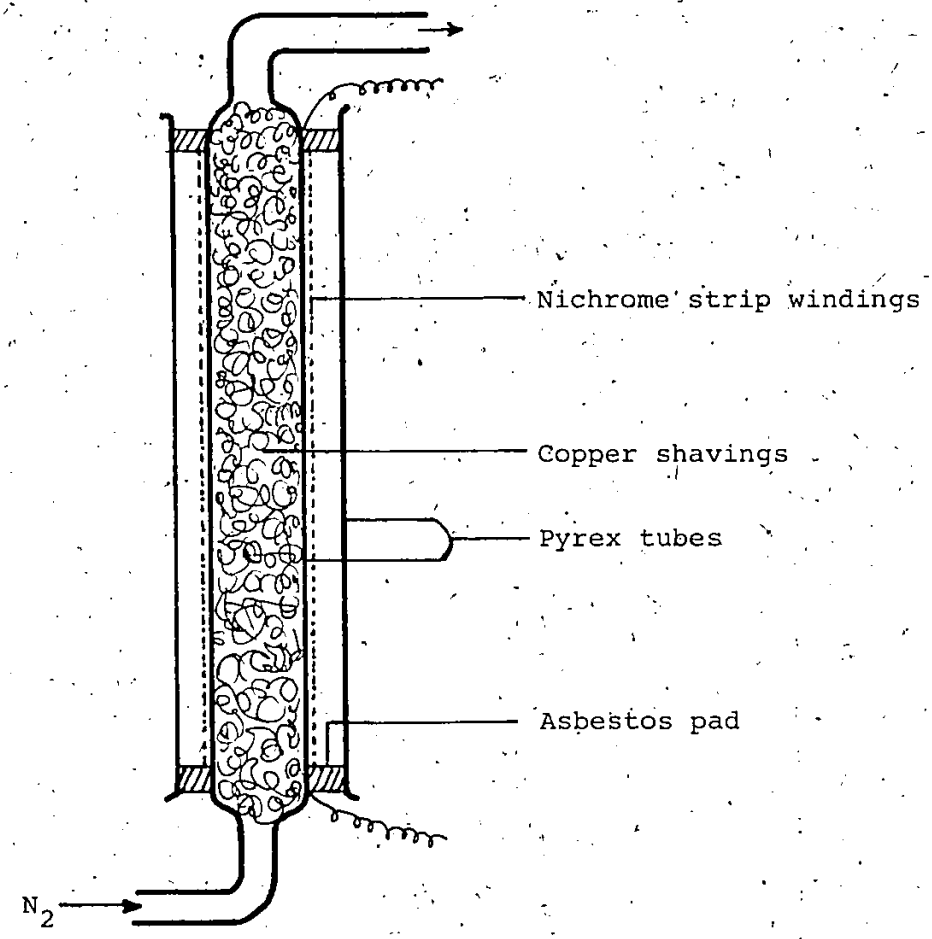

Fig. 15. The copper furnace for removing oxygen from commercially available nitrogen.

METHODS OF HANDLING SENSITIVE COMPOUNDS

The intermediate complexes of thorium and uranium were sensitive to water, oxygen or both. The complexes were prepared in special glass equipment.

(i) Apparatus

Figure 14 shows an apparatus described by Fritz et al. (63) for filtration in an atmosphere of nitrogen. Essentially, the apparatus has three separate parts, viz., two Schlenk tubes A and C, and a middle part, B, provided with a fritted glass disc for filtration. The term "Schlenk tube" will be used to designate a tube such as A. Figure 16 shows ampoules used for storing air sensitive samples for a long period and for weighing.

(ii) Procedure

Samples to be Stored and Weighed

The ampoule (Fig. 16) was fitted on to the filtration apparatus (Fig. 14) and the substance was transferred to the ampoule system. With nitrogen running through the system, the ampoule was sealed at constriction 1 (Fig. 16). To recover a sample from the sealed ampoule tube, the desired amount of the substance was transferred to one of the side tubes. One of the other side tubes was cooled in liquid nitrogen and the tube with the desired amount of the sample was cut from the rest with a blow torch, e.g., at constriction 2 (Fig. 16). A scratch was made on the ampoule containing the sample with a glass-cutter

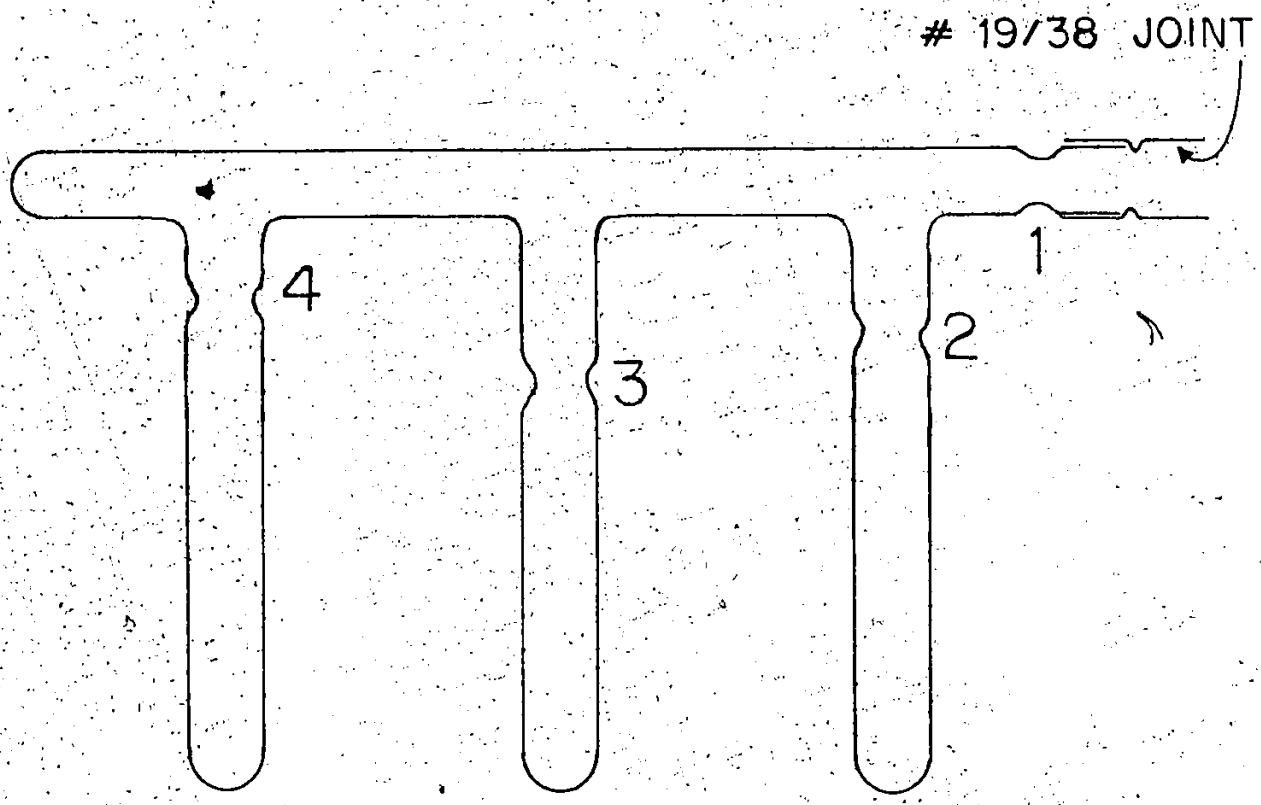

Fig. 16. Ampoules for storing and weighing air-sensitive compounds.

and was weighed along with two stoppers. The ampoule was broken open and quickly emptied, and the sample transferred. The two pieces of the ampoule with the stoppers in place were re-weighed to obtain the weight of the sample.

2. PHYSICAL MEASUREMENTS

The conductivity cell (Fig. 17) and NMR tube were normally cleaned several times with water, and finally rinsed several times with acetone or ethanol and allowed to dry in air. The NMR tube was finally dried in an electric oven (90-100°C) for 6 h.

(i) Conductivity

Conductivities were measured at 25.00±0.05°C in purified nitromethane, nitrobenzene, methanol and dimethyl sulfoxide, using an Industrial Instruments Model RC16B2 conductivity bridge and a cell of the Washburn type with platinized electrodes. Solutions were held between two platinum electrodes in the conductivity cell shown in Fig. 17. The cell was calibrated with 0.1000N potassium chloride and it had a cell constant of 0.762 cm^{-2}. A solution of known concentration, normally 5×10^{-4} M, was prepared from a suitable, purified solvent. The conductance cell was rinsed with solution, then filled, stoppered and put in a water thermostat set at 25°C and left for at least half an hour before determining the conductance. The conductance of the pure solvent was also determined.

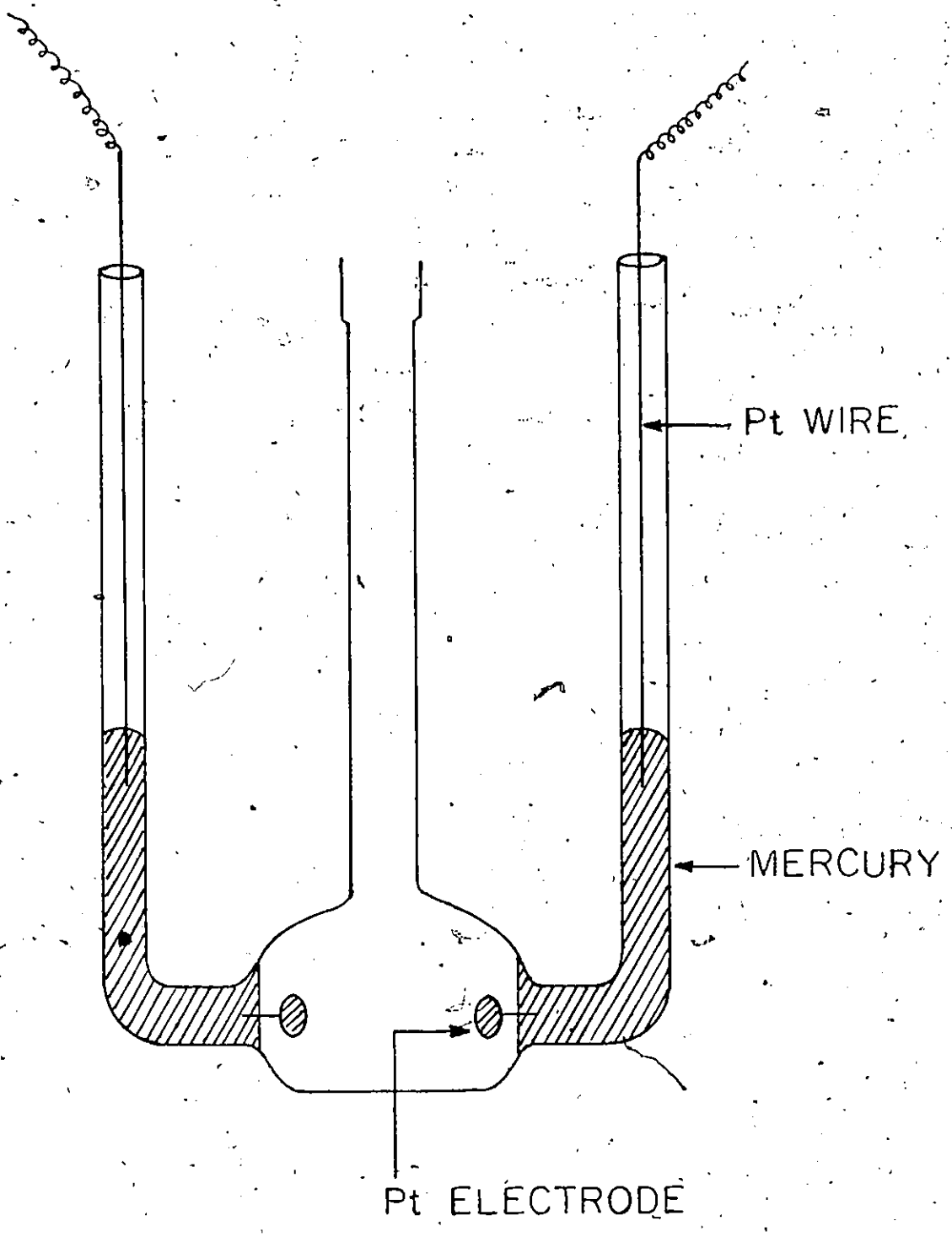

Fig. 17. Conductivity cell.

Preparation of the solutions for the intermediate complexes of thorium and uranium were done in a nitrogen-filled glove box.

(ii) Infrared Spectra

(a) Instrumentation

Infrared spectra (Nujol mulls) were recorded with a Pye Unicam SP 1100 or a Beckman IR-20 spectrophotometer. Spectra between 1500 and 200 cm^{-1} were obtained with a Perkin-Elmer 283 spectrophotometer.

(b) Procedure

The samples were put in an agate mortar, thoroughly powdered and then mulled with Nujol. The mulls were held between two alkali halide discs and the spectra recorded. Rock salt discs were used in the 4000-600 cm^{-1} range, while caesium iodide plates were used for recording the spectra between 1500-200 cm^{-1}. The Nujol mulls for the intermediate complexes were prepared in a nitrogen-filled glove box.

(c) Calibration of Spectra

Spectra recorded with a Pye Unicam SP 1100 or a Beckman IR-20 spectrophotometers were calibrated against the 1601.8 cm^{-1} peak for polystyrene.

Spectra obtained by the Perkin-Elmer 283 spectrophotometer were considered accurate to within ± 1.0 cm^{-1}.

(iii) Nuclear Magnetic Resonance Spectra

Proton and ^{13}C NMR spectra were obtained with Varian T-60 and FT-80 spectrophotometers. Tetramethylsilane (TMS) was employed as an internal standard. Deuterated chloroform and DMSO-d_6 were employed as solvents to obtain proton and ^{13}C NMR spectra respectively.

(iv) Raman Spectra

Raman spectra of the solids were obtained with a Spectra-Physics Model 125A He-Ne laser operated at 50-60 mW. The 6328A° line was used, and the spectra were calibrated by means of the neon lines.

Samples were ground to a fine powder and were transferred to glass capillary tubes, which were sealed by a flame.

(v) Diffuse Reflectance Spectra

The diffuse reflectance spectra of the solid complexes were measured from 250 mμ to 1200 mμ on a Beckman DU spectrophotometer equipped with a Beckman 2580 reflectance attachment. The samples were uniformly ground. The stainless steel cell used is shown in Fig. 18. The samples were contained in a depression and protected from the atmosphere by a quartz disc resting on a neoprene O-ring. Ground magnesium carbonate was used as a reference substance.

(vi) Mass Spectra

Mass spectra of some organic compounds were measured with a AEI MS902S model mass spectrometer.

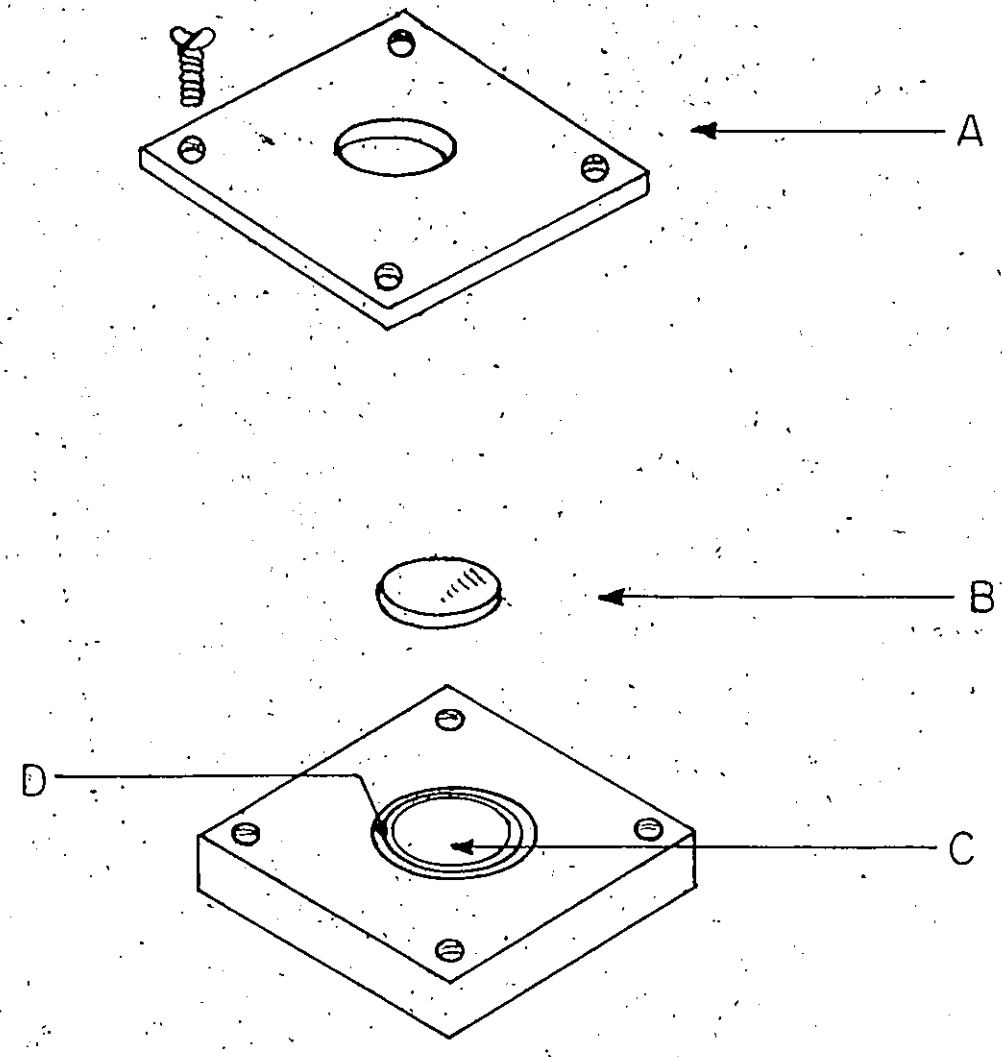

Fig. 18. Cell used for measurement of diffuse reflectance spectra.
A = cell cover
B = quartz window.
C = sample well
D = neoprene O-ring

3. ANALYTICAL TECHNIQUES

(i) General

Carbon, hydrogen and oxygen were determined by Schwarzkopf Microanalytical Laboratory, Woodside, N.Y. A few uranium compounds were analyzed for carbon and hydrogen by Galbraith Laboratories, Inc., Knoxville, Tenn. Determination of thorium and uranium were carried out by the author following a standard literature method (64-65).

(ii) Determination of Thorium and Uranium by Weighing as the Oxide (64-65)

Thorium was determined as the dioxide produced by direct ignition. Uranium was also determined in the same way as U_3O_8. Direct ignition was employed when the compounds were free of interfering elements, namely phosphorous and arsenic.

Procedure

A known weight of the sample (0.2-0.3 g) was put in a previously heated, cooled, and tared platinum crucible. It was heated slowly at the tip of a Bunsen burner until organic matter was destroyed. The crucible was finally heated in the full heat of a Meker burner to constant weight (±0.03 mg).

(iii) Determination of Uranium in Compounds Containing Phosphorous and Arsenic

A known weight of the sample (0.3-0.4 g) was dissolved in a minimum volume (ca. 60 mL) of methanol and treated with sufficient aqueous ammonia to ensure complete precipitation of

uranium hydroxide, $U(O)(OH)_4$. This was separated by filtration on a Whatman No. 41 paper. The precipitate was washed in succession with dilute ammonia solution and methanol. The precipitate was heated in a platinum crucible at the lowest temperature possible, without inflaming, until the carbonaceous matter was burned off. It was then heated strongly over a Meker burner to a constant weight of U_3O_8.

(iv) Determination of Chloride in $ThCl_4$ and UCl_4 by the Volhard Method (66-67)

A quantity (1-2 g) of sample was transferred into a 250 mL volumetric flask. The sample was dissolved in water to which three pellets of potassium hydroxide had been added. Aliquots (25 mL) were acidified with 2-3 mL of concentrated nitric acid and three 25 mL (pipette) portions of standard silver nitrate solution (ca. 0.1N) were added to each aliquot. This was followed by the addition of 2 mL ferric alum solution and 2 mL of chloride-free nitrobenzene. The mixture was shaken vigorously and the excess silver ion was titrated with standard KSCN solution (ca. 0.1N) until a permanent pale buff colour of $FeSCN^{2+}$ was attained.

(v) Determination of the Number of Active Oxygen Atoms in Peroxo Complexes of Uranium by Ce(IV) (68)

A known quantity of the sample (0.5-1.0 g) was dissolved in a minimum volume of methanol (ca. 100-150 mL) which was acidified with 25 mL of sulfuric acid (2N) and was followed by

the successive addition of three drops of osmic acid and one drop of ferroin as an indicator. It was then titrated against previously standardized ceric sulfate solution (ca. 0.1N) until there was transition from orange-red to very pale blue colour of the solution. As_2O_3 (0.1N) solution was used to standardize ceric sulfate solution.

(vi) Alkalimetric Titrations of Some Uranium Complexes with Sodium Hydroxide Solution

A known weight of the sample (0.8-1.5 g), dissolved in methanol (ca. 130-200 mL) was titrated with standard sodium hydroxide solution (0.1N). After each addition of 0.5 mL portions of sodium hydroxide solution, the pH of the solution was recorded with a Fisher Accumet Model pH meter.

CHAPTER 4

PREPARATIVE WORK

Introduction

In this chapter, the preparation of individual compounds and attempts to prepare specific compounds are described. In order to avoid unnecessary repetition, general procedures will be given for those cases where two or more compounds can be made similarly with just a variation of reagents. The various procedures or attempted preparations are indicated with numerals, the first of which is 4 and indicates Chapter 4. The first procedure, for example, is 4.1; the second one is 4.2; and so on.

Preparation of Schiff Bases

4.1 N-(2-Hydroxyphenyl)salicylidenimine (L)

A solution of 2-aminophenol (0.1 mol, 10.9 g) in a 1:1 mixture of benzene and ethanol (100 mL) was added to a solution of salicylaldehyde (0.1 mol, 12.2 g) in benzene (20 mL). The resulting mixture was boiled for 3 minutes and then cooled in an ice-salt bath whereupon bright reddish-yellow crystals formed. These were separated, washed several times with hot ethanol, and dried in vacuo over magnesium perchlorate; yield 16.1 g (75.6%). Recrystallization was from methanol. M.P. 185°C. Anal. Calcd. for $C_{13}H_{11}NO_2$: C, 73.23; H, 5.16. Found: C, 73.22; H, 5.16.

4.2 N-(2-Carboxyphenyl)salicylidenimine (L')

This was obtained when a solution of 2-aminobenzoic acid (0.1 mol, 13.7 g) in a 1:1 mixture of benzene and ethanol (100 mL) was added to a solution of salicylaldehyde (0.1 mol, 12.2 g) in benzene (20 mL). The resulting solution was heated on a steam bath for 5 minutes and then cooled in an ice-salt bath. Yellow crystals were separated and washed with benzene and ethanol; yield 17.0 g (70.5%). Recrystallization was from methanol. M.P. 206°C. Anal. Calcd. for $C_{14}H_{11}NO_3$: C, 69.70; H, 4.56. Found: C, 69.70; H, 4.55.

The structures of Schiff bases L and L' are shown in Fig. 19.

Thorium Complexes

4.3 Thorium Tetrachloride

ThO_2 used to prepare $ThCl_4$ was obtained by the thermal decomposition of $Th(NO_3)_4 \cdot 4H_2O$ (Fisher). $ThCl_4$ formed when CCl_4 vapour entrained in a stream of dry N_2 was passed over ThO_2 at 600°C for 3 h.

Procedure

Refer to Fig. 20. ThO_2 in a porcelain boat (K) was placed in quartz tube I (1.5 cm diameter), held in tube furnace J (2.5 cm diameter). The furnace was maintained at 600°C. Dried N_2 was bubbled through hot CCl_4. The vapour entrained in the stream of N_2 was passed over ThO_2 for 3 h (Fig. 20). The product was cooled under the N_2 flow and the quartz tube

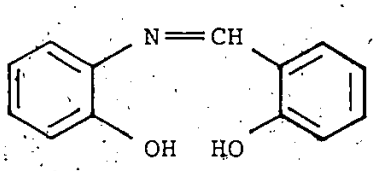

L

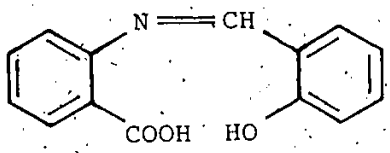

L'

Fig. 19. Structure of the Schiff bases L and L'.

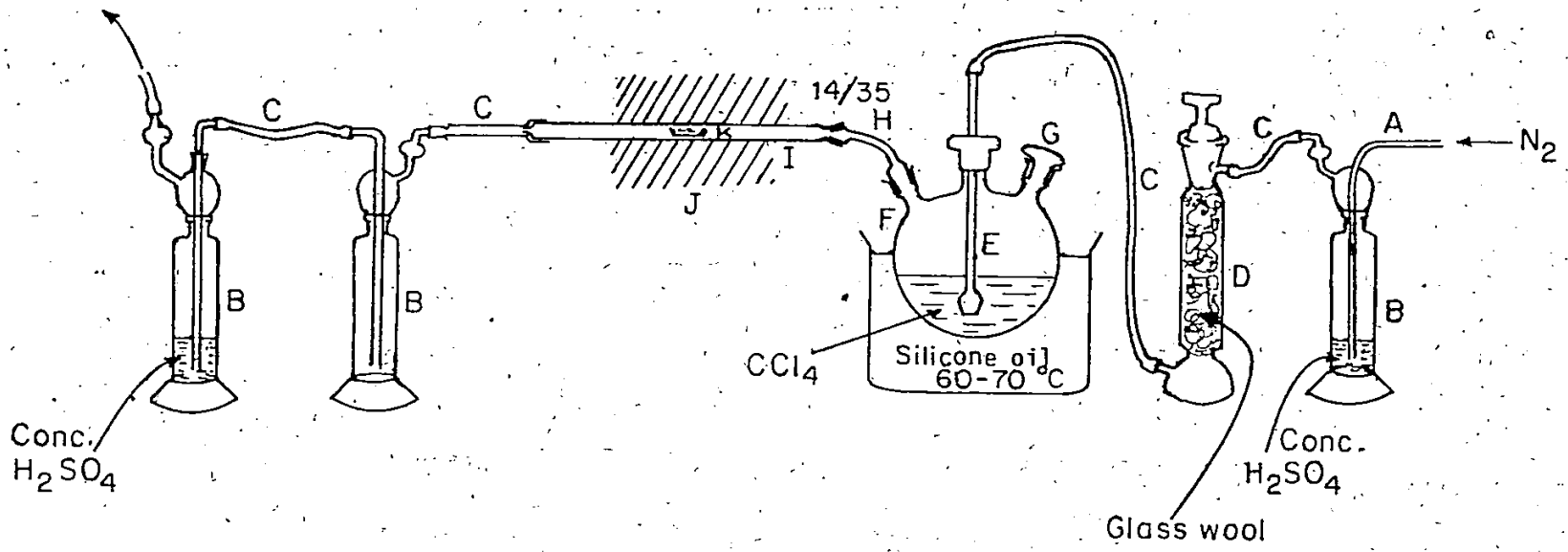

Fig. 20. Preparation of $ThCl_4$ or UCl_4.

Fig. 20. Apparatus for preparing MCl_4 (M=Th and U).

A	= nitrogen inlet
B	= Drechsel bottles
C	= rubber tubing
D	= gas drying tower
E	= bubbler, fritted glass tube
F	= 3 necked 250 mL round bottom flask
G	= glass stopper
H	= glass joint
I	= quartz tube
J	= tube furnace
K	= porcelain boat which holds substance in it

was stoppered at both ends and quickly transferred to a glove box where the substance was transferred into a glass ampoule system as shown in Fig. 16 and stored. Anal. Calcd. for $ThCl_4$: Cl, 37.93; Found: Cl, 36.37.

For the purpose of thermochemistry work, Section B of this thesis, vacuum sublimation of $ThCl_4$ in a platinum tube was desirable. The detailed procedure will be presented in Section B, which yields $ThCl_4$ of high purity.

Preparation of Complexes

The complexes and their element analyses are listed in Table 2, page 72.

4.4 Dichlorobis(pyridine-2-carboxylato)thorium(IV), $[Th(C_5H_4NCOO)_2Cl_2]$

Apparatus

A modified Schlenk tube, illustrated in Fig. 21, was used. The contents were stirred with a 1½ inch Teflon covered stirring bar magnet.

Procedure

The ground joints of the Schlenk tube and its stopper, S, were lightly greased with Apiezon Grease, N. The tube was connected to the vacuum line through stop-cock T_1. Stop-cock T_2 was closed, and stop-cock T_1 opened and the Schlenk tube was thoroughly evacuated while being flamed out. Stop-cock T_1 was closed and the Schlenk tube filled with dry oxygen-free nitrogen through stop-cock T_2.

As nitrogen was still passing through the system, $ThCl_4$ (4.45 g, 0.0119 mol) was suspended in 20 mL of acetonitrile in the Schlenk tube. A solution of the stoichiometric amount of picolinic acid, C_5H_4NCOOH (2.93 g, 0.0238 mol) in the same solvent (20 mL) was added to the suspension of $ThCl_4$. With the stop-cock T_1 closed and stop-cock T_2 open to the nitrogen line, the mixture was heated with a hot-water bath while stirring the mass vigorously for 3 minutes.

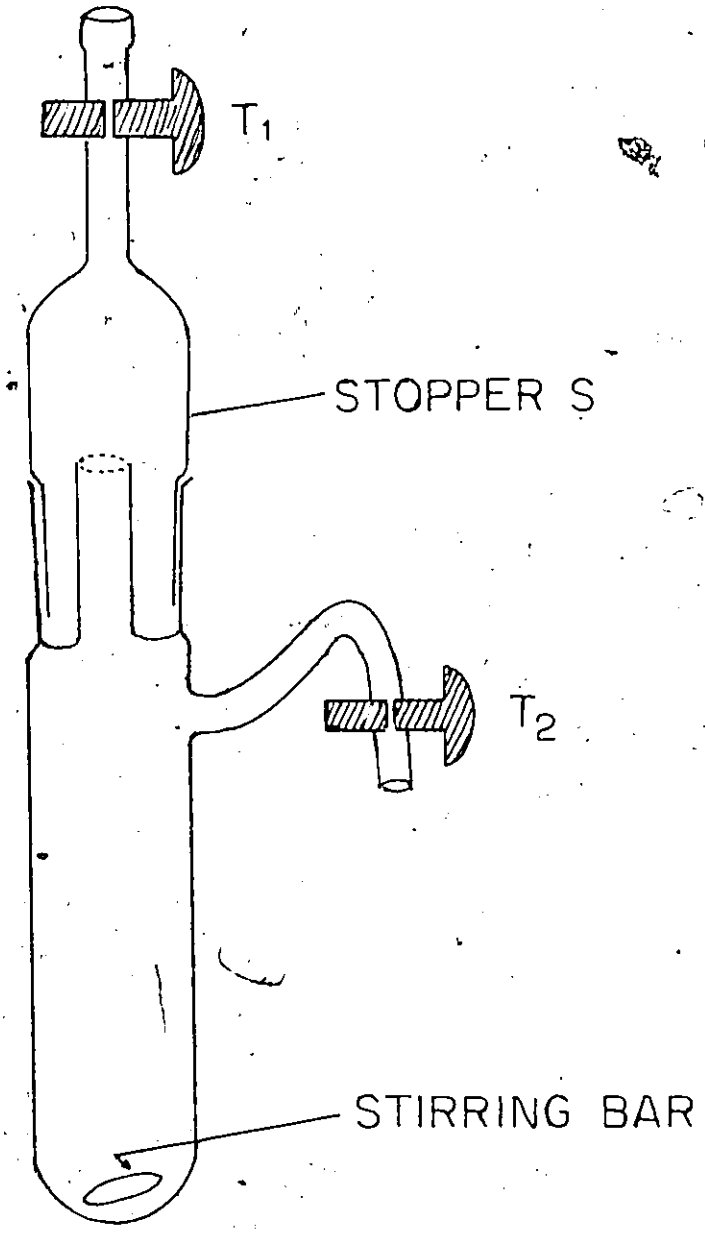

Fig. 21. A Schlenk tube, apparatus for preparation of $Th(C_5H_4NCOO)_2Cl_2$, $Th(C_6H_4NH_2COO)_2Cl_2$, $Th(C_6H_4NH_2O)_2Cl_2$, $Th(C_5H_3N(COO)2)2$, $Th(C_{14}H_9NO_3)_2$ and uranium(IV)-complexes.

Tube C in Fig. 14 was removed and the filtration apparatus fitted onto the Schlenk tube containing the thorium complex. The apparatus was inverted so that the reaction mixture was emptied into the space above the fritted glass in Tube B and filtered. The product was washed with a few mL of acetonitrile and dried in vacuum for a few minutes and the material was recrystallized from hot acetone using the apparatus shown in Fig. 22 as follows.

The apparatus, which was essentially a 500 mL flask converted into a Schlenk vessel, was put in place of tube A (Fig. 14) while the solid was on the frit B. The solid was dissolved in hot acetone and the solution filtered into the 500 mL flask, concentrated by pumping off half of the solvent. The solution was cooled and ether was added dropwise to induce recrystallization. A white solid product was isolated, dried, and stored in an ampoules system (Fig. 16). Elemental analysis showed that the product was $Th(C_5H_4NCOO)_2Cl_2$ (Table 2).

4.5 General Method of Complex Formation

The complexes, 2-5 (Table 2) were prepared by adding a stoichiometric quantity of the ligand in acetonitrile (25-50 mL) to about 3 g of $ThCl_4$ suspended in the same solvent (20 mL) as described for $Th(C_5H_4NCOO)_2Cl_2$. Recrystallization of the complexes from hot acetone was carried out in the similar way as described above.

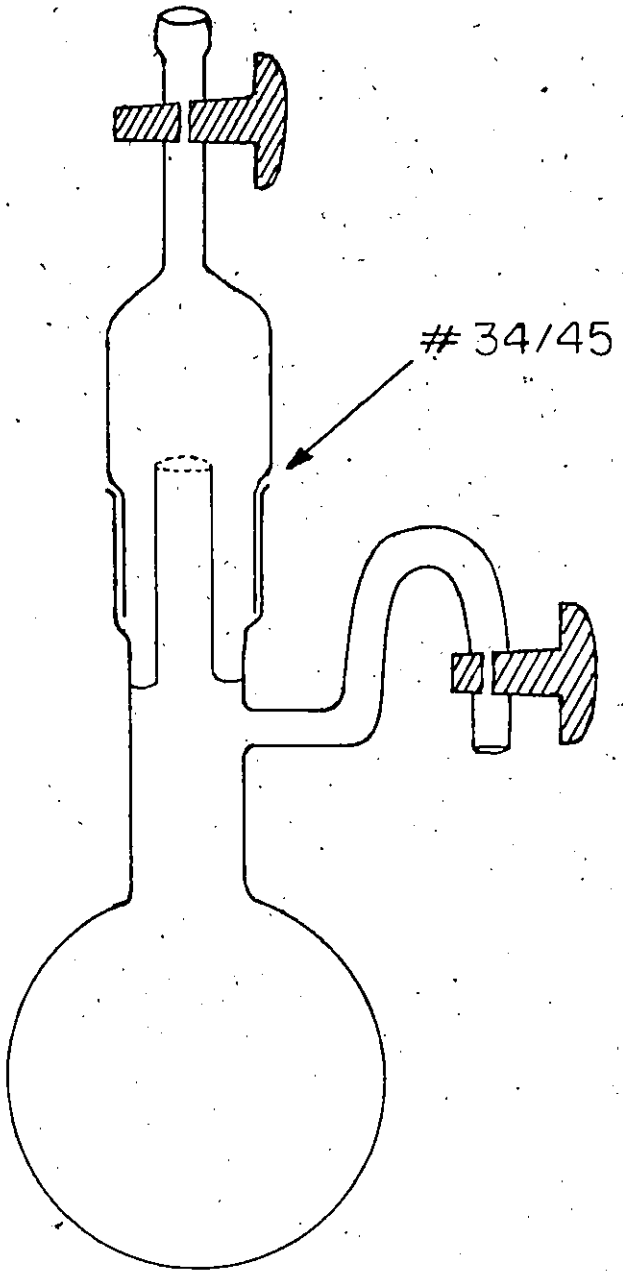

Fig. 22. Apparatus for crystallizing sparingly soluble air-sensitive compounds.

Peroxo Complexes of Thorium

4.6 Peroxobis(pyridine-2-carboxylato)thorium(IV), $[Th(C_5H_4NCOO)_2(O_2)]$

$Th(C_5H_4NCOO)_2Cl_2$ (2.5 g, 0.0045 mol), dissolved in 1:1 acetone and methanol (150 mL), was treated with 30% H_2O_2 (10 mL) in the presence of pyridine (0.5 mL). The resulting solution was boiled for 5 minutes and cooled. A precipitate of complex 6 was separated and washed with acetone and dried in vacuo. Yield: 1.95 g (85.3%).

4.7 Peroxobis(aniline-2-carboxylato)thorium(IV), $[Th(C_6H_4NH_2COO)_2(O_2)]$

The same procedure applied to 2.3 g (0.004 mol) of $Th(C_6H_4NH_2COO)_2Cl_2$ which gave 1.8 g of complex 7 (83.9% yield).

4.8 Peroxobis(2-aminophenylato)thorium(IV), $[Th(C_6H_4NH_2O)_2(O_2)]$

The analogous complex 8 was prepared similarly from 2.1 g (0.004 mol) of $Th(C_6H_4NH_2O)_2Cl_2$. Yield: 1.5 g (77.2%).

4.9 Peroxo(pyridine-2,6-dicarboxylato)thorium(IV) hydrate, $[Th(C_5H_3N(COO)_2)(O_2)H_2O]$

The same procedure was applied to 1.5 g of $Th(C_5H_3N(COO)_2)_2$ (0.0026 mol) and afforded 0.95 g (79.7% yield) of complex 9.

4.10 Peroxo(N-(2-carboxylatophenyl)salicylideniminato) thorium(IV) hydrate, $[Th(C_{14}H_9NO_3)(O_2)H_2O]$

By the same procedure, 1.3 g of complex 10 (68.1% yield) was obtained from 2.6 g (0.0037 mol) of $Th(C_{14}H_9NO_3)_2$.

Oxidation of Organic Substrates with Peroxo Complexes of Thorium

Unless otherwise specified, all oxidation reactions that employed peroxo complexes were carried out under a nitrogen atmosphere.

4.11 Reaction of 6 with Trans-Stilbene

Trans-Stilbene (1.56 g, 0.0086 mol) was added to a suspension of 6 (4.37 g, 0.0086 mol) in CH_2Cl_2 (30 mL). The mixture was stirred under reflux for 24 h after which the solution was filtered and the solvent evaporated. The residue was extracted with ether, and the extract was placed on a 25 g column of alumina (Shawinigan Chemicals; pH of aqueous slurry was 9.0). The material on the column was eluted with 250 mL of petroleum ether followed by 250 mL of benzene. A 1.1 g quantity of unreacted trans-stilbene was recovered from the petroleum ether fraction. Evaporation of the benzene solution yielded 0.49 g (97% yield based on conversion) of trans-stilbene oxide, m.p. 59-61°C (lit. m.p. 65-67°C) (22,69). Anal. Calcd. for $C_{14}H_{12}O$: C, 85.71; H, 6.12; O, 8.16. Found: C, 85.57; H, 6.06; O, 8.13.

4.12 Catalytic Reaction of 6 and H_2O_2 with Trans-Stilbene

A 0.96 g quantity (0.0053 mol) of trans-stilbene was added to 0.048 g of 6 suspended in 20 mL of dioxane and 20 mL of 30% H_2O_2. The mixture was heated under reflux at 90°C for 24 h. It was cooled and filtered, and the filtrate was evapo-

rated to dryness. The residue was extracted with ether and the extract was dried with Na_2SO_4 and evaporated to dryness. A yellow solid (0.93 g, 82.7% yield) was identified as benzoin by IR, NMR, and mass spectrometry as well as by elemental analysis; m.p. 137-138°C (lit. m.p. 134-136°C) (22,69). Anal. Calcd. for $C_{14}H_{12}O_2$: C, 79.24; H, 5.66; O, 15.09. Found: C, 79.38; H, 5.79; O, 15.23. No starting material was detected. The spectroscopic data are discussed in Chapter 5.

4.13 Catalytic Reaction of 6 and H_2O_2 with Trans-Stilbene in Presence of Acetic Acid

A 0.92 g quantity (0.0051 mol) of trans-stilbene was added to 0.053 g of compound 6 suspended in 15 mL of dioxane and 20 mL of 30% H_2O_2 and 2 mL of glacial acetic acid were added. The reaction mixture was heated under reflux at 90°C for 20 h. It was cooled, filtered and the filtrate evaporated to dryness. The residue was extracted with ether, and the extract was dried with Na_2SO_4 and evaporated to dryness. A yellow solid was isolated (0.90 g, 83.3% yield) which was identified as benzoin in the similar way as mentioned in Section 4.12.

4.14 Attempted Reaction of Trans-Stilbene with H_2O_2

Trans-stilbene (1.4 g) was dissolved in 30 mL of dioxane to which 25 mL of 30% H_2O_2 was added. The mixture was heated under reflux at 90°C for 24 h; no reaction was found to occur.

4.15 Reaction of Trans-Stilbene Oxide with H_2O_2

Trans-stilbene oxide (1.0 g, 0.0055 mol) was dissolved in 10 mL of dioxane to which 15 mL of 30% H_2O_2 was added. The mixture was heated under reflux at 85°C for 20 h. The solution was concentrated in a rotary evaporator to a yellow oil which was extracted with ether and dried by Na_2SO_4. Solvents were removed under high vacuum and the oil was placed on a 25 g column of silica gel (Baker Analyzed Reagent, 60-200 Mesh) and eluted with ether:hexane (5:5). Three fractions were collected. Evaporation of the first fraction gave 0.41 g of unreacted trans-stilbene oxide, evaporation of other two fractions produced benzoin (0.35 g, 32.4% yield) and diol, 1,2-dihydroxy-1,2-diphenyl ethane, $C_{14}H_{14}O_2$ (0.16 g, 14% yield), m.p. 146-148°C (lit. value 149-150°C) (69) respectively.

4.16 Reaction of 7 with Allyl Alcohol

Compound 7 (2.5 g, 0.0047 mol) was suspended in 8 mL of tetrahydrofuran, and the stoichiometric amount of allyl alcohol was added. The mixture was stirred under reflux at 60°C for 36 h. Microdistillation under ca. 20 mm Hg pressure yielded the epoxide (glycidol) as a high-boiling fraction (149-153°C) (0.12 g, ca. 35 % yield). The glycidol was identified from its boiling point and its ^1H NMR spectrum.

4.17 Catalytic Reaction of 7 and H_2O_2 with Allyl Alcohol

A 20 mL quantity of allyl alcohol (17.04 g, 0.294 mol) was dissolved in 20 mL of dioxane, and 0.91 g of 7 was added

followed by 20 mL of 30% H_2O_2. The mixture was kept under reflux at 90°C for 20 h. The reaction mixture was filtered and the filtrate distilled at 20 mm Hg pressure until the oil-bath temperature reached 210°C. Continued distillation at 0.002 mm Hg pressure yielded a product at 130-135°C that was identified as glycerol (12.0 g, 44.3% yield). In a second attempt, a yield of 49.3% was obtained.

Uranium Complexes

4.18 Uranium Tetrachloride

U_3O_8 used to prepare UCl_4 was obtained by the thermal decomposition of $UO_2(NO_3)_2{\cdot}6H_2O$ (Baker Analyzed Reagent). UCl_4 formed when CCl_4 vapour entrained in a stream of dry N_2 was passed over U_3O_8 in a quartz tube held at 500°C for 2.5 h (see Fig. 20). At the temperature of the reaction, UCl_4 was found to have partially sublimed to the cooler zone of the quartz tube.

Procedure

The procedure for preparing and storing the sample is the same as outlined in Section 4.3. Anal. Calcd. for UCl_4: Cl, 37.33. Found, Cl, 36.75.

Preparation of Complexes

The complexes and their elemental analyses are listed in Table 6, page 99.

4.19 Tetrachlorobis(pyridine-N-oxide)uranium(IV), $[UCl_4{\cdot}2ONC_5H_5]$

UCl_4 (1.5 g, 0.0039 mol) was dissolved in acetone (15 mL) in a Schlenk tube (Fig. 21) to which a solution of ONC_5H_5

(0.74 g, 0.0078 mol) in the same solvent (15 mL) was added. About one-third of the solvent was pumped off whereupon green crystals appeared. These were separated with the filtering apparatus shown in Fig. 14, washed with acetone and stored in the same way as described in Section 4.4.

4.20 General Method of Complex Formation

The U(IV) complexes, 12-19 (Table 6), were prepared by adding of a stoichiometric quantity of the ligand in acetone (15-60 mL) to about 2 g of UCl_4 dissolved in the same solvent (15 mL) as described in Section 4.4.

Peroxo Complexes of Uranium

4.21 Oxodiperoxobis(pyridine-N-oxide)uranium(VI) hydrate, $[U(O)(O_2)_2 2ONC_5H_5]H_2O$

Compound 11, $UCl_4 \cdot 2ONC_5H_5$ (2.1 g, 0.0036 mol) was moistened successively with acetone and H_2O_2 (50%) and warmed. A yellow product which formed was washed successively with hot water, acetone and finally with n-hexane. The product was dried in vacuo over P_2O_5. Yield 1.3 g (67.0%).

4.22 Oxodiperoxobis(triphenylphosphine oxide)uranium(VI) hydrate $[U(O)(O_2)_2 2OPPh_3]H_2O$

The same procedure applied to $UCl_4 \cdot 2OPPh_3$ (1.95 g, 0.0021 mol) afforded 1.4 g of the complex 21 (75.3% yield).

4.23 Oxodiperoxobis(triphenylarsine oxide)uranium(VI) hydrate $[U(O)(O_2)_2 2OAsPh_3]H_2O$

The analogous complex 22 was prepared similarly from $UCl_4 \cdot 2OAsPh_3$ (2.2 g, 0.0021 mol) which gave 1.7 g of complex 22 (80.7% yield).

4.24 Oxomonoperoxo(pyridine-2,6-dicarboxylato)uranium(VI) hydrate, $[U(O)(O_2)C_5H_3N(COO)_2H_2O]$

$U(C_5H_3N(COO)_2)_2$ (1.5 g, 0.0026 mol) was dissolved in methanol (75 mL) to which 50 % H_2O_2 (10 mL) was added. The solution was heated to expel two-thirds of the solvent whereupon a yellow precipitate formed. The product was separated, washed with hot acetone followed by n-hexane, and dried in vacuo over P_2O_5. Yield 1.0 g (80.8%).

4.25 Hydrogen dioxomonoperoxo(2-aminophenylato)uranium(VI) hydrate, $H^+[U(O)_2(O_2)(C_6H_4NH_2O)H_2O]^-$

$U(C_6H_4NH_2O)_2Cl_2H_2O$ (1.4 g; 0.0032 mol) was dissolved in a 1:1 mixture of acetone and methanol (50 mL) and treated with 50% H_2O_2 (10 mL) solution. The mixture was cooled to 0°C whereupon a yellow precipitate appeared. This was separated and washed successively with water and acetone. The product was stored at -20°C. Yield 1.1 g (79.6%).

4.26 Hydrogen dioxomonoperoxo(pyridine-2-carboxylato) uranium(VI) hydrate, $H^+[U(O)_2(O_2)(C_5H_4NCOO)H_2O]^-$

$U(C_5H_4NCOO)_2Cl_2C_5H_4NCOOH$ (2.0 g, 0.0029 mol) dissolved in a 1:1 mixture of acetone and methanol (60 mL) was treated with 50% H_2O_2 (10 mL) solution. The mixture was boiled for 2 minutes and cooled to room temperature whereupon a muddy yellow product formed. This was separated and washed successively with water, acetone and n-hexane. It was dried in vacuo over P_2O_5. Yield 0.95 g (72.5%).

Complexes 26 and 27 (Table 6) were prepared in the same way as described in 4.26. Further details follow.

4.27 Hydrogen dioxomonoperoxo(aniline-2-carboxylato) uranium(VI) hydrate, $H^+[U(O)_2(O_2)(C_6H_4NH_2COO)H_2O]^-$

2.1 g of $U(C_6H_4NH_2COO)_2Cl_2C_6H_4NH_2COOH$ (0.0029 mol) afforded 0.94 g of the peroxo complex 26 (Table 6). Yield 70.3%.

4.28 Oxomonoperoxo(N-(2-carboxylatophenyl)salicylideniminato) uranium(VI) hydrate, $[U(O)(O_2)(C_{14}H_9NO_3)H_2O]$

1.5 g of the U(IV)-complex, $U(C_{14}H_9NO_3)_2$ (0.0021 mol) yielded 0.72 g of the peroxo complex 27 (Table 6) (63.3% yield).

Oxidation of Organic Substrates with Peroxo Complexes of Uranium

4.29 Reaction of 26 with trans-stilbene

Trans-stilbene (1.2 g, 0.0066 mol) was added to a suspension of 26 (3.0 g, 0.0066 mol) in tetrahydrofuran (20 mL). The mixture was stirred under reflux for 24 h after which the solution was filtered and the solvent evaporated. The residue was extracted with ether and evaporated to dryness. The substance was placed on a 25 g column of silica gel (Baker Analyzed Reagent, 60-200 Mesh) and eluted with ether:benzene (5:5). Evaporation of the first fraction produced unreacted trans-stilbene (0.85 g), the other two fractions produced trans-stilbene oxide (yield 0.29 g; 76.1% based on conversion), m.p. 61-62°C (lit. m.p. 65-67°C) (22,69) and 2-aminobenzoic acid (0.2 g), m.p. 143-145°C (lit. m.p. 144-146°C) (69).

4.30 Reaction of 26 with trans-stilbene in presence of H_2O_2

A 1.0 g quantity (0.0055 mol) of trans-stilbene dissolved in 20 mL of dioxane was added to 2.5 g (0.0055 mol) of complex 26 suspended in 15 mL of dioxane and 15 mL of 30% H_2O_2. The reaction mixture was kept under reflux at 90°C for 24 h when it was filtered and the filtrate was evaporated to dryness. The residue was extracted with ether and the extract was placed on a 25 g column of silica gel (Baker Analyzed Reagent, 60-200 Mesh) and eluted with ether:benzene (5:5) mixture. Evaporation of the first fraction gave unreacted trans-stilbene (0.35 g) and the other two fractions produced benzoin (0.55 g, 77.7% yield based on conversion), m.p. 133-135°C (lit. m.p. 134-136°C) (69) and 2-aminobenzoic acid (0.35 g), m.p. 142-145°C, respectively.

4.31 Reaction of 25 with allyl alcohol

4.4 g of 25 was added to a large excess of allyl alcohol (25 mL) and refluxed for 20 h at 80°C. The reaction mixture was subsequently cooled to -78°C for 1 h. Formation of epoxide was monitored by thin layer chromatography (TLC) and proton NMR of the reaction product.

4.32 Attempted reaction of 23 and t-butylhydroperoxide with 2-methylcyclohexanone

A 2 g quantity of compound 23 was suspended in 2-methylcyclohexanone (15 mL) and the mixture was refluxed at 120°C for 36 h. Monitoring by TLC and NMR revealed no indication of reaction.

A further attempt to oxidize the ketone was made by adding 5 mL of $(CH_3)_3COOH$ to the reaction mixture which was refluxed for a further 48 h at 120°C. Again, the TLC and NMR results suggested that there had been no reaction; the unaltered peroxo complex was quantitatively recovered.

4.33 Attempted reaction of 20-22 and 25 with cyclohexene or cyclooctene

Typically 0.0006 mol of the complexes 20-22 and 25 were suspended in mesitylene and stoichiometric quantity of cyclohexene or cyclooctene was added. Refluxing for 36 h failed to produce a reaction.

CHAPTER 5

RESULTS AND DISCUSSION

Thorium Complexes

The elemental analyses along with molar conductance values of the thorium complexes are given in Table 2.

Complexes 1-5

These compounds, which served as precursors of the peroxo complexes, were prepared from the reaction of $ThCl_4$ with the stoichiometric amount of an organic ligand in acetonitrile. These intermediate complexes were soluble in all of the polar solvents tried, e.g., acetone, methanol, DMSO, etc.

The analytical and molar conductance data were consistent with six-fold coordination of the thorium atom (Table 2) in compounds with the general empirical formulae, ThL_2Cl_2 and ThL'_2, where L and L' are the bidentate, uninegative and tridentate, dinegative ligands, respectively. The electrical conductivities of $5x10^{-4}$ M solutions of complexes in DMSO (Table 2) indicate that compounds 4 and 5 are nonelectrolytes, hence, the compounds can be formulated as $[ThL'_2]$, but 1-3 exhibited conductance values intermediate between those typical of 1:1 and 2:1 electrolytes. By comparison, the 2:1 electrolytes $UO_2(NO_3)_2 6H_2O$ and $MgCl_2 6H_2O$ gave values of 60.0 and 60.6 Ω^{-1} cm^2 mol^{-1}, respectively at a concentration of $5x10^{-4}$ mol L^{-1}. Also potassium iodide at the same concentration exhibited a

Table 2. Analytical data and other physical properties of the Th(IV) complexes.

No.	Compound	% Th		% C		% H		Molar Conductance $ohm^{-1}cm^2mol^{-1}$
		Calcd.	Found	Calcd.	Found	Calcd.	Found	
1	$[Th(C_5H_4NCOO)_2Cl_2]$	42.49	42.61	26.37	26.42	1.46	1.45	43.05
2	$[Th(C_6H_4NH_2COO)_2Cl_2]$	40.41	39.96	29.26	29.22	2.09	2.11	48.0
3	$[Th(C_6H_4NH_2O)_2Cl_2]$	44.78	44.83	27.79	27.74	2.31	2.33	45.5
4	$[Th(C_5H_3N(COO)_2)_2]$	41.28	41.35	29.89	29.78	1.06	1.06	7.8
5	$[Th(C_{14}H_9NO_3)_2]$	32.67	32.71	47.32	47.53	2.53	2.55	3.3
6	$[Th(C_5H_4NCOO)_2(O_2)]$	45.66	45.79	28.34	28.52	1.57	1.59	0.60
7	$[Th(C_6H_4NH_2COO)_2(O_2)]$	43.28	43.36	31.34	31.45	2.23	2.23	4.40
8	$[Th(C_6H_4NH_2O)_2(O)_2]$	48.33	48.35	30.00	30.18	2.50	2.52	3.04
9	$[Th(C_5H_3N(COO)_2)(O_2)H_2O]$	51.90	51.98	18.79	18.87	1.11	1.21	0.22
10	$[Th(C_{14}H_9NO_3)(O_2)H_2O]$	44.52	44.81	32.24	32.35	2.11	2.16	1.5

* The values are for 5×10^{-4} M solutions of the complexes in DMSO.

The organic moieties are as follows:

Compounds 1 and 6: 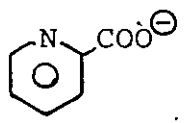

Compounds 2 and 7: 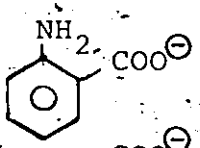

Compounds 3 and 8: 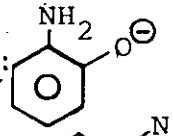

Compounds 4 and 9: 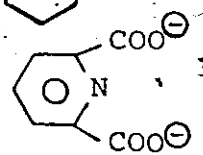

Compounds 5 and 10: 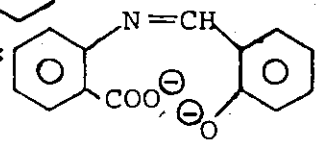

value of 29.7 Ω^{-1} cm^2 mol^{-1}. Literature values of molar conductance for 2:1 and 1:1 electrolytes in DMSO are ~60 and ~35 Ω^{-1} cm^2 mol^{-1} respectively (70-71), comparable to ours. It is suggested that the conductivity of solutions of 1-3 arises by displacement of chloride ion from the coordination sphere as shown:

$$[ThL_2Cl_2] + DMSO = [ThL_2ClDMSO]^+ + Cl^- \quad [30]$$

$$[ThL_2ClDMSO]^+ + DMSO = [ThL_2(DMSO)_2]^{2+} + Cl^- \quad [31]$$

where L refers to the bidentate, uninegative ligands, $C_5H_4NCOO^-$, $C_6H_4NH_2COO^-$ and $C_6H_4NH_2O^-$, respectively (Table 2).

In order to understand the electrolytic behaviour of complexes 1-3 in DMSO, conductivities were measured at different molar concentrations. Plots of molar conductivities against (concentration)$^{\frac{1}{2}}$ (Fig. 23) show that the molar conductivities decrease with increasing concentration and approach values typical of 1:1 electrolytes at the upper end of the concentration range. The ^{13}C NMR spectrum of 1 (Table 5) indicated that the picolinato ligand is not displaced in DMSO solution; therefore the conductivity arises from ionization of chloride rather than the organic group.

The infrared spectra of the chloro complexes (Table 3) display strong bands at 220-250 cm^{-1}, which we assign to Th-Cl stretching (72-74). Therefore, the solid-state formulations for 1-3 were evidently $[ThL_2Cl_2]$. The organic ligands

Fig. 23. Plot of molar conductivities vs (concentration)$^{\frac{1}{2}}$ in DMSO solutions.

(A) $[Th(C_6H_4NH_2COO)_2Cl_2]$

(B) $[Th(C_6H_4NH_2O)_2Cl_2]$

(C) $[Th(C_5H_4NCOO)_2Cl_2]$

(D) KI.

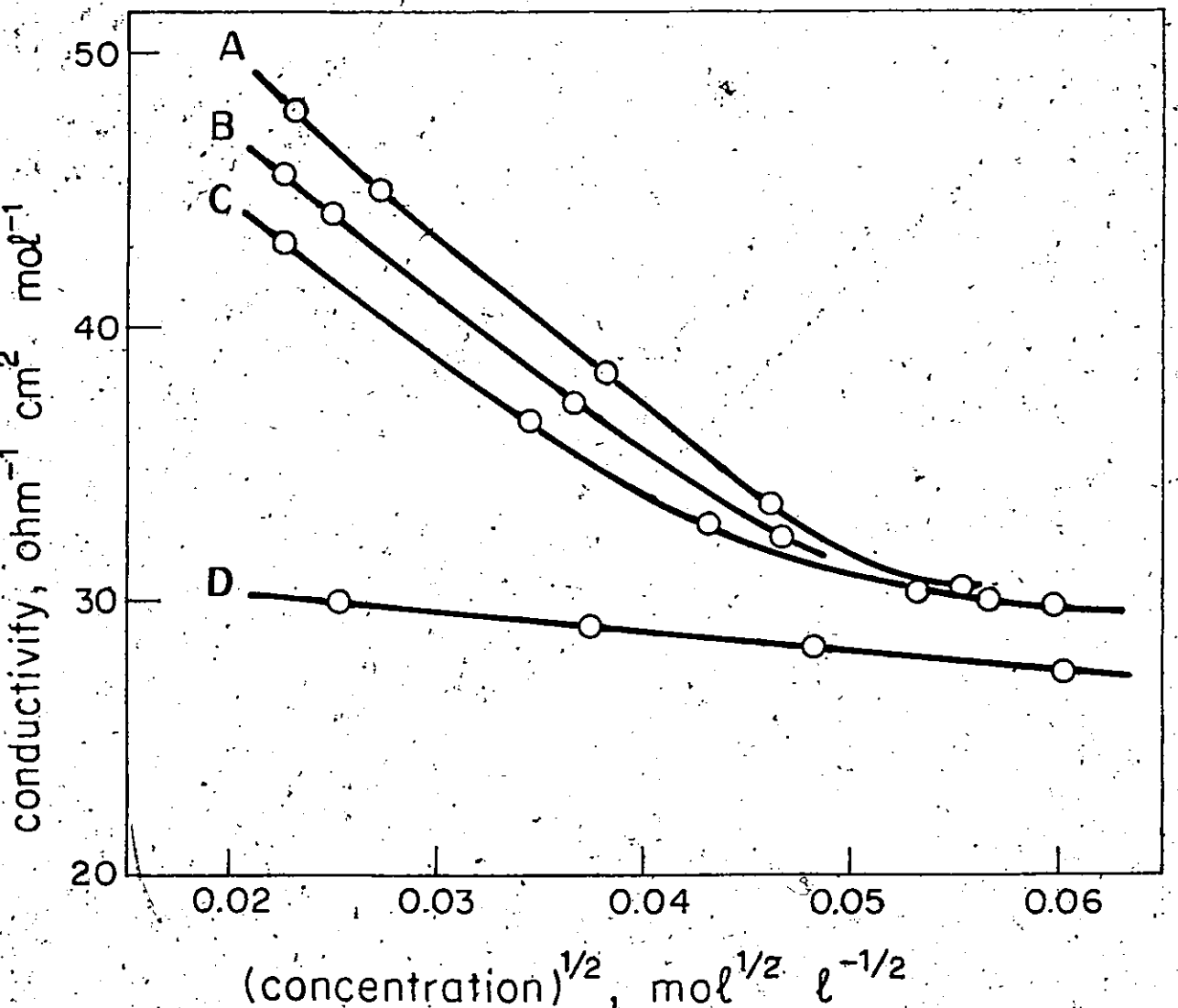
A
B
C
D
50
40
30
20
0.02
0.03
0.04
0.05
0.06
conductivity, ohm^{-1} cm^2 mol^{-1}
(concentration)$^{1/2}$, mol$^{1/2}$ $\ell^{-1/2}$

reveal characteristic frequencies that confirm their expected bi- and tridentate character. In 1, the ν(C=O) appears at 1655 cm^{-1} (Table 3), 70 cm^{-1} lower than the free ligand value (Table 4). This indicates coordination by the oxygen of the carboxylic group of the picolinato ligand. Complexes 2 and 3 show two medium intensity bands due to ν(N-H) at (2, 3170 and 3100; 3, 3230 and 3150 cm^{-1} (Table 3) - significantly lower in frequency than the corresponding bands of the free ligands, 2-aminobenzoic acid and 2-aminophenol respectively (Table 4). This indicates coordination by amino nitrogen of the ligands. Similarly, ν(C=O) bands in 2, 4 and 5 have frequencies 50-70 cm^{-1} lower than the free ligand values. This shows that the carboxylato groups are coordinated to the metal atom in each case.

The Schiff bases behaved as tridentate, dinegative ligands coordinating at the imino nitrogen and two oxygen atoms. The assignments shown in Tables 4 and 3 are based on comparisons with related compounds (75-77). In complex 5, the decrease in ν(C=N) by 25 cm^{-1} relative to the frequency for the free Schiff base indicates that the imino nitrogen is coordinated to the metal atom (78). The ν(O-H) band at 3120 cm^{-1}, observed in the Schiff base, disappears upon coordination, which indicates that there is deprotonation and coordination at the oxygen site.

Table 3. Infrared and Raman spectral data for the Th(IV) complexes*. Band maxima, cm^{-1}.

Comp. No.	ν(O-H)	ν(N-H)	ν(C=O)	ν(C=N)	ν_1(O-O)	ν(Th-O)	ν(Th-N)	ν(Th-Cl)
1			1655 vs.			396 sh.	350 s.	225 vs.
2		3170 ms. 3100 m.	1615 s.			388 vs.	335 ms.	250 sh.
3		3230 m. 3150 m.				390 vs.	325 s.	220 vs.
4			1600 s.			400 s.	325 ms.	
5			1650 br.	1600 ms.		392 s.	330 s.	
6			1650 br.		822 br.			
7		3125 ms. 3090 m.	1590 br.		820 s.			
8		3200 w. 3110 ms.			825 ms.			
9	3400 br.		1650 s.		840 ms.			
10	3405 br.		1645 s.	1600 m.	825 br.			

* Relative band intensities are denoted by vs, ms, s, m, w, br, sh, meaning very strong, medium strong, strong, medium, weak, broad and shoulder, respectively.

Table 4. Characteristic infrared spectral data for the ligands[a]; band maxima, cm^{-1}.

Compound	ν(O-H)	ν(N-H)	ν(C=O)	ν(C=N)
pyridine-2-carboxylic acid			1725 vs.	
pyridine-2,6-dicarboxylic acid			1710 vs.	
2-aminobenzoic acid		3390 s. 3300 s.	1680 vs.	
2-aminophenol		3414 s. 3342 s.		
N-(2-hydroxyphenyl) Salicylidenimine, (L)	3290 br.			1640 ms.
N-(2-Carboxyphehyl) Salicylidenimine, (L')	3120	1700 br.		1625 ms.

a Relative band intensities are denoted by vs, ms, s, br, meaning very strong, medium strong, strong and broad, respectively.

Further, the far infrared spectra of the complexes indicate the presence of Th-O and Th-N bonds. In complexes 1-5, these give rise to bands at 388-400 (Th-O) and 325-350 cm^{-1} (Th-N) (79-81), data which also support the multidentate nature of the organic ligands.

In order to obtain additional information on the mode of coordination of the substituted pyridines, we obtained ^{13}C NMR spectra with solutions of 1 and 4 and their peroxo analogues, (compounds 6 and 9) in DMSO-d_6 (Table 5). These afforded comparisons with an analogous uranium compound (see uranium section) and several pyridine complexes (82).

Assignments were based in part upon the proton couplings in off-resonance spectra and in part upon a consideration of nuclear Overhauser enhancement (NOE). There is no ambiguity in the assignment of different carbon signals. Signals of the substituted ring carbon in position 2 of picolinic acid are less intense than for position 6 (Fig. 24), where the substituent is hydrogen. One is led to conclude that the assignment of the spectrum by Jacobson et al. (46) is incorrect, the bands for carbons in positions 2 and 6 having been reversed. We agree with the assignments reported by Moore et al. (83).

The resonance of the carboxylic carbon, C-7, is far downfield from all other resonances and is marked by a low intensity that is expected from the lack of NOE enhancement. Amongst the ring carbons, C-2 and C-6 appear downfield compared

Table 5. Chemical shift[a], relative to Me_4Si in ^{13}C NMR of some Th(IV) complexes.

Compound	Ring Carbons					Carboxylic Carbons	
	C-2	C-3	C-4	C-5	C-6	C-7	C-8
Pyridine-2-carboxylic acid	148.3	124.8	137.8	127.2	149.4	166.3	
1	151.0	124.3	139.0	126.8	148.3	169.2	
6	150.8	124.4	138.6	126.7	147.8	169.3	
Pyridine-2,6-dicarboxylic acid	148.0	127.7	139.4	127.7	148.0	165.5	165.5
4	150.5[b]	125.8	142.0	125.8	149.9[b]	170.4[b]	170.0
9	150.2[b]	125.6	141.7	125.6	149.6[b]	170.1[b]	169.8

a ppm downfield relative to TMS as internal standard.

b The assignment of these narrow doublets to C-2 and C-6 or to C-7 and C-8, respectively, is arbitrary. A reversed assignment is equally likely.

to the other ring carbons because of electron density depletion from these two positions owing to the presence of nitrogen and the carboxylic group. The signals due to C-2 and C-6 should not be confused, C-6 carries a hydrogen atom while C-2 does not. NOE enhancement clearly identifies C-6. Moreover, in the off-resonance spectrum (Fig. 24b), C-6 is a clear doublet while C-2 is only slightly split probably by long range coupling. Further, it has also been suggested that due to the carboxylic group, the bond order between N-1 and C-2 is lower than that between N-1 and C-6 which causes a slight upfield shift of C-2 (84-85). It should be pointed out, however, that this theory of chemical shifts is not universally accepted (86).

The C-4 resonance is influenced by the inductive effect of the nitrogen heteroatom. The C-3 and C-5 resonances occur at upmost field. The higher field band was attributed to C-3 on the basis of off-resonance ^{1}H decoupling (83). The relative positions of the C-3 and C-5 resonances are governed by the carboxylic group which causes the order of the C-2-C-3 bond to be less than that of the C-4-C-5 or C-5-C-6. Apparently, this effect is caused by polarization of electron density from C-2 toward the carboxylic group which in turn causes a polarization of the density from C-3. Presumably, this is compensated in part by a shift in density toward C-3 from C-4. The net effect is anisotropic with respect to C-3 (82,85). This effect would be significantly smaller for C-5 which is remote from the

carboxylic group or the hetero atom. In the off-resonance spectrum, C-4, C-3 and C-5, all appear as clear doublets.

Upon coordination with thorium, there are significant shifts of all the carbon resonances other than those for the atoms in positions 3 and 5 of the ligand, picolinic acid. The C-3 and C-5 resonances in the complexes appear slightly upfield compared to the free ligand values (Table 5). Paramagnetic anisotropy attributable to the metal is a major influence in causing upfield shifting. Upon coordination through nitrogen of the ring and the carboxylato group of the picolinato ligand, there will presumably be an anisotropic effect with respect to C-3 and C-5 which causes upfield shifting for these two carbons. It can be seen from Table 5 that the resonances for the C-2 carbons in the complexes are only slightly downfield from the values for the free ligand. Lavallee et al.(82) pointed out that the shifts of the C-2 resonances in coordinated pyridines are governed by factors that are poorly understood. On the other hand, the carboxylic carbon resonances are shifted considerably farther downfield. The C-4 resonance in complex 1 displays a downfield shift of 1.2 ppm with respect to the free ligand. This obviously arises because of the inductive effect originating at the nitrogen atom is strengthened upon coordination to the metal. These results indicate that the picolinato ligand is bidentate and is not dissociated in DMSO. The ^{13}C NMR spectrum of compound 1 is shown in Fig. 25.

The ^{13}C NMR spectra of pyridine-2,6-dicarboxylic acid (Fig. 26) were rather straightforward. The resonance of the carboxylic carbons (C-7 and C-8) is far downfield from all other resonances. A singlet resonance band of C-2 and C-6 appears downfield compared to the other ring carbons. The band due to C-3 and C-5 occurs at upmost field as a singlet. The relative positions of the different ring carbon resonances are probably governed by the inductive effect of the nitrogen hetero atom. The off-resonance proton decoupled spectrum of pyridine-2,6-dicarboxylic acid (Fig. 26b) reveals the influence of C-H coupling on C-4, C-3 and C-5.

In the ^{13}C NMR spectra of the complexes containing pyridine-2,6-dicarboxylic acid, there is evidently a small difference between the 2- and 6-carbons and also the 7- and 8-carbons. This could arise if the complex lacks a plane of symmetry. This would be the case if the nitrogen atoms of the two ligands were in a mutually cis-arrangement. Alternatively, there may be coordination by a solvent molecule in two different orientations. The direction of changes are analogous to those of picolinato complexes but in complex 4 (Fig. 27), it is interesting to note that the C-4 and carboxylic carbon resonances display much stronger downfield shifts of 2.6 and 4.5-4.9 ppm respectively, compared to the free ligand values.

The C-4 position is the least influenced by magnetic anisotropy; therefore changes in the chemical shifts of the C-4

resonances are believed to be due to inductive effect through the nitrogen hetero atom for coordination to the metal. The downfield shift of the C-4 resonances in complexes 1 and 4 shown in Table 5 are 1.2 and 2.6 ppm respectively, from the free ligand values. These are much smaller shifts than the corresponding shift reported by Lavallee et al. for pyridine complexes of Co(III) and Rh(III) (82). The C-4 resonances in the pyridine complexes of Co(III) and Rh(III) appear at 5.2 and 4.4 ppm downfield from the C-4 resonance of pyridine itself. This indicates that the electron density depletion from the heterocyclic ring towards the metals is in the order Co(III)> Rh(III)>>Th(IV). The present data on Th(IV)-complexes refer to solutions in DMSO while Lavallee et al. employed D_2O as solvents, and although there is a solvent effect, particularly with the free ligands, the effect is small compared to that of complexing. It may be concluded that Th(IV) is a significantly weaker acceptor than the smaller trivalent ions.

The ^{13}C NMR data of complex 4 are consistent with the conductivity data for a fully covalent structure of the complex. This again reveals the tridentate nature of the pyridine-2, 6-dicarboxylic acid.

The proton spectra failed to reveal splitting, but the hydrogen atoms are rather remote from the first coordination sphere and are presumably not much influenced by the point symmetry at the thorium atom.

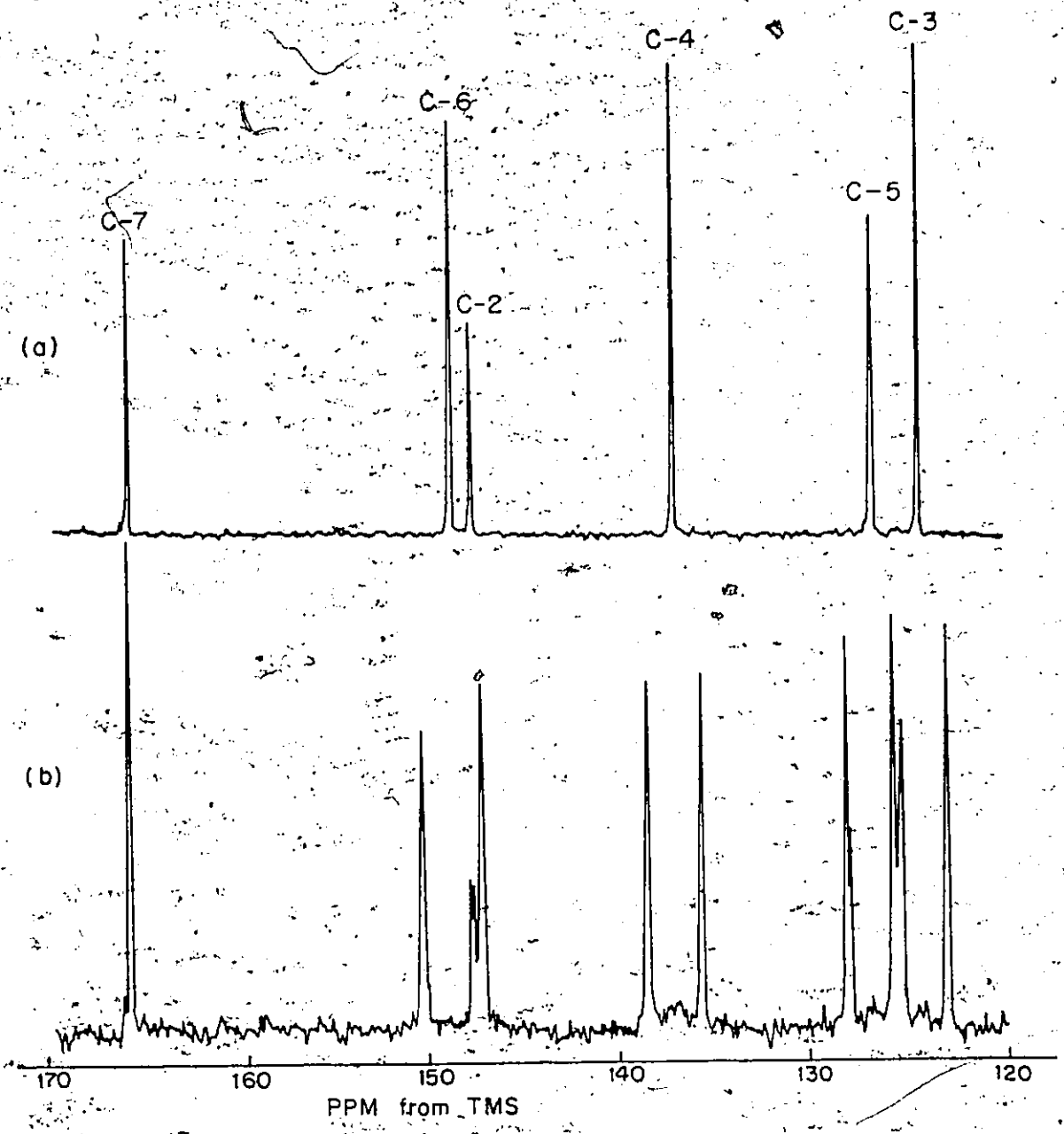

Fig. 24. ^{13}C NMR spectra of picolinic acid in DMSO-d_6.

(a) proton spin decoupled.

(b) single frequency off resonance proton spin decoupled.

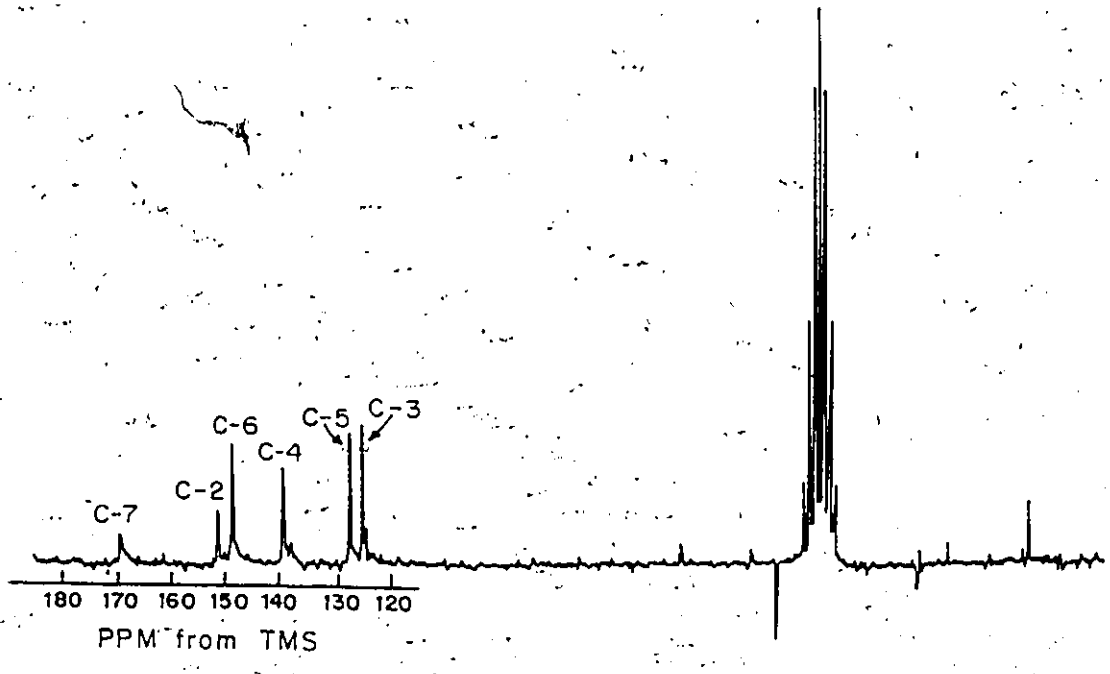

Fig. 25. ^{13}C NMR spectrum of $Th(C_5H_4NCOO)_2Cl_2$ in DMSO-d_6 (proton spin decoupled).

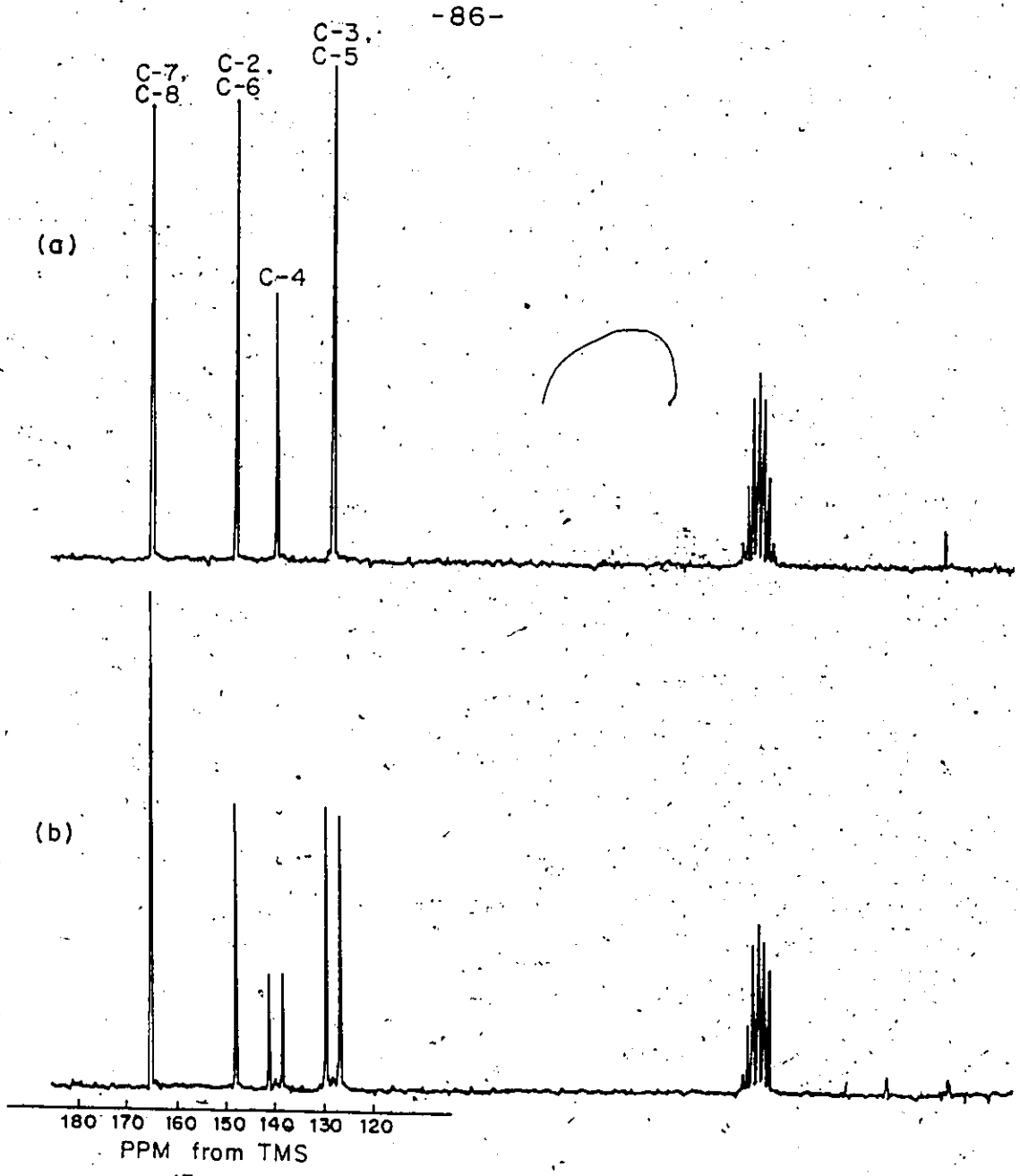

Fig. 26. ^{13}C NMR spectra of pyridine-2,6-dicarboxylic acid in DMSO-d_6

(a) proton spin decoupled.

(b) single frequency off resonance proton spin decoupled.

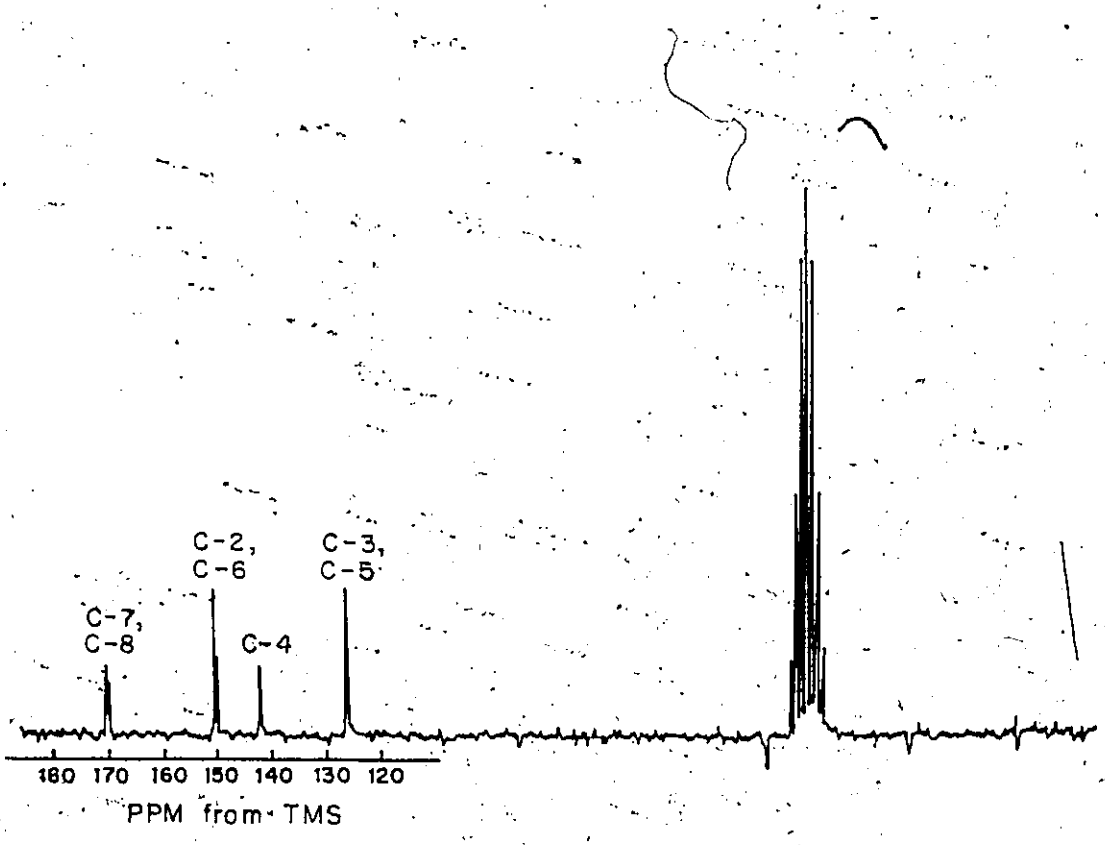

Fig. 27. ^{13}C NMR Spectrum of Th $(C_5H_3N(COO)_2)_2$ in DMSO-d_6 (proton spin decoupled)

Peroxo Compounds, 6-10 (Table 2)

Treatment of compounds 1-5 with a solution of H_2O_2 in the presence of a small amount of pyridine resulted in partial replacement of the ligands. With complexes 1-3, two chloro groups were replaced by a peroxo group while one of the organic ligands in 4 and 5 was replaced by a peroxo group and an aquo group. Pyridine was used to scavenge hydrogen ion that was generated in the course of the synthesis reactions. In the absence of pyridine, only ThO_2 was recovered from the reaction mixtures. Attempts to prepare organo-peroxo complexes from $ThCl_4 2L$ (L=$OPPh_3$ and $OAsPh_3$) were unsuccessful.

The resulting complexes from the reactions of the intermediate complexes of thorium with H_2O_2 were soluble in polar solvents such as methanol and DMSO. The analytical and molar conductance data indicate that the complexes are apparently hexacoordinate with the general formulae, $[ThL_2(O_2)]$ and $[ThL'(O_2)H_2O]$. L and L' were defined at the beginning of this chapter. Formulations as above follow from conductivity data (Table 2) which reveal that all the peroxo complexes, 6-10, behave as non-electrolytes in DMSO.

The metal peroxo grouping (local C_{2v} symmetry) gives rise to three infrared and Raman-active vibrational modes. These are predominantly O-O stretching (ν_1), the symmetric M-O stretch (ν_2) and the antisymmetric M-O stretch (ν_3). The characteristic stretching vibrations, ν_1(O-O) of the present

peroxo complexes are infrared inactive, as is the case with peroxo complexes of uranium (25) (see uranium section), but in the Raman spectra it appears at 820-840 cm^{-1} (Table 3). By contrast, the ν_1(O-O) mode is infrared active in complexes of light transition elements and it occurs with higher frequencies. It is to be presumed that, in the actinide complexes, the peroxo group has more nearly the character of the O_2^{2-} ion, i.e., it is ionic. In particular, the ν_1(O-O) frequencies in the present peroxo complexes are somewhat lower than those reported for some peroxofluoro complexes of Zr (87) having the general formula $M_3[Zr_2(O_2)_2F_7]nH_2O$, (M=NH_4, k, Rb, Cs; n=0.6-2) where ν_1(O-O) appears at 840-850 cm^{-1}. Further, the ν_1(O-O) bands of thorium peroxo complexes are considerably lower than the value, ~900 cm^{-1}, reported for complexes of Ti, e.g., $TiC_{36}H_{44}N_4O_2$ (88) and $M_2TiCl_4(O_2)H_2O$ (89) (M=Rb and Cs). Very recently Mimoun et al. (26) have reported a value of 895 cm^{-1} for ν_1(O-O) for the complex $Ti(O_2)(C_5H_4NCOO)_2HMPT$. The present data, thus clearly reveal that ν_1(O-O) stretching frequencies decrease with the increase of atomic number in a particular group. The infrared spectra of the peroxo complexes were unsatisfactory in the low-energy region so that the two ν(Th-O) modes associated with the $Th(O_2)$ grouping and the ν(Th-N) modes could not be located with certainty and that Th-O and Th-N assignments were not attempted.

The remaining features of the infrared spectra were similar to those obtained for complexes 1-5 with the exception of broad bands at ~3400 cm^{-1} in complexes 9 and 10, which arise from the coordinated water molecule.

In brief, the spectral data could be interpreted as follows. Compound 6 displays ν(C=O) 75 cm^{-1} lower than the free ligand value, indicating that the picolinato ligand is bonded to the metal through the carboxylato group. Complexes 7 and 8 show two medium intensity bands corresponding to ν(N-H) stretchings at 3090-3200 cm^{-1} (Table 3) which are significantly lower in frequency than the corresponding bands of the free ligands. This clearly suggests coordination by the amino group in complexes 7 and 8. Further, compound 7 displays ν(C=O) 90 cm^{-1} lower than the free ligand value, characteristic of the carboxylato binding with the metal. Infrared spectra of 9 and 10 also reveal the presence of a metal-bonded carboxylato group. In compound 10, the decrease in ν(C=N) was similar to that observed in 5 which thereby indicates that imino nitrogen is coordinated to the metal atom.

The ^{13}C NMR spectra (Table 5) of compounds 6 (Fig. 28) and 9 (Fig. 29) were also obtained in DMSO-d_6. The direction of changes of different carbon resonances were analogous to those observed in complexes 1 and 4 respectively. This again supports the nitrogen and carboxylato binding by the ligands in complexes 6 and 9. In other words, picolinato and pyridine-2,6-

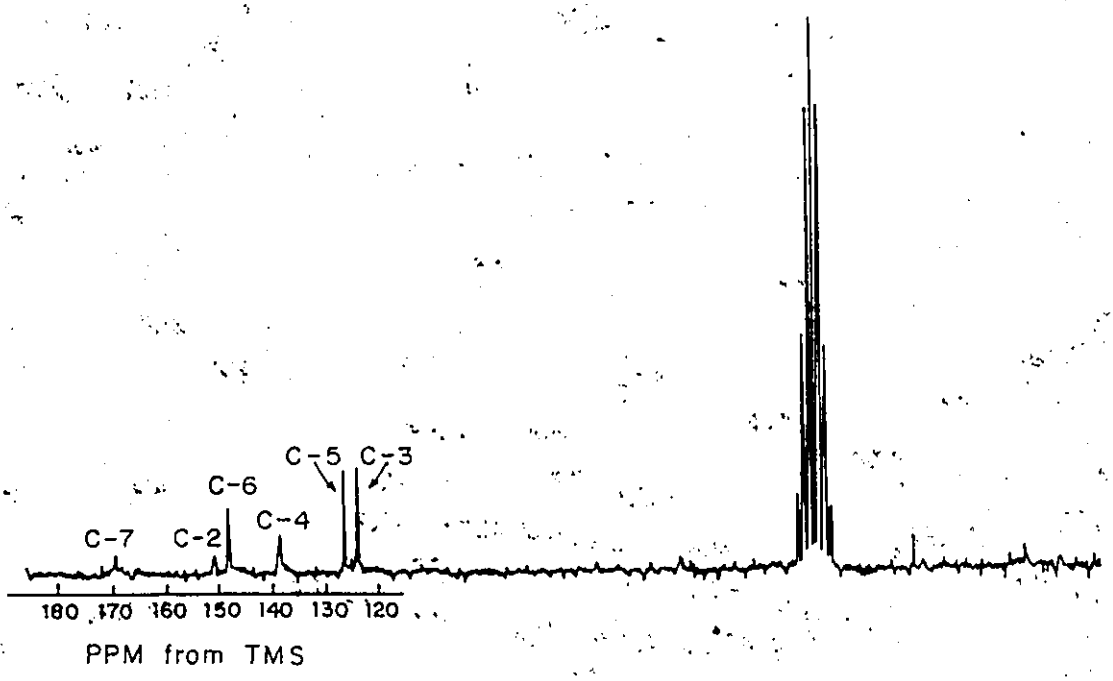

Fig. 28. ^{13}C NMR spectrum of Th (O_2) $(C_5H_4NCOO)_2$ in DMSO-d_6 (proton spin decoupled).

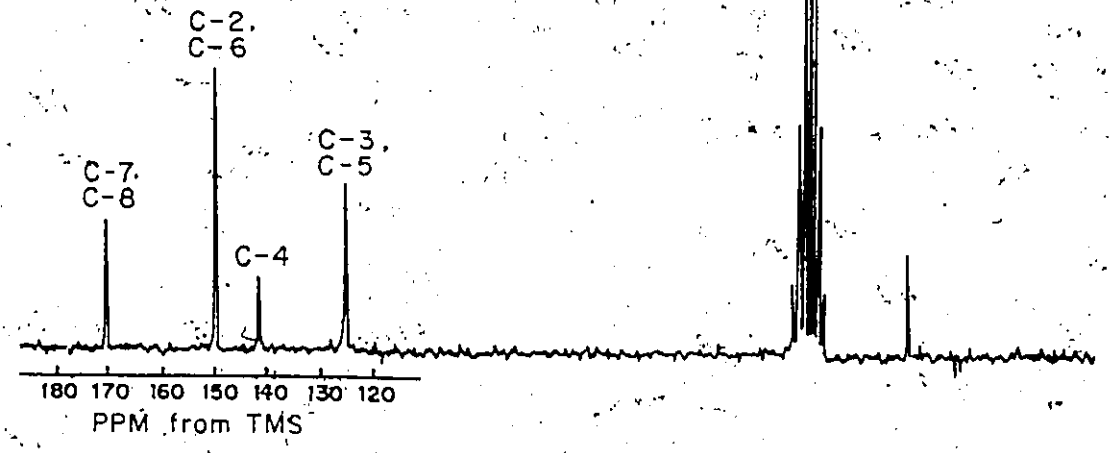

Fig. 29. ^{13}C NMR spectrum of $Th(O_2)\ C_5H_3N(COO)_2 \cdot H_2O$ in DMSO-d_6 (proton spin decoupled).

dicarboxylato ligands coordinate in bidentate (complexes 1 and 6) and tridentate (complexes 4 and 9) fashions respectively.

Reactivity

The thorium peroxo complexes were not found to be explosive. Treatment with aqueous iodide gave a discernible liberation of I_2 within 3-4 minutes.

Reactions with Olefinic Compounds

Titanium isopropoxide has been used with tert-butyl hydroperoxide to convert allylic alcohols to epoxides (61). Recently, Mimoun et al. (26) have reported that triphenylphosphine was converted to the phosphine oxide by a stoichiometric amount of organo peroxo complexes of titanium. As thorium is also quadrivalent, and the last member of group 4B, it was of interest to study oxygen transfer reactions of peroxo complexes of thorium towards organic substrates. The behaviour of a peroxo-thorium complex toward trans-stilbene will be described. In addition, a similar reaction with allyl alcohol has also been investigated. The reaction conditions are to be found in the Experimental section.

Reaction of 6 with trans-stilbene (reaction 4.11) produced trans-stilbene oxide as indicated by a medium-strong infrared band at 1060 cm^{-1} assigned to the C-O-C stretching mode and the ^1H NMR spectrum, which showed a methine absorption at 3.8 ppm as required for trans-stilbene oxide. Further, the mass spectrum of the product gave a molecular ion peak at m/e

196 which was followed by the diagnostic peaks at m/e 167, 105, 77, 51 and 39 respectively. A possible mechanism of epoxidation is shown in Scheme 1.

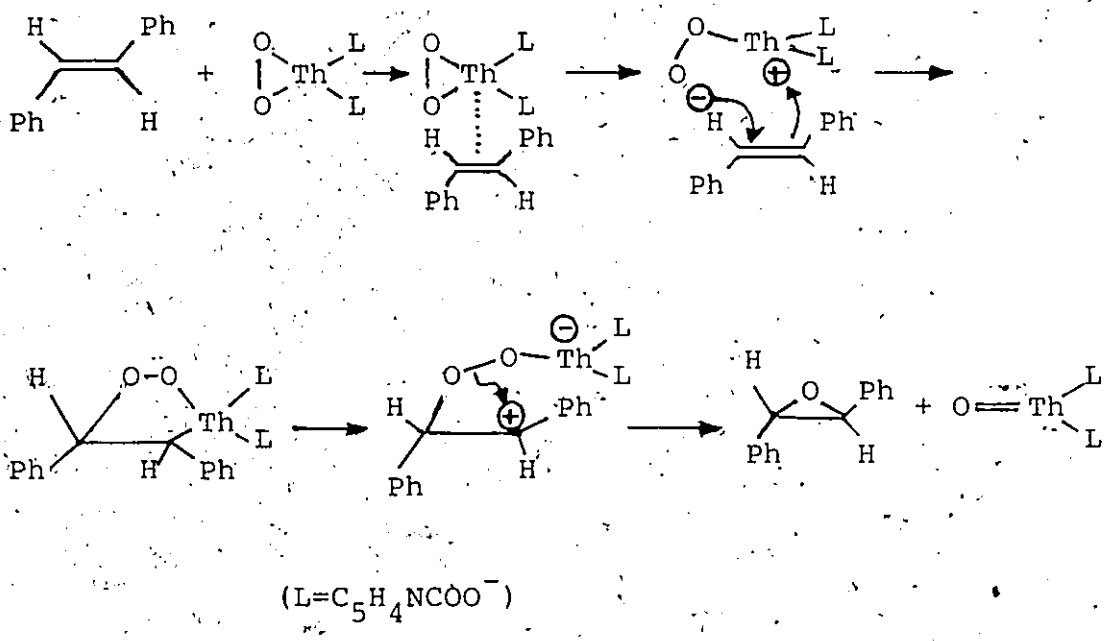

Scheme 1

Catalytic reaction of 6 and H_2O_2 with trans-stilbene (reaction 4.12) produced a high yield of product that, however, in this case was benzoin. The infrared spectrum of the product (Nujol mull) displayed ν(C=O) at 1685 (s) cm^{-1} and ν(O-H) at 3380 (s) cm^{-1}. The ^1H NMR spectrum showed methine absorption at 6.0 ppm. The mass spectrum showed a molecular ion peak at m/e 212 as well as further diagnostic peaks at m/e 178, 152, 107, 105, 77, 51, 28 and 18 respectively. A possible reaction path is shown in Scheme 2.

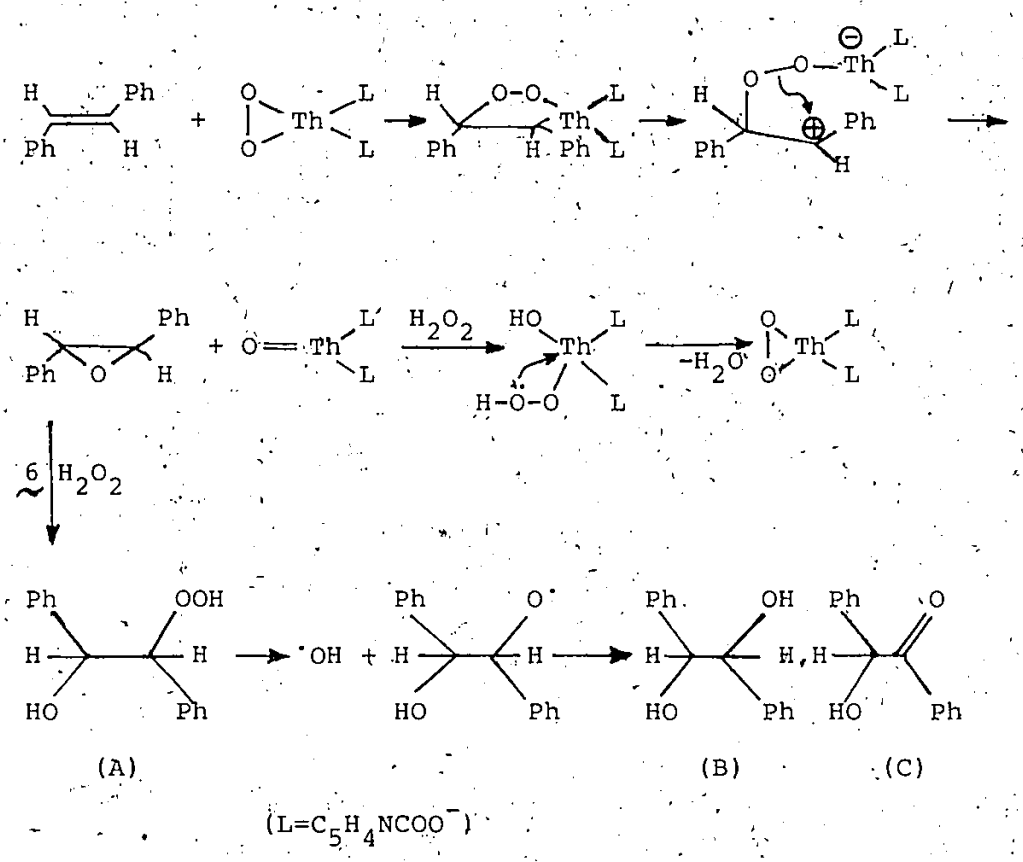

(L=$C_5H_4NCOO^-$)

Scheme 2

The various steps are analogous to mechanistic processes suggested by Mimoun et al.(16), Olah et al.(22) and Dzhemilev et al.(90). Support for the mechanism was provided by the fact that, in addition to benzoin, the diol, 1,2-dihydroxy-1,2-diphenylethane, $C_{14}H_{14}O_2$ (14% yield) was also isolated from the reaction of trans-stilbene oxide with H_2O_2 in dioxane (reaction 4.15). The infrared spectrum of the diol indicates ν(O-H) at 3300 cm^{-1} and the absence of ν(C=O). The ^1H NMR spectrum shows

methine absorption at 6.0 ppm. Opening of the epoxide ring has been shown to occur readily in the presence of excess oxidant (90-91) with the subsequent formation of diol and α-hydroxy ketone. In the presence of catalyst and oxidant, diols may be oxidized further to α-hydroxy ketones (90).

Catalytic reaction of 6 and H_2O_2 with trans-stilbene in the presence of acetic acid (reaction 4.13) also produced benzoin.

It is noteworthy that refluxing of trans-stilbene with H_2O_2 in dioxane (reaction 4.14) did not produce any reaction, which reveals that in the epoxidation process, a peroxo complex plays an important role in oxygen transfer mechanisms.

The epoxide glycidol was obtained by oxidation of allyl alcohol with 7 (reaction 4.16). This was evident from the ^1H NMR spectrum, which showed three multiplets centered at 2.7, 3.2 and 3.7 ppm. With H_2O_2 and only a catalytic amount of thorium complex 7 (reaction 4.17), the product isolated was glycerol. Its ^1H NMR spectrum showed methylene and methine absorptions at 3.61 and 5.15 ppm, respectively, as required by glycerol. The mass spectrum produced peaks at m/e 74, 61, 44, 43, 39, 31, 29, 18 and 15, identical with that of an authentic sample. A possible reaction path is shown in Scheme 3.

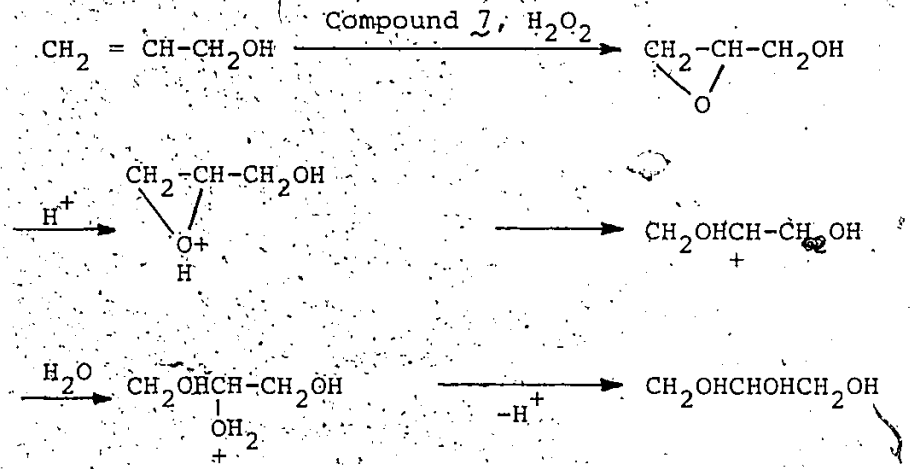

Scheme 3

Katsuki and Sharpless (61) comment on the low yields of epoxide whenever the product is water soluble. Possibly the hydrolysis involved in the above mechanism is more facile when the epoxide is soluble.

Compounds 9 and 10 failed to oxidize the organic substrate (trans-stilbene) even when refluxing at 120°C was continued for 24 h. This is presumably due to the enhanced stability afforded by the tridentate ligands.

Uranium Complexes

The elemental analyses along with other physical properties are listed in Table 6.

Complexes of Uranium(IV)

Several complexes, which served as precursors of the peroxo compounds, are described below. Compounds 12 and 13 have been reported previously (92-93). The complexes of U(IV) were prepared by addition of a stoichiometric quantity of the ligand to UCl_4 dissolved in acetone. These complexes were soluble in almost all of the polar solvents tried.

Formulations as shown in Table 6 follow from elemental analyses and conductivity measurements. The electrical conductivities (Table 7) of 5×10^{-4} M solutions of complexes 11-19 in nitromethane or nitrobenzene indicated that all of the complexes were undissociated.

Infrared data are shown in Table 8. Complex 11 shows a decrease in ν(N-O) compared to the value for the free pyridine-N-oxide (1242 cm^{-1}) (94). The decrease is attributed to a reduction in the N-O bond order as a result of coordination to the metal atom. Complex 11 also displays ν(U-Cl) at 250 cm^{-1} (95).

Complex 14 exhibits a strong carboxylato band at 1675 cm^{-1}. This is significantly shifted with respect to the uncoordinated pyridine-2,6-dicarboxylic acid (1710 cm^{-1}). As discussed in connection with the thorium complexes, this ligand

Table 6. Analytical data and other physical properties of the U(IV)- and U(VI) complexes.

No.	Compound	% U		% C		% H			M.P.[a] (°C)
		Calcd.	Found	Calcd.	Found	Calcd.	Found	Colour	
11	$[UCl_4.2ONC_5H_5]$	41.90	41.85	21.12	21.11	1.76	1.73	green	270
12	$[UCl_4.2OPPh_3]$	25.48	25.37	-	-	-	-	pale green	319-322
13	$[UCl_4.2OAsPh_3]$	23.28	23.26	42.27	42.15	2.94	3.0	pale green	310-311
14	$[U(C_5H_3N(COO)_2)_2]$	41.90	41.78	29.57	29.41	1.05	1.04	green	345-347
15	$[U(C_6H_4NH_2O)_2(H_2O)Cl_2]$	43.91	43.86	26.56	26.39	2.58	2.51	green	330-331
16	$[U(C_5H_4NCOO)_2Cl_2].C_5H_4NCOOH$	35.25	35.01	32.0	31.65	1.92	1.95	pale green	275
17	$[U(C_6H_4NH_2COO)_2Cl_2].C_6H_4NH_2COOH$	33.19	33.3	35.14	34.78	2.37	2.43	green	280
18	$[U(C_{13}H_9NO_2)_2]$	36.06	36.25	47.27	46.79	2.72	2.62	greenish-brown	291-293
19	$[U(C_{14}H_9NO_3)_2]$	33.24	33.07	46.92	46.85	2.51	2.63	brownish-green	319-322
20	$[U(O)(O_2)_2.2ONC_5H_5].H_2O$	45.24	45.21	22.81	22.64	2.28	2.29	yellow	335-338
21	$[U(O)(O_2)_2.2OPPh_3].H_2O$	26.28	26.61	48.43	48.65	3.58	3.57	yellow	>360
22	$[U(O)(O_2)_2.2OAsPh_3].H_2O$	24.28	24.40	44.08	43.69	3.26	3.13	pale yellow	>360
23	$[U(O)(O_2)(C_5H_3N(COO)_2)(H_2O)]$	50.74	50.90	17.91	18.30	1.06	1.05	yellow	351-353
24	$H^+[U(O)_2(O_2)C_6H_4NH_2O)(H_2O)]^-$	55.47	55.25	-	-	-	-	deep yellow	-[b]
25	$H^+[U(O)_2(O_2)(C_5H_4NCOO)(H_2O)]^-$	53.72	53.88	18.96	18.67	1.58	1.60	yellow	>360
26	$H^+[U(O)_2(O_2)(C_6H_4NH_2COO)(H_2O)]^-$	52.07	52.32	18.38	18.62	1.96	2.01	pale yellow	>360
27	$[U(O)(O_2)(C_{14}H_9NO_3)(H_2O)]$	43.83	43.72	30.93	31.25	2.02	2.03	deep yellow	336-340

a Uncorrected

b The complex decomposes at room temperature on standing.

Table 7. Molar conductivities of the uranium complexes (Ω^{-1} cm^2 at 25°C).

Complex No.	Nitromethane	Nitrobenzene	Methanol
11	11.98		
12	12.2		
13	17.02		
14	12.66		
15		0.19	
16		0.03	
17		0.06	
18		0.21	
19		0.50	
20	12.16		12.2
21	15.02		16.0
22	8.30		9.63
23	10.72		10.76
24		12.20	12.56
25		10.03	10.93
26		10.04	12.5
27		0	0

Table 8. Infrared and Raman spectral data for the U(IV)- and U(VI) complexes*. Band maxima, cm^{-1}.

Comp. No.	ν(O–H)	ν(N–H)	ν(C=O)	ν(U=O)	ν(C=N)	ν(B=O)	ν_1(O–O)	ν_3(U(O)(O))	ν_2(U(O)(O))	Other Bands
11						1215 vs				ν(U–Cl) 250 vs
12						1060 vs				250 vs
13						845 vs				264 vs
										ν(U–N)
14			1675							268
15	3500	3365 m 3290 m								
16			1725 vs 1675 vs							
17		3230 m 3130 m 3390 br 3300 w	1680 vs 1615 vs							
L	3290 br				1640 ms					
L'	3120 ms		1700 br		1625 ms					
18					1605 ms					
19			1675 br		1600 ms					
20	3525 br			915 vs		1209 vs	820 s	630 w	600 m	485 s, 200 s 250 w
21	3500 br			922 vs		1070 vs	830 s	685 ms	606 ms	410 m, 250 m 200 w
22	3500 br			907 vs		847 vs	805 s	670 ms	612 m	400 br, 240 s 342 s
23	3500 br		1680 vs 1660 vs	940 vs			860 vs 825 s	661 w	588 w	415 br, 140 vs
25	3400 br		1650 s	930 vs			803 s	670 ms	610 w	490 w, 395 br, 238 s
26	3400 br	3200 m 3105 m	1600 s	920 vs			825 ms	680 w	600 w	420 br, 240 s
27	3330 br		1634 br	915 vs	1590		805 s	670 ms	610 w	460 br, 240 m 185 br

* Relative band intensities are denoted by vs, ms, s, m, w, br, meaning very strong, medium strong, strong, medium, weak and broad respectively. E stands for As, N and P.

is tridentate, the coordination sites being the nitrogen atom and the two carboxylato groups. The very strong band of compound 14 at 268 cm^{-1} can be tentatively attributed to the ν(U-N) mode (96). In order to gain additional evidence that the ligand nitrogen is bonded to uranium, an attempt was made to obtain a ^{13}C NMR spectrum of compound 14. Dimethyl sulfoxide was the only effective solvent but the solutions rapidly formed a green precipitate which was presumably an adduct of DMSO. The infrared spectrum of the precipitate displayed a strong band at 960 cm^{-1} characteristic of ν(S-O) in adducts of DMSO (65). ^{13}C NMR spectra of thorium complexes of pyridine-2,6-dicarboxylic acid reveals nitrogen coordination. Further, Jacobson et al. (46) found by x-ray structure determination and spectroscopic measurements that the nitrogen atom of the pyridine-dicarboxylato ligand is coordinated to the metal atom in a number of compounds of Mo and W. Similarly, for complex 14, elemental analysis, conductivity, and infrared data indicate a six-coordinate complex in which two coordination sites are occupied by nitrogen atoms.

The infrared spectra of complexes 15 and 17 show two medium intensity bands due to ν(N-H) at (15, 3365 and 3290; 17, 3230 and 3130 cm^{-1}) - significantly lower than the values for 2-aminophenol and 2-aminobenzoic acid (3414, 3342 and 3390, 3300 cm^{-1} respectively, Table 4) which indicate coordination by nitrogen. Complexes 16 and 17 show very strong carboxylato

bands at 1675 and 1615 cm^{-1}, respectively. However, these complexes also show bands at 1725 and 1680 cm^{-1} as expected for the free carbonyl group in pyridine-2-carboxylic acid and aminobenzoic acid, respectively. In addition, two weak bands appear at 3390 and 3300 cm^{-1} in complex 17, characteristic of the uncoordinated amino group. Jacobson et al. (46) reported some compounds of Mo and W containing uncoordinated ligand molecules in the solid state.

So that additional information on coordination of the picolinato ligand in complex 16 could be obtained, a ^{13}C NMR spectrum in DMSO-d_6 was obtained. The spectrum was weak (Fig. 30), but it appeared to show two types of carboxylic carbons with chemical shifts of 167.2 and 166.0 ppm (the values of carbon resonances of free pyridine-2-carboxylic acid are listed in Table 5). The signals assigned to carbon in positions 6 and 2 appeared at 144.9 and 143.4 ppm, respectively, whereas the signal of the carbon in position 4 was shifted downfield by 1.2 ppm to 139.0 ppm. The spectrum showed a broad band at 129-130 ppm which presumably arises from carbon 3 and carbon 5. However, only one set of ring carbons were observed. Presumably one picolinic acid molecule serves as a monodentate ligand by utilizing its ring nitrogen to form a seven-coordinate uranium species in solution. Apparently this does not occur in the crystal.

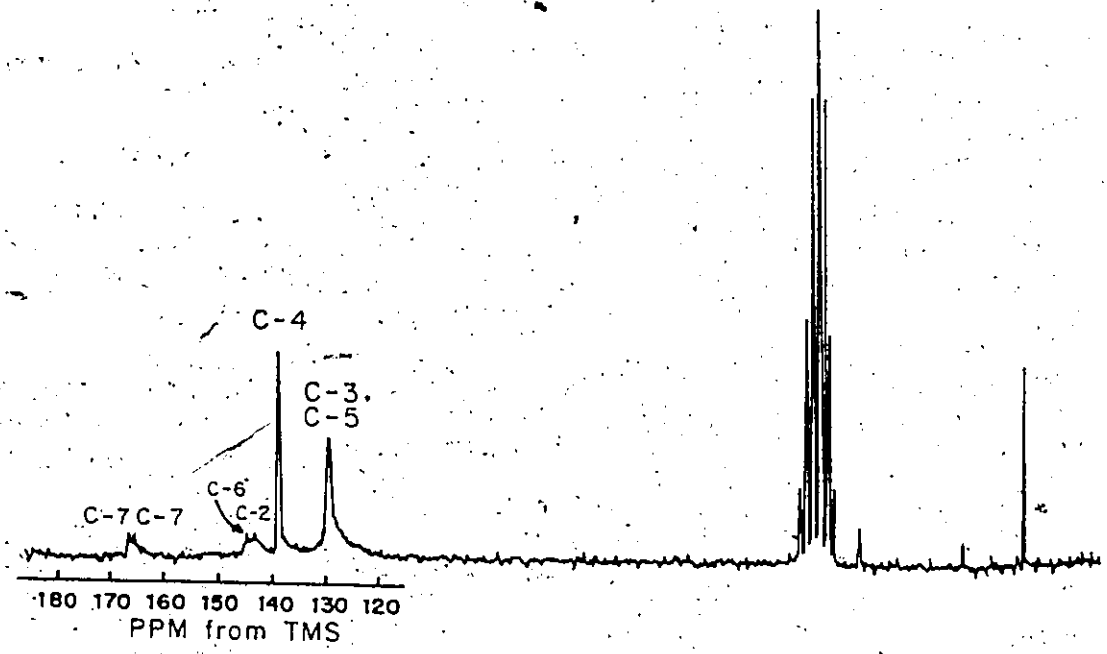

Fig. 30. ^{13}C NMR spectrum of $U(C_5H_4NCOO)_2Cl_2 \cdot C_5H_4NCOOH$ in DMSO-d_6 (proton spin decoupled).

The directions of changes in chemical shifts are analogous to those observed on protonation of pyridine (82). Similar changes were also observed in the Mo and W complexes of picolinic acid (46). The C-4 resonance, which is strongly influenced upon coordination through the nitrogen of the picolinato ligand, appears at 139.0 ppm in $Th(C_5H_4NCOO)_2Cl_2$ dissolved in DMSO-d_6, i.e. at virtually the same field as that with the uranium compound. Larger shifts were reported for Mo(VI) and W(VI) complexes of picolinic acid (21,46).

Alkalimetric titrations of 16 and 17 dissolved in methanol exhibited inflection points at pH 3.6 and 3.8, respectively, at a stoichiometry of ca. 1.1 mol of NaOH per mol of the complex (Table 9). This is attributed to the neutralization of the free carboxylic acid protons.

As indicated earlier, the Schiff bases behaved as tridentate, dinegative ligands coordinating at the imino nitrogen and two oxygen atoms. In complexes 18 and 19, the decrease in ν(C=N) by 35 and 25 cm^{-1} (Table 8) relative to the free ligands (for comparison, characteristic bands of the free Schiff bases are also included in Table 8) indicates that bond formation takes place through the imino nitrogen atom (78). The ν(O-H) band observed in the Schiff bases disappears upon coordination which indicates deprotonation and coordination at the oxygen site. Furthermore, in complex 19, the coordination of the carboxylato group is evident from the decrease in ν(C=O) by 25 cm^{-1} from the free ligand value.

Table 9. Titration of methanolic solution of the complexes by aqueous sodium hydroxide.

Complex No.	Equivalence Point, pH	No. of NaOH Equiv./Mol. of the Complex
16	3.6	1.15
17	3.8	1.1
24	6.8	0.74
25	4.0	0.95
26	3.4	1.06

The solid-state reflectance spectra of complexes 11 and 14-19 exhibited bands at $18x10^3$ and $29x10^3$ cm^{-1}. The former is due to a transition from the ground state A_1 ($^3H_4$) to higher levels within the $5f^2$ configuration (93) and the latter is caused by charge transfer.

Complexes of Uranium(VI)

Two different approaches were used to synthesize peroxo complexes of uranium from their precursor compounds. The U(IV)-complexes containing monodentate ligands were successfully converted to peroxo complexes of U(VI) by moistening the crystals in succession with acetone and H_2O_2 (50%) and warming. When U(IV) adducts of the unidentate ligands were dissolved in boiling acetone or methanol prior to the addition of H_2O_2, the product was $UO_4 4H_2O$, whereas peroxo complexes containing multidentate ligands were prepared by adding H_2O_2 (50%) to solutions of the U(IV) intermediates in methanol (compound 23) or a 1:1 mixture of acetone and methanol (compounds 24-27). Attempts to isolate a peroxo complex containing the Schiff base L, N-(2-hydroxyphenyl)salicylidenimine were unsuccessful as the compound quickly decomposed as soon as it formed.

The peroxo complexes were soluble in polar solvents such as DMSO, methanol, nitromethane and nitrobenzene. The formulations shown in Table 6 follow from the elemental analyses, conductivity measurements, and titrations with base (Table 9) and ceric ion (Table 10). The peroxo complexes are formulated

Table 10. Titration of methanolic solutions of the peroxo-complexes by aqueous acidified standard ceric sulfate solution.

Complex No.	No. of Ceric Sulfate Equiv./Mol. of the Complex
20	4.2
21	4.1
22	3.95
23	2.2
24	2.05
25	1.95
26	2.08
27	1.75

as seven-coordinate by analogy to similar complexes of Mo and W (46). It is conceivable that compounds 20-22 are actually eight-coordinate with the water molecule contained in the coordination sphere.

The conductivity measurements of 5×10^{-4} molar solutions of the complexes in nitromethane or nitrobenzene indicate that the complexes behave virtually as non-electrolytes in solution. Molar conductances of all the peroxo complexes were also obtained in methanol (Table 7) which provides further evidence for their non-electrolytic behaviour in solutions.

The complexes 24-26 are anionic. Alkalimetric titrations (Table 9) indicated an inflection point at pH 3.4-6.8 which corresponds to the neutralization of the acid proton. The molar conductivities of 5×10^{-4} molar solutions were about $10\ \Omega^{-1}\ cm^2$ at 25°C in both nitrobenzene and methanol, i.e., they are weak electrolytes. It is proposed that the low conductivities result from the formation in organic media of structures like 26a and 26b. Analogous conclusions were reached by Jacobson et al. (46) for analogous compounds of Mo and W.

Methanolic solutions of the peroxo complexes were titrated with Ce(IV) to determine the number of active oxygen atoms present (68). The titrations (Table 10) indicated that complexes 20-22 and 23-27 are di- and monoperoxo complexes, respectively.

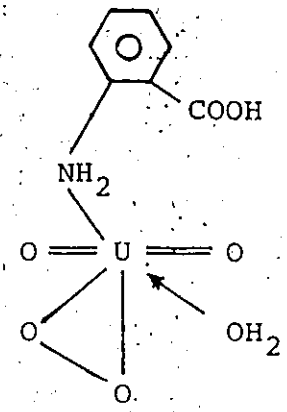

26a

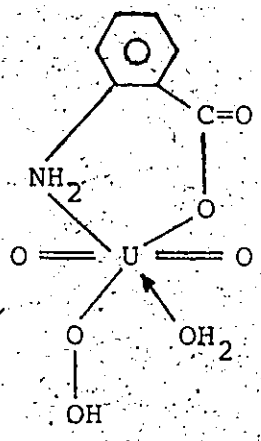

26b

The infrared spectra of all the peroxo complexes display a very strong band at 907-940 cm^{-1} (Table 8) corresponding to the ν(U=O) stretch (94,97-98). In complex 20, complexing causes a decrease in ν(N-O) by 33 cm^{-1} compared to the free ligand value (94). In complex 21, there is a decrease of ν(P-O) by 122 cm^{-1} compared to the free ligand value (1192 cm^{-1}) (95) which reveals coordination by the oxygen of $OPPh_3$. In complex 22, the ν(As-O) is decreased by 33 cm^{-1} from the free ligand value (880 cm^{-1}) (99). It is indicative of coordination through the oxygen of $OAsPh_3$. Further, in the far infrared region, the compounds 20-22 exhibit single bands at 485, 410 and 400 cm^{-1} assigned to the U-O' stretching (O' = oxygen in organic ligand). The absence of band splitting possibly indicates a trans-arrangement of the ligands although coupling of independent oscillators may be damped by the heavy metal atom (92).

As indicated in the thorium section, the metal-peroxo grouping (local C_{2V} symmetry) gives rise to three infrared- and Raman-active vibrational modes. These are predominantly O-O stretching (ν_1), the symmetric M-O stretch (ν_2), and the antisymmetric M-O stretch (ν_3). Wendling (89) and Griffith (100) have clearly established that the ν_1 mode in compounds of Mo and W appears at 800-900 cm^{-1}, and bands at 500-650 cm^{-1} are likely to arise from ν_2 and ν_3 modes. There is, however, a decrease in ν_1 upon passing from a molybdenum complex to the corresponding tungsten complex (23,89,100). The present work extends the above trend to uranium where there is further decrease in ν_1 to 803-860 cm^{-1}. In the present examples, ν_2 and ν_3 modes appear at 588-612 and 661-685 cm^{-1}, respectively, i.e., somewhat higher than in the Mo and W complexes. The Raman spectrum for 23 shows two well-defined bands in the O-O stretching region which presumably arise from two of several possible isomers.

Westland et al. (23) have reported that the O-O stretching frequency in peroxo complexes of Mo and W is decreased by replacing a given ligand by one which is a stronger donor. They suggested that the peroxide modes depend on the degree of ionic character in the M-O bonds and this may in turn be affected by the other ligands in the molecule. Griffith has noted that when fluorine replaces a less electronegative element bonded to the central atom of a peroxo complex, the O-O stretching frequency is increased (100). The phosphorus

and arsenic-containing ligands (e.g., $OPPh_3$ and $OAsPh_3$) are spatially very much alike while the Pauling electronegativities of phosphorus and arsenic are 2.19 and 2.18 respectively - practically identical (101). Nevertheless, the frequency of the ν_1 mode is lower in the arsenic compounds than in the phosphorus analogues. The polarity or the polarizability of the bond from the group 5A element to oxygen should influence charge displacement toward the metal atom. Reynold and Meek report the following bond moments for Ph_3EO (E=P or As): P-O, 3.27; As-O, 4.77 D (102). The derived charge separations in the E-O bonds show that the oxygen in the arsine oxide is more negative, and values of 2.45×10^{-10} and 1.78×10^{-10} e.s.u. were obtained for arsine oxide and phosphine oxide respectively, using 0.74, 1.10 and 1.21 A° as the covalent radii for oxygen, phosphorus and arsenic, respectively (103). Proton basicities have been determined by titration of compounds R_3EO with $HClO_4$ in nitromethane (104). The following p^{Ka} values were obtained for the protonated oxides: R_3PO, 9.72; R'_3PO, 8.54; R_3AsO, 16.14 (R = cyclooctyl, R' = n-butyl). This evidence again points to a greater polarity in the case of arsine oxides and hence ≡As-O is a stronger donor than ≡P-O. This argument seems to apply again in accounting for the lower ν_1 value observed for 22 compared to 21.

It is noteworthy that the ν_1 mode of the peroxouranium group is observed only in the Raman spectrum. The group appears

to be behaving as if it has essentially linear symmetry, i.e. it is ionic. The same is observed with thorium complexes (27).

The remaining features of the infrared spectra of the peroxo complexes of uranium were similar to their precursors with the exception of a broad band at 3330-3525 cm^{-1} in complexes 20-27 which arises from the coordinated water molecule.

In brief, the spectral data could be described as follows. Compounds 23 and 25-27 display ν(C=O) at 1600-1680 cm^{-1}, significantly lower in frequency than the corresponding bands of the free ligands. This clearly suggests coordination by the oxygen of the carboxylato group in complexes 23 and 25-27. Complex 26 displays two medium intensity bands due to ν(N-H) stretching at 3200 and 3105 cm^{-1} (Table 8), considerably lower in frequency than the corresponding bands of the free ligand, 2-aminobenzoic acid (Table 4). This indicates amino coordination in complex 26. In compound 27, the decrease in ν(C=N) by 35 cm^{-1} relative to the frequency for the free Schiff base indicates that the imino nitrogen is coordinated to uranium.

Reactivity

Peroxo complexes of uranium were not explosive under the experimental conditions cited in Chapter 4. However, a violent explosion was noticed when compound 21, $[U(O)(O_2)_2 2OPPh_3]H_2O$, was heated on a hot plate. There was sufficient violence to shatter the hot plate. The reduction of the peroxo complexes

of uranium by iodide was very slow and 3-4 h elapsed before any discernible brown coloration appeared in the solution.

Reactions with Olefinic Compounds

Peroxo complexes of molybdenum and tungsten have attracted interest as oxidants in organic synthesis (16,23-24,59-60,105). As uranium somewhat resembles the group 6B elements, it was of interest to investigate some oxygen transfer reactions of peroxo-uranium complexes towards olefinic compounds. Also, an attempt was made to use a peroxo uranium complex for a Baeyer-Williger oxidation of 2-methylcyclohexanone. The various conditions are described in the Experimental section, Chapter 4.

Reaction of 26 with trans-stilbene (reaction 4.29) produced trans-stilbene oxide as was evident from an infrared band at 1060 cm^{-1}, assigned to the C-O-C stretching mode and the characteristic methine absorption at 3.8 ppm in the ^1H NMR spectrum. 2-aminobenzoic acid (0.2 g) was also recovered from the reaction mixture. It was identified from the m.p. and infrared data. The infrared spectrum contained two medium intensity bands at 3390 and 3300 cm^{-1} corresponding to ν(N-H) modes and a band at 1680 cm^{-1} is assigned to ν(C=O) stretching. A possible reaction path is shown in Scheme 4.

Reaction of 26 with trans-stilbene in presence of H_2O_2 (reaction 4.30) produced benzoin, identified from its m.p. and spectral data. The infrared spectrum showed ν(C=O) at 1685 cm^{-1} and ν(O-H) at 3380 cm^{-1} and the ^1H NMR showed characteristic

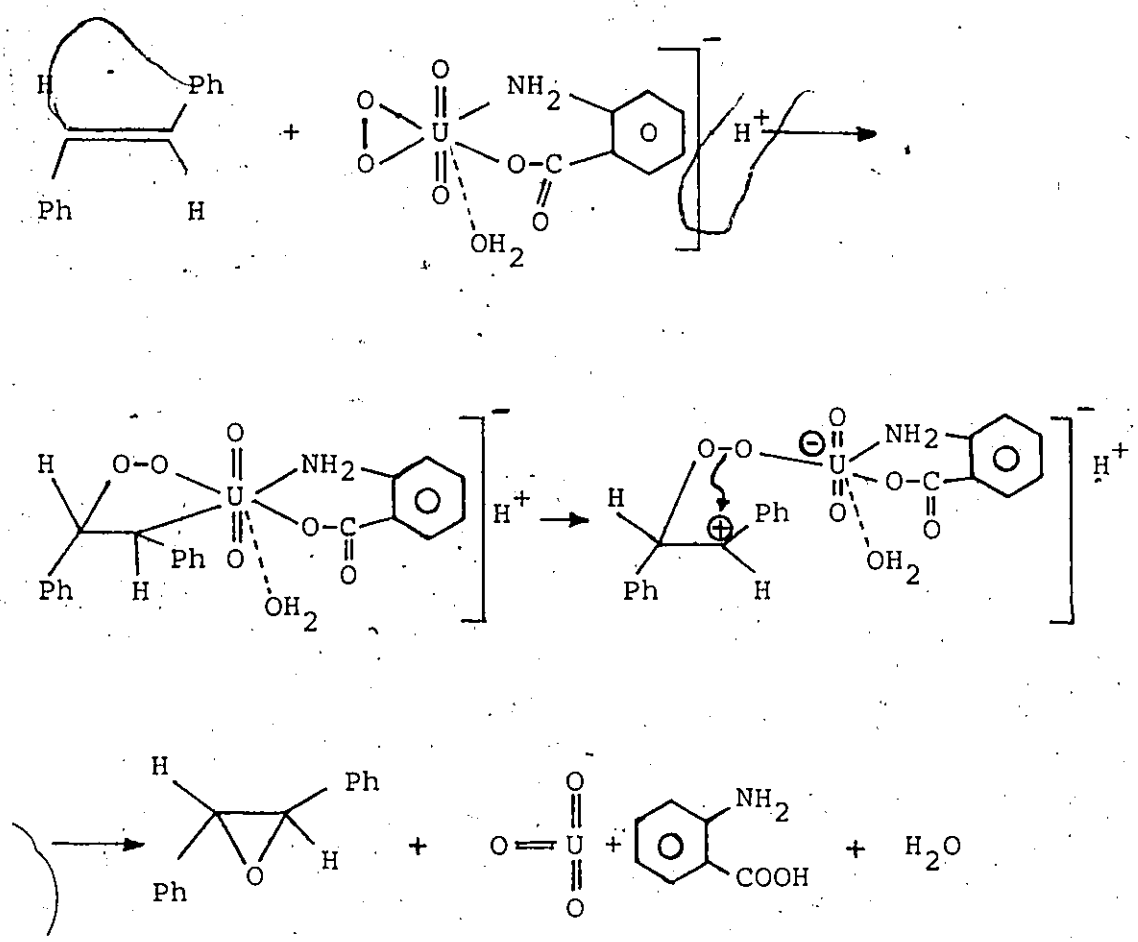

Scheme 4

methine absorption at 6.0 ppm. 2-aminobenzoic acid which was also isolated had an infrared spectrum identical with that of an authentic sample. A possible reaction path, analogous to Scheme 2, is shown in Scheme 5.

It has been suggested by Dzhemilev et al. that this type of reaction, which employs excess H_2O_2, can be used generally to prepare α-hydroxyketones (90). The present result supports their prediction.

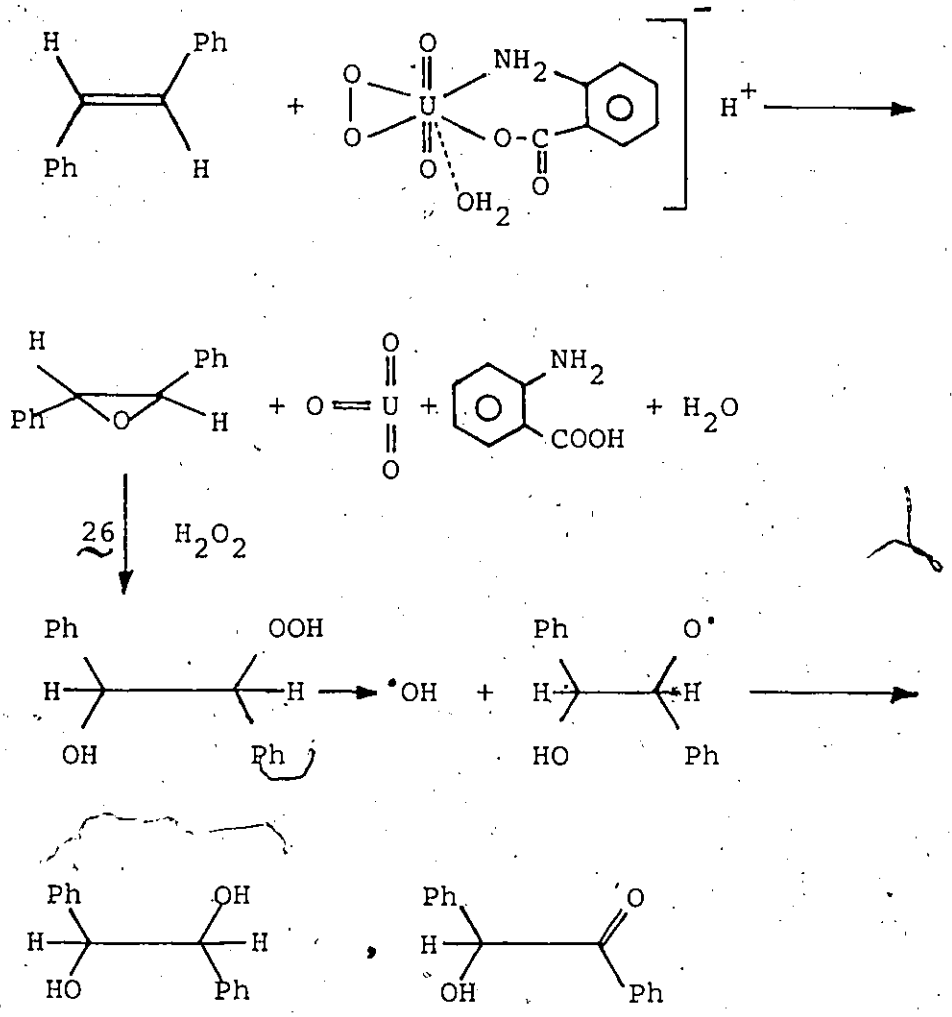

Scheme 5

Reaction of 25 with allyl alcohol (reaction 4.31) produced allyl alcohol epoxide as monitored by thin layer chromatography. This conclusion is supported by the proton NMR spectrum of the reaction product which showed narrow multiplets centered at 2.7, 3.1 and 3.6 ppm as required for allyl alcohol epoxide.

Reaction of 23 with 2-methylcyclohexanone (reaction 4.32) did not produce Baeyer-Villiger oxidation. The reaction was also continued in presence of t-butyl hydroperoxide, the same absence of reactivity was observed. In contrast, a similar molybdenum peroxo complex produced δ-valerolactone from the reaction of $[Mo(O)(O_2)C_5H_3N(COO)_2]H_2O$ and the substrate cyclopentanone (59).

Reactions of 20-22 and 25 with cyclohexene or cyclooctene (reaction 4.33) failed to produce a reaction. Negative results were also found by Olah and Welch for the very stable, coordinatively saturated salt, $Na_4[U(O)_2(O_2)_3]$ (22).

Conclusion

The present work has been carried out against a background of information about the behaviour of titanium, molybdenum, and tungsten complexes. Titanium complexes of the type $Ti(A\text{-}B)_2(O_2)$ HMPT* (26) are unusually stable and relatively inactive toward simple olefins, allylic alcohols, and cyclic ketones. For example, no reaction was observed between $Ti(C_5H_4NCOO)_2(O_2)$HMPT and a highly nucleophilic olefin such as tetramethylethylene. On the other hand, titanium tetraisopropoxide, a four-coordinate species, is highly reactive toward organic substrates (61-62)

---

* A-B is a bidentate, uninegative ligand (see Fig. 9, Chapter 1).

and has been used to catalyze the epoxidation of allylic alcohols by tert-butylhydroperoxide. The reaction probably involves an alkylperoxotitanium intermediate as the active catalyst. It is suggested that the difference between these two types of titanium complexes is kinetic in nature. The former type of complex, containing HMPT, is 7-coordinate and since all the ligands, the HMPT included, are tightly held, a substrate molecule can not be readily coordinated. Neither replacement of a ligand nor expansion to eight coordination is favourable. Thus, oxygenation of substrates for which coordination to the metal is necessary prior to oxygen transfer (see Eqn. [10]) is precluded.

In contrast to the behaviour of the 7-coordinate titanium complexes, two of the thorium complexes were found in the present work to oxidize olefinic compounds to epoxides. They also catalyzed the oxidation of the olefins with H_2O_2 to form more highly oxygenated products, benzoin and glycerol. This difference in behaviour between the thorium and titanium complexes may be attributed to the six-fold coordination of thorium and the greater readiness with which thorium may adopt an expanded coordination shell. Alternatively, as it is a large ion, Th^{4+} may bond its ligands less strongly and ligand substitution may therefore involve a lower activation energy. Some features of the bonding energy of thorium (and uranium) will be examined in Part B of this thesis.

The thorium complexes reacted with trans-stilbene and allyl alcohol to produce epoxides only when the reaction medium was strictly anhydrous. The epoxide ring opened when aqueous H_2O_2 was present. Low yields of epoxide have been reported in metal-catalyzed epoxidations with H_2O_2 owing to facile reactions of H_2O_2 with the epoxide. These latter reactions are also catalyzed by the metal complex (106-107). The metals, in their high oxidation states, perhaps act as Lewis acids.

The relative thermodynamic stability of peroxides of the group 4B elements and thorium is of some interest. Titanium peroxides are the least stable with respect to the formation of normal oxide and dioxygen while peroxides of thorium are the most stable (108). The trend can be explained by the greater lattice energies of the oxides of the lighter elements. An alternative view takes account of the high charge to radius ratio of Ti^{4+} compared to the other group 4B ions. The Ti^{4+} ion therefore has the greatest polarizing ability, which causes greater covalency in its attached peroxo groups and hence thermodynamic instability. On the other hand, Th^{4+} has the least charge to radius ratio and therefore its peroxo compounds should be predominantly ionic and stable. This behaviour is also evident from the fact that in the present examples of organoperoxo complexes of thorium, the peroxo stretch appears only in the Raman spectrum. These trends are similar to that in groups 1A and 2A where, for example, it is observed that

BaO_2 can be formed from BaO and oxygen while CaO_2 cannot be so prepared.

The observed reactivity of the organo peroxo complexes of thorium towards organic substrates is attributed to their kinetic instability. The organo peroxo complexes of titanium prepared by Mimoun et al. are kinetically stable (26), while the thorium complexes are not.

The uranium peroxo complexes were not reactive towards simple olefinic compounds, e.g., cyclohexene or cyclooctene (see reaction 4.33) but were found to be reactive towards trans-stilbene and allylalcohol.

The uranium peroxo complex, 26, was employed to oxidize trans-stilbene to the oxide. The reaction was also investigated in presence of 30% H_2O_2 which, however, produced benzoin. As indicated earlier, the epoxide ring opens in the presence of a large excess of aqueous H_2O_2. The UO_4 entity acts as a strong Lewis acid. In the case of uranium peroxo complex, catalytic reaction was not achieved; rather, the complex decomposed to give UO_3 and free ligand (reactions 4.29 and 4.30, see Schemes 4 and 5). The compound UO_3 is very inert and its reaction with H_2O_2 to regenerate peroxo-uranium species is not feasible.

Compound 25 was employed to oxidize allyl alcohol to the epoxide.

Investigations of oxidation reactions with uranium-peroxo complexes indicated that these compounds are less reactive than the peroxo complexes of Mo and W (16, 24, 59-60, 105). This could be because of a high thermodynamic stability of the $U(O_2)$ grouping or it could be for a kinetic reason. The peroxo-uranium complexes are all 7-coordinated.

Similar to the peroxo complexes of group 4B, the peroxo complexes of 6B elements exhibit analogous trends in properties. On the basis of ionic potentials (charge to radius ratio), the metal-peroxo bonds in the peroxo complexes of Mo and W would be more covalent whereas that for the uranium-peroxo moiety should be predominantly ionic. This is obvious from the appearance of the $\nu_1(O\text{-}O)$ stretch only in the Raman spectra of the uranium peroxo complexes as was the case also with the thorium peroxo complexes.

The peroxo complexes of uranium are somewhat less reactive than the peroxo complexes of thorium. As discussed earlier, the peroxo complexes of thorium are all 6-coordinated and in the reactions with olefinic compounds, coordination leading to 7-coordinated species is probably more facile than the uranium compounds, which are 7-coordinated.

THE CHEMISTRY OF THORIUM AND URANIUM

PART 2. THERMOCHEMISTRY

CHAPTER 1

Introduction

Thermochemical data for thorium and uranium compounds are likely to be of importance for the technology of these metals. Their broadening use in metallurgy and nuclear technology has called for the development of new energy-efficient and economical processes of production. Electrolysis of the anhydrous chlorides in a melt of alkali chloride is one of the promising methods of producing and refining these and other refractory metals and alloys. Complexes, such as $ThCl_6^{2-}$ and UCl_6^{2-} for example, may be implicated in chemical reactions of molten salts proceeding in electrolytic cells. These salts are chemically less reactive, thermally stable, and relatively nonvolatile at high temperatures. Further basic knowledge must precede more detailed study of such intermediates.

Our thermochemical studies on the ternary salts of thorium and uranium tetrahalides have revealed some of their fundamental properties, e.g., class a and class b behaviour, comparative Lewis acidity, etc.

There have been no reports of thermochemical measurements on ternary salts of thorium tetrabromide. It therefore seemed desirable to initiate work in this area. An early calorimetric investigation of A_2ThCl_6 salts (109) (A=Li,

Na, K, Rb and Cs) shows a lack of internal consistency and the value -62.3 KJ mol^{-1} obtained for the process $2CsCl + ThCl_4 = Cs_2ThCl_6$ disagrees with the value -73.6 KJ mol^{-1} obtained by Fuger and Brown (110). In the earlier work, the ternary salts were prepared by fusing a mixture of the component chlorides while the later workers obtained hydrated Cs_2ThCl_6 from ethanolic hydrochloric acid by saturating the solution with gaseous hydrogen chloride at ice-temperature. The product was vacuum-dried at room temperature for two days and was refluxed with thionyl chloride for 2-3 h and was vacuum-dried. In a previous research (111), Westland et al. found that Cs_2NbCl_6 prepared by crystallization from solution provided an enthalpy of solution which was several KJ mol^{-1} less negative than that of a sample prepared in the dry way. A redetermination of the heats of solution of choloro complexes prepared in the dry way appeared to be desirable as well as the study of bromothorates.

Russian workers have studied the thermochemistry of the A_2UCl_6 (112) and A_2UBr_6 (113) salts. Also, Fuger and Brown (110) determined the enthalpy of formation of Cs_2UCl_6 and obtained a result in fairly good agreement with that in reference 112.

The present work was intended to achieve the following objectives:

(a) Determination of the heat of complexing of A_2ThX_6 (A=K, Cs, and X=Cl,Br) salts and the comparative stabilities of A_2ThX_6 and A_2UX_6 salts and their anions.

(b) A thermochemical investigation of the process,

$$MX_4(g) + 2X^-(g) \rightarrow MX_6^{2-}(g), \quad (M=Th \text{ and } U)$$

was of interest in order to further our understanding of the bonding of these actinide elements to non-metal atoms. The enthalpy of the above reaction, which is the double halide in affinity of the gaseous MX_4, affords comparison between the acceptor strengths of thorium and uranium.

(c) Examination of the thermochemical bond energies of M-X systems.

CHAPTER 2

REVIEW OF PREVIOUS WORK

1. Thermal Studies

As stated earlier, the French chemist, E. Chauvenet (109), was the first to claim the existence of the complex salts A_2ThCl_6 where A=Na, K, Rb and Cs. These compounds were more recently identified by phase equilibrium studies. It was claimed by several groups of workers that the potassium salt melts incongruently (114-116) and by another group that it melts congruently (117). The reader may see the inconsistency in the published phase diagrams reproduced here as Fig. 31.

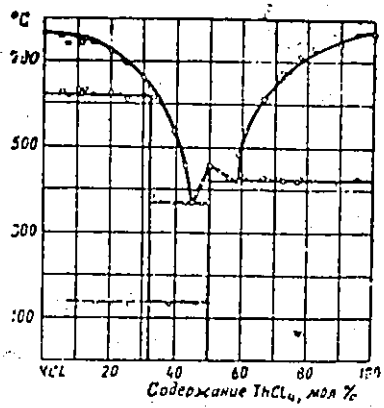

Диаграмма плавкости системы KCl—$ThCl_4$ (115).

(a)

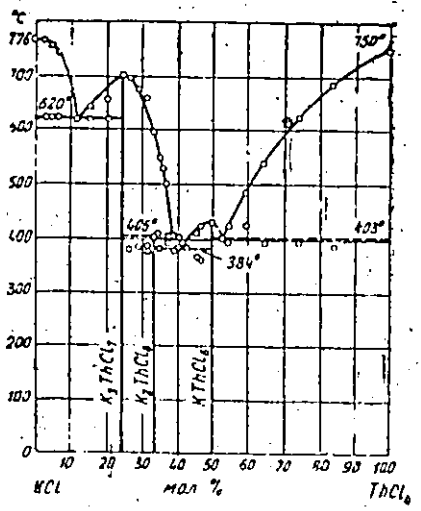

Диаграмма плавкости системы KCl—$ThCl_4$ (116).

(b)

Fig. 31. Comparisons of the published phase diagrams of K_2ThCl_6.

We shall return later to the conclusions which can be drawn from the above figure. The rubidium salt, Rb_2ThCl_6, is reported to melt incongruently (117). The sodium and caesium salts, Na_2ThCl_6 (115) and Cs_2ThCl_6 (117) melt congruently. The melting points of different compounds are shown in Table 11.

Table 11. Melting points of A_2ThCl_6 complexes (117).

Complex	m.p. (°C)
Na_2ThCl_6	435 ± 2
K_2ThCl_6	705 ± 2
Rb_2ThCl_6	710 ± 2
Cs_2ThCl_6	710 ± 2

Although he had by no means characterized his products, Chauvenet believed that he had prepared the A_2ThCl_6 salts by fusing a stoichiometric mixture of the component chlorides (109). His calorimetric results for the assumed reactions, $2ACl + ThCl_4 \xrightarrow{\Delta H_c} A_2ThCl_6$, are listed in Table 12.

Table 12. Heats of complexing, ΔH_c, of the alkali metal-hexachlorothorates (109).

Complex	$-\Delta H_c$/KJ mol^{-1}
Na_2ThCl_6	18.0
K_2ThCl_6	38.2
Rb_2ThCl_6	80.7
Cs_2ThCl_6	62.3

Fuger and Brown (110) obtained -73.6 KJ mol^{-1} as the heat of complexing for Cs_2ThCl_6. Their method of preparing Cs_2ThCl_6 by an aqueous route was described in the Introduction. It is evident that there is uncertainty about the reported enthalpy values.

Thermochemical data on A_2ThBr_6 systems are not available.

A_2UCl_6 and A_2UBr_6 systems (A=Na, K, Rb and Cs) are all congruently melting compounds (118). The melting points of A_2UX_6, where X=Cl and Br, are given in Table 13.

Table 13. Melting points of A_2UX_6 complexes (118).

Complex	m.p. (°C)
Na_2UCl_6	420-445
K_2UCl_6	605-654
Rb_2UCl_6	676
Cs_2UCl_6	670
Na_2UBr_6	533
K_2UBr_6	672
Rb_2UBr_6	722
Cs_2UBr_6	736

Reported values for the heat of complexing for A_2UX_6 salts are given in Table 14.

Table 14. Heats of complexing, ΔH_c, of the alkalimetal hexahalouranates.

Complex	$-\Delta H_c$/KJ mol^{-1}	Reference
Na_2UCl_6	7.1	112
K_2UCl_6	39.3	112
Rb_2UCl_6	67.4	112
Cs_2UCl_6	100.8	112
Cs_2UCl_6	106.6	110
Na_2UBr_6	5.0	113
K_2UBr_6	43.5	113

2. Lattice Energies

The published crystal symmetries and the lattice parameters of different A_2MX_6 salts are shown in Table 15.

Table 15. Crystal symmetries and lattice parameters of A_2MX_6 complexes.

Complex	Symmetry	Lattice Constant (A°)	Reference
Cs_2ThCl_6	Trigonal (space group $P\bar{3}m1$)	a=7.629 c=6.050	119-120
Cs_2UCl_6	Trigonal (space group $P\bar{3}m1$)	a=7.507 c=6.050	120
K_2UBr_6	Tetragonal	a=10.94 c=10.67	113
Rb_2UBr_6	Face centered cubic lattice of rubidium	-	118
Cs_2UBr_6	Face centered cubic lattice of caesium	-	118

The complexes Cs_2ThCl_6 and Cs_2UCl_6 are isomorphous.

The calculations for the lattice energy, U, reported in references 112 and 113, used the Kapustinskii and Yatsimirskii (121) expression,

$$U = \frac{1201.6(\Sigma n) Z_+Z_-}{r}\left(1 - \frac{0.345}{r}\right) + 10.5(\Sigma n) Z_+Z_- \text{ kJ mol}^{-1} \quad [32]$$

where Σn is the number of ions in the molecule of the complex salt, Z_+ and Z_- are the charges of the ions and r (in Angstroms) is the sum of the radii of the complex anion and cation (i.e., $r = r_- + r_+$), obtained by the method of Yatsimirskii (see discussion section). The lattice energies so obtained are given in Table 16.

Table 16. Lattice energies of A_2UX_6 salts.

Compound	$U_{A_2UX_6}$/KJ mol^{-1}	Reference
Na_2UCl_6	1579.0	112
K_2UCl_6	1518.4	112
Rb_2UCl_6	1536.0	112
Cs_2UCl_6	1507.0	112
Na_2UBr_6	1504.1	113
K_2UBr_6	1484.1	113
Rb_2UBr_6	1473.2	113
Cs_2UBr_6	1459.4	113

Jenkins and Pratt (122-125) have developed a sophisticated method to evaluate lattice energies and they have reported the values, 1315 and 1352 KJ mol^{-1} for Cs_2ThCl_6 and Cs_2UCl_6 respectively.

Jenkins and Pratt's approach to evaluate lattice energies requires precise knowledge of the "basic" radii of $r_{MX_6^{2-}}$ and the charge distribution in the complex anion MX_6^{2-}. The total lattice energy of a salt, A_2MX_6, is given by,

$$U = U_{elec.} + U_{dd} + U_{qd} - U_R \qquad [33]$$

where $U_{elec.}$, U_{dd}, U_{qd} and U_R are the electrostatic, dipole-dipole, quadruple-dipole dispersion and repulsion energies respectively.

The simplified form of the lattice energy expression is given by Jenkins and Pratt as,

$$\text{Const. } \exp\left(\frac{2\bar{r}_{x^-}}{\rho}\right) + \text{Const. } \exp\left(\frac{\bar{r}_{x^-}}{\rho}\right) + \text{const.} = 0$$

$$= \left(\frac{\partial U}{\partial i}\right)_{i=i_o,d} \qquad [34]$$

where

$\bar{r}_{x^-}$ = Huggins' "basic" radii (= $\bar{r}_{MX_6^{2-}}$) (125)

ρ = repulsion constant

i = a,b,c = the unit cell parameters, minimization being carried out with respect to a single parameter i, while maintaining the other cell constants

at their equilibrium values, i_o and preserving the M-X distance (=d) in the complex ion constant (125).

Equation [34] can be solved as a function of q_x (q_x = charge on the halogen atom of the complex ion) and a plot of $\bar{r}_x$- versus q_x in the case of the six halogen model leads to a determination of the basic radius of x^{q_x} . In the case when MX_6^{2-} is assumed to be a homogeneous spherical ion, a plot of $\bar{r}_{MX_6^{2-}}$ versus q_x gives the basic radius of MX_6^{2-} ion. The charge distribution q_x is obtained from the intersections of the curves generated from the specific derivatives i (usually a and c in the non-cubic salts).

CHAPTER 3

EXPERIMENTAL TECHNIQUES

This chapter deals with the following matters:

1. The purification and handling of materials
2. Physical measurements
3. Analytical method.

Preparative work will be discussed in Chapter 4.

The purity and sources of certain of the compounds and the purification of solvents have been discussed in Chapter 3, Section A.

1. PURIFICATION AND HANDLING OF MATERIALS

Because all of the halides and their derivatives were extremely susceptible to hydrolysis, closed systems which were evacuated or filled with dry N_2 gas, were used in all preparations and experiments. All materials were rigorously dried and stored in evacuated containers. A glove box was also employed and a continuous flow of dry N_2 gas was maintained through it and an abundant supply of freshly exposed phosphorus pentoxide was kept inside in order to remove excess moisture.

A typical sample transferring apparatus is shown in Fig. 32. The apparatus was connected to a vacuum line,

Fig. 32. An all-glass sample transferring apparatus.

A and B = seal-off points

C = connection to vacuum system and nitrogen supply

D = 24/40 ground glass cap.

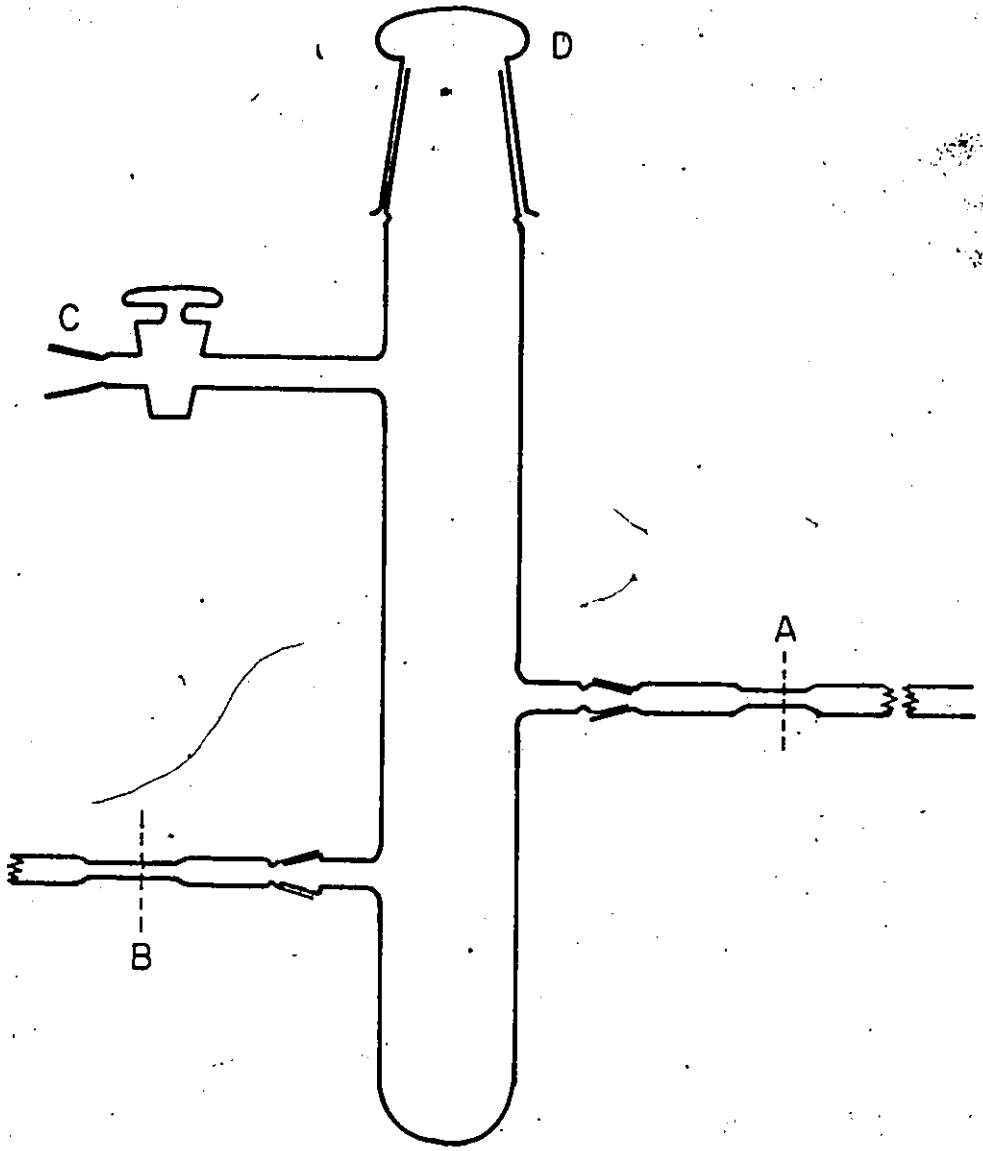
D
C
A
B

evacuated and flamed out to ensure complete dryness. Dried N_2 gas was then admitted. The 24/40 joint was disconnected while N_2 gas was passing through, and a nitrogen-filled ampoule containing the sample was broken over the opening and the sample poured in. The ground cap was replaced and the assembly re-evacuated. At this stage, if the properties of the material permitted, it was heated under vacuum to ensure complete dryness. The stopcock was closed and the apparatus was removed from the vacuum line. The sample was then transferred to the reaction tubes (A and B in the diagram) and these were sealed off at the points indicated, either under a dynamic vacuum or under N_2 gas.

Materials

Metal

(i) Thorium powder (99.9% purity) was supplied by Alpha Ventron.

(ii) Bromine (J.T. Baker Analyzed Reagent) was dried over P_2O_5 for several days under N_2-atmosphere and distilled immediately prior to use.

(iii) Alkali metal halides

The potassium halides were J.T. Baker Analyzed Reagent grade material. The other alkali halides (99.9% purity) were supplied by K and K Laboratories of Hollywood, California and were used without further purification other than drying.

All alkali metal halides were dried under vacuum by heating in a quartz tube to 500°C.

(iv) Acid

Hydrochloric acid was supplied by McArthur Chemical Co. Ltd. of Montreal, Canada.

2. PHYSICAL MEASUREMENTS.

(i) X-ray diffraction

X-ray diffraction patterns were obtained by the Debye-Scherrer method using Ni-filtered CuK_α radiation and a camera with a diameter of 114.7 mm. The line spacings were determined by the Straumanis technique and the resulting lattice parameters for each line were extrapolated against the Nelson-Riley function (126).

Nelson-Riley function:

$$\left(\frac{\cos^2\theta}{\sin\theta} + \frac{\cos^2\theta}{\theta} \right), \quad (\theta = \text{Bragg angle}) \qquad [35]$$

This reduced systematic errors due to self-absorption, and off-centering of the specimen. The extrapolated value from the best drawn line gave the resulting lattice constants.

Samples were ground to a fine powder and were transferred to 0.3 mm capillary tubes made of Lindemann glass. The operation was carried out under N_2-atmosphere in a glass

transferring apparatus. The capillaries were sealed with a low flame. The exposure time to X-rays varied from 3 to 8 hours depending on the sample.

The d-spacings were calculated from the formula,

$$n\lambda = 2d \sin \theta \qquad [36]$$

with the weighted mean wavelength λ = 1.5406 A°.

The relative intensities of the lines were estimated visually.

(ii) Calorimetry

Construction of calorimeter

(a) Thermostat:

The thermostat consisted of a glass jar which was insulated with vermiculite. The temperature was controlled by a mercury contact thermoregulator. The temperature was controlled at 25.0° ± 0.1°C. The thermostat heater was controlled by an electronic relay supplied by Precision Scientific Co., Chicago. A copper cooling coil was connected to the mains water.

(b) Calorimeter:

The present modelling of the calorimetric system is based upon Greenwood and Perkins (127) all-glass calorimeter but some improvements were incorporated. Westland et al. (111) have described its construction and calibration previously. Some important features will be described here. Figure 33 shows the construction of the calorimeter.

Fig. 33. A schematic diagram showing the calorimeter assembly.

A = Dewar flask

B = an empty glass well for rapid heating and cooling

C = glass stirrer

D = hard polyethylene well for calibration heater

D' = gold-plated copper tube

E = glass well for thermistor

F = sample bulb holder

G = sample bulb

H = protective well around the bulb holder (made from teflon)

I = thermobath

J = thermometer

K = thermoregulator

L = thermostat stirrer

M = thermostat heater

N = cooling water

O = water level in the thermobath

P = jacks

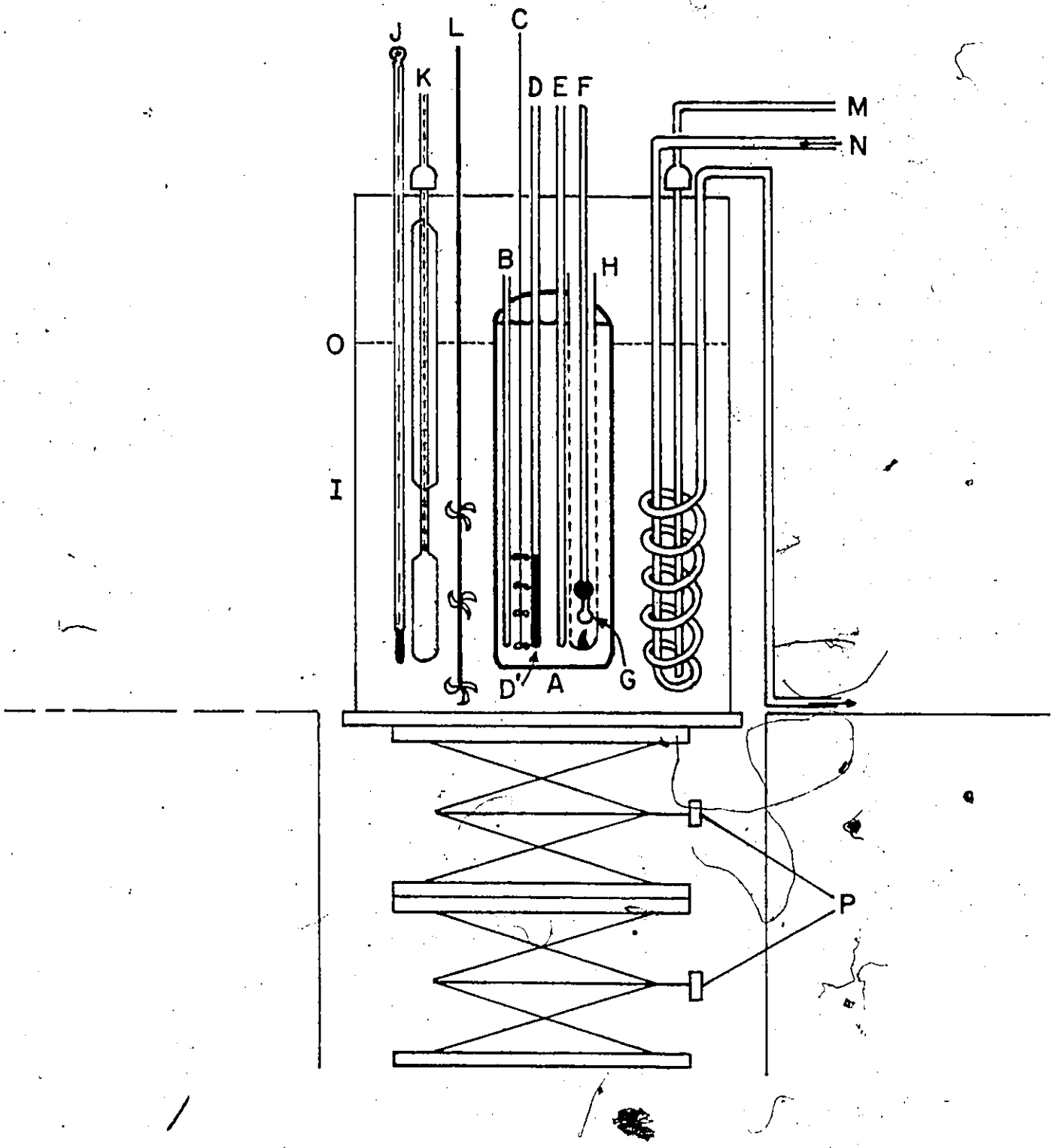
J
L
C
K
D E F
M
N
B
H
O
I
D'
A
G
P

It essentially consisted of a Dewar flask, A (600 cm^3 capacity, Pope Scientific Inc., Wisconsin, U.S.A.) (Fig. 33) which was insulated at the top by a polystyrene cover plate. Through the holes made in the cover plate, an empty glass well, B; a glass stirrer, C; a hard polyethylene well for calibration heater, D; a glass well for thermistor, E and a sample bulb holder, F were introduced into the Dewar flask. The bulb holder was a teflon rod which had an inner hole at the bottom in which the stem of the glass bulb G was introduced and fixed to the teflon bar with wax. There was a protective teflon cover H, around the bulb and the bulb holder which had numerous holes in it and a silver spike at the bottom. At the appropriate time, the thin-walled glass bulb containing the sample was crushed by hitting it against the spike as shown in Fig. 33. The Dewar flask with these accessories was immersed in the glass thermobath.

The temperature sensing element

The temperature changes were detected by means of a Sargent-Welch model thermistor immersed in silicone oil. This was connected through a Sargent-Welch model S-81601 thermistor bridge to a 10 mV recorder which was used as a null instrument.

(c) The calibration heater

The calibration heater, made from two ½ watt carbon resistors connected in series, was immersed in silicone oil.

The heater had a total resistance of 122.8 ohms which was standardized with a resistance thermometer bridge, type J-1003, supplied by M. Tinsley Co. Limited. The bottom of the calibration heater well consisted of a ¼ inch diameter gold-plated copper tube for the transmission of heat into the calorimeter liquid. Current was drawn from a 12 volt lead-acid battery. In order to achieve a steady e.m.f. from the battery, current was drawn through a dummy heater for at least one hour before a measurement. The duration of the electrical heating was timed by means of an electric timer (reading to 0.1 second) which was synchronized with the heater by a three pole double throw switch as shown in Fig. 34.

The current was measured by means of a potentiometer, supplied by Derritron Electronics Limited, connected across six one ohm standard resistors connected in parallel to give a resistance of 0.1667 ohm.

(d) Calorimetric liquid

The calorimetric liquid was 4.02 N HCl. This was prepared in bulk from concentrated 12 N acid. The solution was stored in a large glass container fitted with a dispensing burette. The strength of the acid was determined by titration from time to time and found to be quite constant.

Fig. 34. Synchronization circuit of calibration heater and the timer used for calorimetric measurements.

A = 12 volt lead storage cells

B = 110 volt supply

C = timer

D = calibration heater

E = dummy heater

F = standard 1 ohm resistors

G = potentiometer

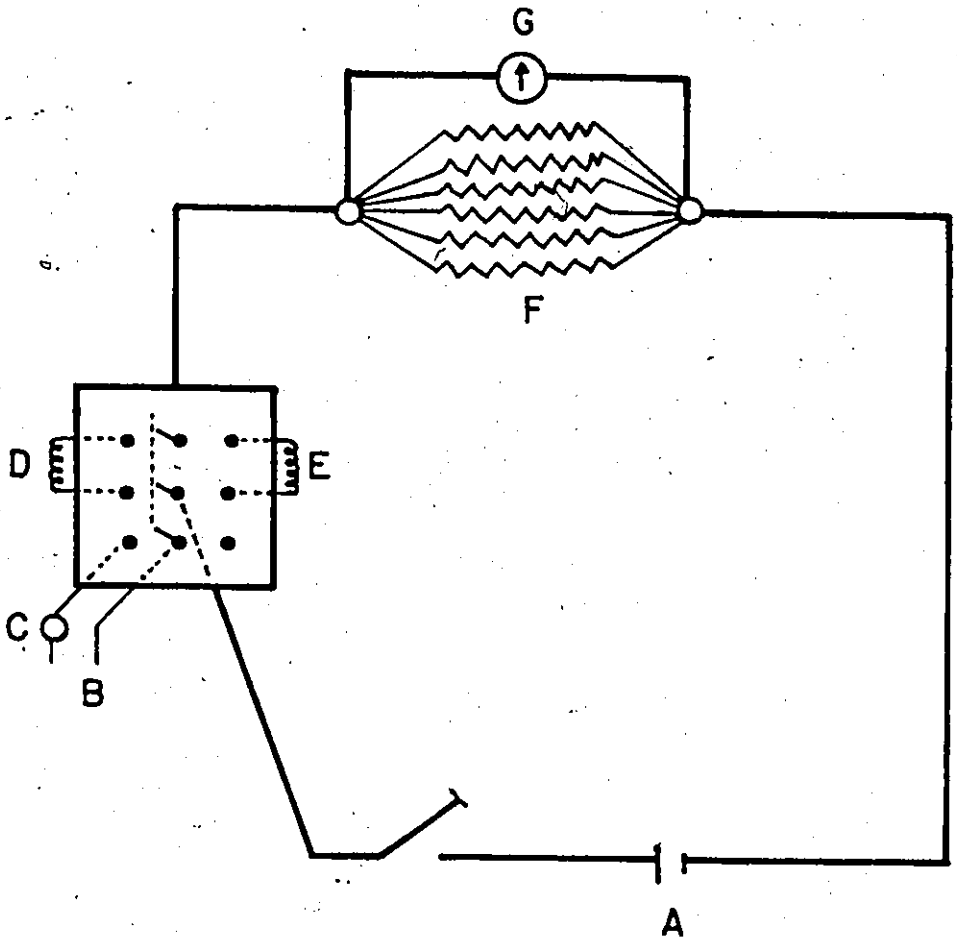
G
F
D
E
C
B
A

(e) Measurement

Thin-walled sample bulbs were filled with the finely ground samples. The bulb was sealed under N_2 gas. The bulb was then attached to the bulb holder by means of wax and suspended in calorimeter.

About 300 cm^3 of 4.02 N HCl was introduced into the calorimeter. When the calorimeter liquid and the bath had reached approximately the same temperature, the heating circuit was closed in the dummy position.

For purposes of evaluating the heat changes in the calorimeter, a correction was made for the exchange of heat between the calorimeter and its surroundings during the process. For this purpose, the course of temperature changes was divided into three periods. The first period was observed for 8-10 minutes prior to the reaction or calibration. In this period, the calorimeter temperature was recorded at one minute intervals until the temperature change was constant over a fairly long period of time (20-30 minutes) and the last 8-10 readings were considered. At this stage with the heating circuit still closed, the sample bulb was crushed under the calorimeter liquid. Dissolution was complete in 4 minutes or less which constitutes the second period of the calorimetric measurements. This period consisted of a sharp jump of temperature. Following the reaction, the third period began when rate of cooling of

the calorimeter followed Newton's law. A schematic diagram, Fig. 35 (graph A_1) shows three periods typically observed for exothermic reactions.

In order to achieve rapid dissolution of the samples, the calorimeter liquid was stirred rapidly. The sample holder was raised from the bottom of the calorimeter after breaking the bulbs, thus preventing trapping of the sample by the upper part of the bulb fragment at the bottom of the calorimeter.

During a calorimetric run, when the third period was complete, the temperature of the calorimeter liquid was restored to 25°C by allowing a few drops of liquid nitrogen to evaporate in a well (tube B, Fig. 33) which extended down into the calorimeter liquid. A new set of readings were recorded which constituted the first period of the calibration. The calorimeter heater was turned on and readings were recorded. The heating was of such a duration (300-725 sec.) so as to achieve the same temperature jump as was obtained during the actual reaction period. The heating time and current were measured with a precision better than ±0.1%. A typical curve for the dissolving of $ThBr_4$ in 4.02 N HCl containing a stoichiometric amount of KBr is shown in Fig. 35.

Evaluation of Data

(f) Heat capacity of the calorimeter

The energy q in joules supplied by calibration heater

Fig. 35. A typical temperature-time curve for dissolution of $ThBr_4$ in 4.02 N HCl containing stoichiometric amount of KBr. (The temperature scale shows the unconverted Helipot reading, the black dots are experimental points.)

Graph A_1:

Curve A-B = initial period

Curve B-C = reaction period

Curve C-D = cooling period

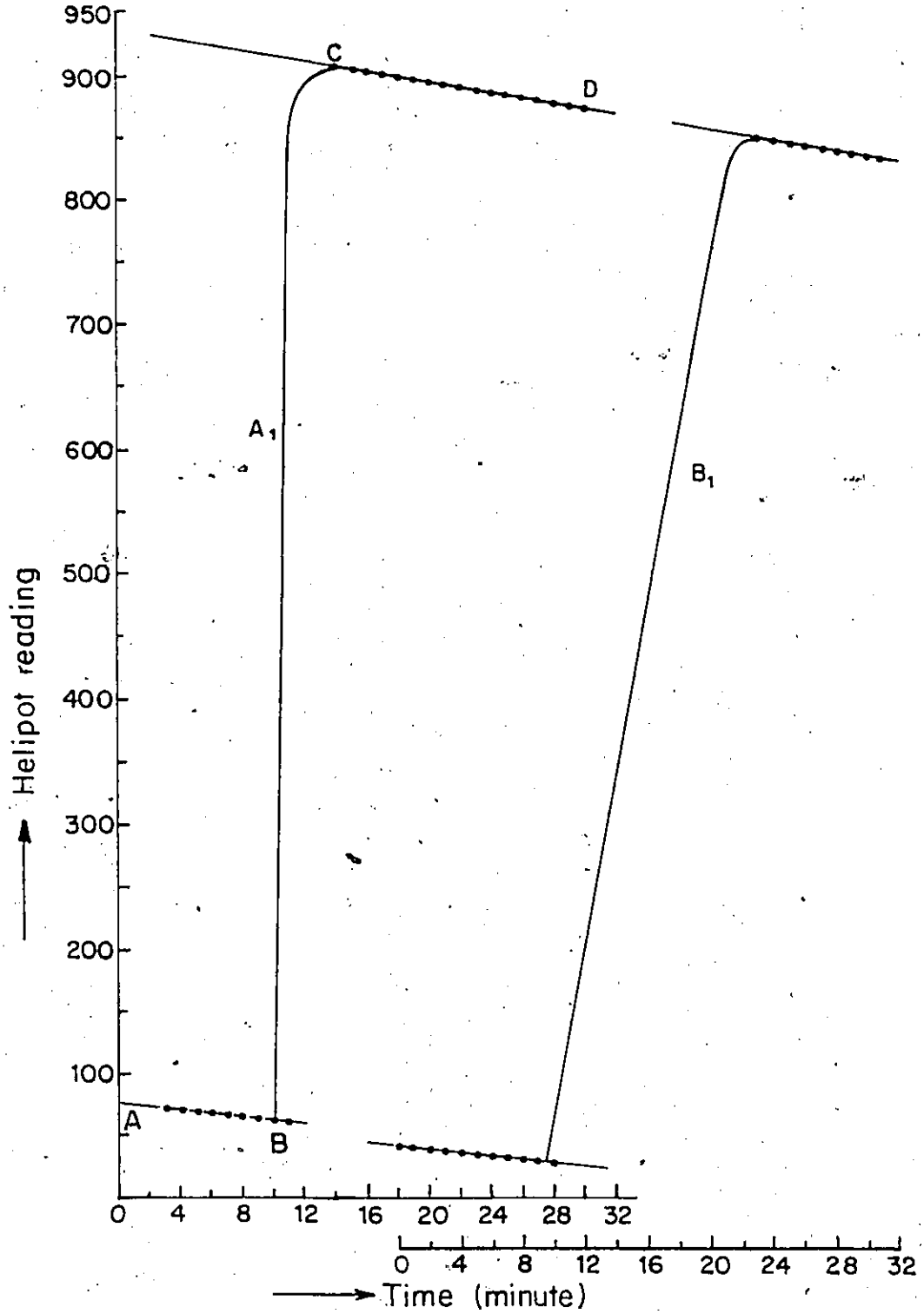
950
900
800
700
600
500
400
300
200
100
Helipot reading
A
B
C
D
A1
B1
0 4 8 12 16 20 24 28 32
0 4 8 12 16 20 24 28 32
Time (minute)

was determined using the equation,

$$q = I^2 Rt \quad \text{Joules} \qquad [37]$$

where R is the resistance of the heater in ohms (= 122.8 ohms), I the current in amperes, and t the time in seconds. In all our experiments, I was found to remain constant for each run. The heat capacity, C, of the calorimeter and its contents was determined (e.g., from curve B_1, Fig. 35) by using the equation,

$$C = \frac{q}{\Delta T} \quad \text{Joules per temperature scale division} \qquad [38]$$

where C is the heat capacity and ΔT represents the true temperature change in units of a Helipot scale*.

(g) Temperature jump

The temperature changes were determined graphically. A vertical line was drawn through the curve at the point corresponding to half the determined reaction time. The temperature time curves in the preperiod and after-period were extrapolated to intersect this vertical line. The difference of the two intersecting points was taken to be the temperature jump in Helipot scale divisions.

---

* 1 Helipot scale division corresponds to about 10^{-3} °C.

A more precise method of evaluation, used when reaction times are rather long, has been described by Kubaschewski et al. (128). This method was employed to check the results obtained by the other method for A_2ThBr_6 salts and in checking the accuracy of the calorimeter by measuring the heat of neutralization of a sample of THAM (tris(Hydroxymethyl)methylamine) with excess of 0.1 N HCl at 26°C. The mean of five values obtained with our calorimeter is 29.6 KJ mol^{-1}. The literature value is 29.56 KJ mol^{-1} (129).

(h) Heats of solution

The molar heats of solution, ΔH_s, were calculated by using the equation,

$$\Delta H_s = \frac{C.\Delta T.MW}{w} \quad \text{Joules mol}^{-1} \qquad [39]$$

where MW is the molecular weight of the sample, w is the mass of the sample, and C and ΔT have been defined earlier.

(iii) Spectra

Raman spectra of the solids were obtained with a Control Laser Model 552A argon laser (5145A°) operated at 2.0 watts. The finely ground samples were held in sealed, pyrex capillary tubes.

3. ANALYTICAL METHOD

Chlorides and bromides in different samples were determined by the Volhard method outlined on Page 50.

CHAPTER 4

PREPARATIVE WORK

Preparation of Compounds

4.1 Thorium Tetrachloride

The preparation of $ThCl_4$ has been discussed on Page 53 (refer to Fig. 20, Page 55). The product was purified by twice subliming in vacuum in a platinum tube heated to 760°C.

Procedure

The entire appratus shown in Fig. 36 was dried under vacuum while being flamed out. Crude, powdered, $ThCl_4$ (6-8 g) was transferred into the platinum tube, B (Fig. 36) in a glove box and its opening was tightly corked by a rubber stopper. The platinum tube containing the substance was quickly introduced into the quartz tube A through the opening G while N_2 gas was flowing through the system and the rubber cork was removed from the platinum tube. The quartz tube along with the Pt-tube was introduced into the tube furnace leaving 1/2 of the Pt-tube outside the furnace. The temperature of the furnace was slowly increased to 760°C and was heated for 6 h. It was found that a very light ashy substance, essentially oxide, was projected towards

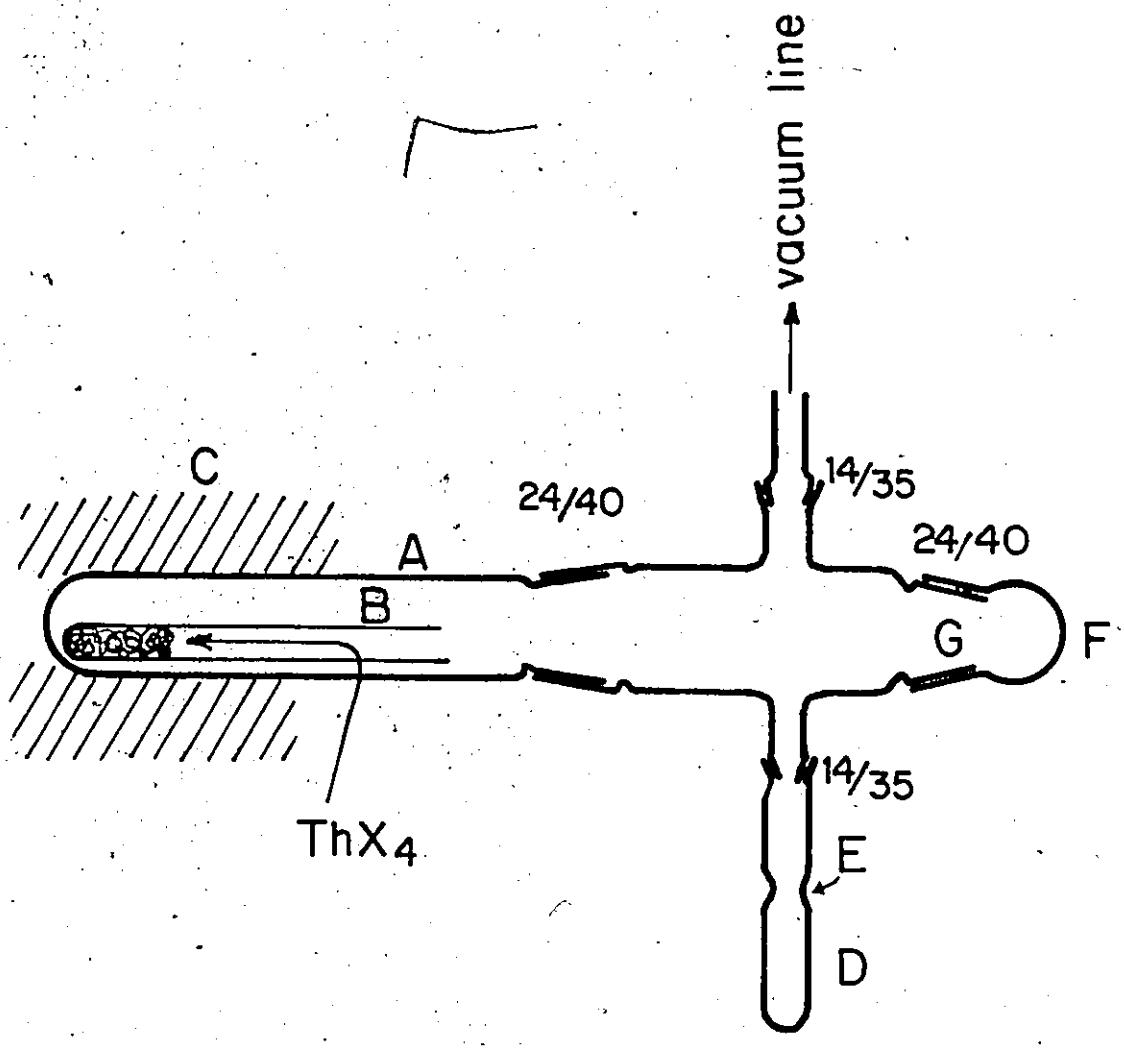

Fig. 36 Vacuum sublimation of $ThCl_4$ or $ThBr_4$.
A = 2.0 cm diameter quartz tube,
B = 1.0 cm diameter Pt-tube,
C = 2.5 cm diameter tube-furnace,
D = glass ampoule,
F = 24/40 male joint.

the opening G during the sublimation while the $ThCl_4$ was left sticking to the platinum tube in the cooler zone. With a stream of N_2 gas passing through the system, the impurities were tilted down through the opening G and the Pt-tube was scratched by a long stainless steel rod to break up the $ThCl_4$ cake. The resultant powder was collected in the ampoule D which was sealed at the constriction E under N_2 gas. After collecting 2-3 batches of product, all were introduced again into the Pt-tube for a second sublimation. The product was finally stored under N_2 gas in a sealed ampoule system, Fig. 16 (Page 43). Anal. Calcd. for $ThCl_4$: Cl, 37.93; Found: Cl, 37.84%.

4.2 Thorium Tetrabromide

Thorium tetrabromide was prepared by a published method (131) with some modification. Bromine (25 mL) was added dropwise to thorium powder (4.18 g) in 5 mL acetonitrile. The mixture was refluxed under N_2 gas for 12 h. The solid product was heated for 4 h at 180°C and was subsequently sublimed (three times) under vacuum in a platinum tube heated to 550°C. The procedure of sublimation was the same as outlined in Section 4.1 above. Finally, the product was stored under N_2 gas in a sealed ampoule system. Anal. Calcd. for $ThBr_4$: Br, 57.93. Found: Br, 57.70%.

Preparation of Ternary Salts

4.3 Potassium Hexachlorothorate, K_2ThCl_6

The preparation of K_2ThCl_6 is typical. A stoichiometric amount of KCl was added to $ThCl_4$. The mixture, with a weight of 7 g, was sealed in vacuo in a quartz tube and this was heated in a tube furnace at 730°C. Once a clear liquid had been formed, the tube was agitated to bring about thorough mixing and the tube was heated again for 0.5 h. The melt was quenched in air and the solidified mass was ground in a dry nitrogen atmosphere and stored in a sealed ampoule system (Fig. 16).

Unless otherwise specified, all other salts, Cs_2ThCl_6, $KThCl_5$, K_3ThCl_7, K_2ThBr_6 and Cs_2ThBr_6 were prepared in the same way as described in Section 4.3 above.

Completeness of reaction was shown by x-ray diffraction patterns which showed no lines that could be attributed to either of the starting materials.

Attempts were made to prepare $KThBr_5$ and K_3ThBr_7 by mixing stoichiometric amounts of KBr with $ThBr_4$ and fusing as described in the case of K_2ThCl_6. X-ray diffraction results and the existence of these salts will be described in the ensuing discussion section.

CHAPTER 5

RESULTS AND DISCUSSION

The enthalpies of complexing, ΔH_c, in forming K_2ThCl_6, Cs_2ThCl_6, K_2ThBr_6 and Cs_2ThBr_6 from the constituent halides, were studied by solution calorimetry.

As mentioned earlier, the calorimeter liquid was 4.02 N HCl. Acid was used as a calorimetric liquid in order to suppress in part the hydrolysis of dissolved thorium compounds. When water was used in the calorimeter, as in Chauvenet's work (109), hydrolysis caused undue evolution of heat, and the calculation of enthalpies of complex formation involved taking differences of large numbers. It is believed that the acid made the calorimetric results more reproducible.

Enthalpies of complexing for A_2ThX_6 salts, i.e., enthalpies of reaction [40], were determined by measuring

$$2AX(C) + ThX_4(C) \xrightarrow{\Delta H_c} A_2ThX_6(C) \qquad [40]$$

the heats of solution of each of the substances appearing in the equation. We assumed that A_2ThX_6 dissolved in hydrochloric acid solution to give the same species as were formed when ThX_4 and AX were dissolved separately. At any rate, the complex, Cs_2ThCl_6 may be crystallized from a solution of the component chlorides in concentrated acid (110).

The following partial reactions were used to calculate the enthalpies of complexing.

$$2AX(c) + \{H_2ThX_6 + nHCl\} \xrightarrow{2\Delta H_1} \{2AX + H_2ThX_6 + nHCl\} \quad [41]$$

$$ThX_4(c) + \{2AX + (n+2)HCl\} \xrightarrow{\Delta H_2} \{2AX + H_2ThX_6 + nHCl\} \quad [42]$$

$$\{2AX + H_2ThX_6 + nHCl\} \xrightarrow{-\Delta H_3} A_2ThX_6(c) + \{(n+2)HCl\} \quad [43]$$

$$\{2AX + H_2ThX_6 + nHCl\} + \{(n+2)HCl\} \xrightarrow{\Delta H_4} \{H_2ThX_6 + nHCl\} + \{2AX + (n+2)HCl\} \quad [44]$$

From which we obtain:

$$2AX(C) + ThX_4(C) = K_2ThX_6(C) \text{ and}$$

$$\Delta H_c = \sum_{i=1}^{4} \Delta H_i .$$

The enthalpy of solution, ΔH_4, is assumed to be zero or negligible with respect to other quantities because the solutes were essentially at infinite dilution. Therefore, the enthalpy of complexing, ΔH_c, of the process [40] is expressed as,

$$\Delta H_c = 2\Delta H_1 + \Delta H_2 - \Delta H_3 \quad [45]$$

Westland et al. (111,130,132) observed with the tetrahalides of various elements, that the measured enthalpies

were essentially independent of sample size. Thus, the solutes behaved as though they are at infinite dilution. We believe this condition to have obtained in the present study as well. The heats of solution, ΔH_1, ΔH_2 and ΔH_3 are recorded in Tables 17, 18 and 19 respectively.

The heats of solutions of the alkali halides at infinite dilution in 4.02 N hydrochloric acid, are not measurably influenced by the presence of small quantities of the solutes, MX_4. Therefore, values of ΔH_1 obtained in the previous researches (130,132) were used in the present work (Table 17). Equivalent amounts of alkali halide were added to the calorimeter liquid when the enthalpies of solution of $ThCl_4$ and $ThBr_4$ were measured, although there was no evidence that such additions had any influence on the measurements.

As a check on the purity of the $ThCl_4$, we obtained the value -186.2 KJ mol^{-1} for the enthalpy of solution in 6.00 N hydrochloric acid. This compares well with the value -185.3 KJ mol^{-1} obtained by Eyring and Westrum (133). A more negative result may suggest a purer sample, i.e., one more free from hydrolysis.

Westland et al. (130) have argued that in the case of MBr_4 and its salts, the bromide mixing according to equation [46]

$$MBr_4 + (6-x)Cl^- \rightarrow (MBr_xCl_{6-x})^{2-} + (4-x)Br^- \qquad [46]$$

Table 17. Enthalpy of solution, ΔH_1, for alkali halides in 4.02 N hydrochloric acid. Values taken from references (130) and (132).

COMPOUND	ΔH_1 KJ mol^{-1}
KCl	18.39 ± 0.11
CsCl	13.70 ± 0.24
KBr	19.87 ± 0.04
CsBr	23.25 ± 0.15

Table 18. Enthalpy of solution of thorium halides, ΔH_2, in 4.02 N hydrochloric acid containing alkali halide.

COMPOUND	SAMPLE WEIGHT g	ΔH_2 KJ mol^{-1}	MEAN
$ThCl_4$	1.7835	-213.2	
	1.3514	-215.4	
	1.2694	-213.9	
	1.2495	-213.3	
	1.6085	-213.0	-213.8 ± 1.0
$ThBr_4$	2.1541	-263.5	
	1.7000	-264.5	
	1.8065	-260.0	
	1.7778	-265.7	
	2.1062	-260.8	-262.9 ± 2.4

Table 19. Enthalpy of solution of alkali-metal hexhal othorates, ΔH_3, in 4.02 N hydrochloric acid.

COMPOUND	SAMPLE WEIGHT g	ΔH_3 KJ mol^{-1}	MEAN
K_2ThCl_6	2.1941	-124.8	
	1.1760	-125.0	
	0.9671	-126.2	
	1.9890	-127.5	
	1.3559	-128.1	-126.3 ± 1.5
Cs_2ThCl_6	3.4708	-104.5	
	2.9195	-104.3	
	3.0215	-107.0	
	2.5034	-105.3	-105.3 ± 1.2
K_2ThBr_6	1.2039	-198.4	
	1.4558	-202.6	
	1.3083	-200.5	
	1.5305	-199.5	-200.2 ± 1.8
Cs_2ThBr_6	2.0607	-144.5	
	2.1315	-142.0	
	1.9867	-144.2	
	2.4398	-143.0	
	2.3357	-142.8	-143.3 ± 1.0

was of little or no significance for the measurements as the complexes are entirely labile. Moreover, there was presumably negligible complexed bromide in the system owing to the large ratio of chloride to bromide in solution. In addition, the halogeno-species were partially hydrolyzed to a mixture of hydroxo- and aquo-species. The validity of calorimetric measurements depends on the ready attainment of the same equilibrium state in each case and the lability of the compounds under study assured this.

The heats of complexing, ΔH_c, of the ternary complexes calculated from data in Tables 17 to 19 are given in Table 20.

Evaluation of Experimental Data

The numerical magnitude of the enthalpy of complexing which is a measure of the thermodynamic stability of alkali-metal hexahalothorates, increases from potassium to caesium (Table 20). This is normal for ternary complexes and may be accounted for by the consideration of the following reactions:

$$A_2ThX_6(C) \xrightarrow{+U_{A_2ThX_6}} 2A^+(g) + ThX_6^{2-}(g) \qquad [47]$$

$$ThX_6^{2-}(g) \xrightarrow{+\Delta H_D} ThX_4(g) + 2X^-(g) \qquad [48]$$

$$2A^+(g) + 2X^-(g) \xrightarrow{-2U_{AX}} 2AX(C) \qquad [49]$$

Table 20. Enthalpy of complexing, ΔH_c, of the alkali-metal hexahalothorates.

COMPOUND	ΔH_c/KJ mol^{-1}
K_2ThCl_6	-50.7 ± 2
Cs_2ThCl_6	-81.1 ± 2
K_2ThBr_6	-23.3 ± 3
Cs_2ThBr_6	-73.1 ± 3

By adding the equations [47] to [49], we obtain the overall reaction,

$$A_2ThX_6(C) \xrightarrow{\Delta H_R} 2AX(C) + ThX_4(C) \qquad [50]$$

and

$$\Delta H_R = \Delta H_D - (2U_{AX} - U_{A_2ThX_6}) \qquad [51]$$

where $U_{A_2ThX_6}$ and U_{AX} represent lattice energies of A_2ThX_6 and AX respectively. ΔH_D is the enthalpy of dissociation of the complex anion ThX_6^{2-} and ΔH_R is the experimentally measured enthalpy of decomposition of the solid A_2ThX_6.

Because of the smaller size of the X^- anion compared to the size of the MX_6^{2-} ion, the difference in the lattice energies $(2U_{AX} - U_{A_2ThX_6})$ increases (or becomes less negative) as the size of the alkali metal ion decreases. As the heat of dissociation, ΔH_D of the MX_6^{2-} ion is common to both potassium and caesium hexahalothorates, it follows that the heat of decomposition, ΔH_R (Eqn. 51), for the hexahalometallates should increase with increasing cationic radius. This is a general result for hexahalometallates.

Table 20 reveals one important property of thorium. We see from the enthalpies of complexing that K_2ThCl_6 is ca. 27 KJ mol^{-1} more stable than K_2ThBr_6. Again, Cs_2ThCl_6 is more stable than Cs_2ThBr_6 (Table 20). This illustrates

that thorium prefers chloride complexation and gives an indication of class a character of Th(IV). A more full description of its class a behaviour will appear in the section dealing with halide-ion affinity.

The uncertainty limits given in Tables 17-19 are the standard deviations of the measurements. These limits do not include an estimate of accuracy as influenced by purity of materials, etc.

An additional uncertainty pertains to the K_2ThCl_6 salt. As mentioned earlier, published reports (114-116) on the phase diagram of K_2ThCl_6 indicate that the salt melts incongruently. However, a recently published phase diagram (117) along with an examination of Figures 31a and 31b, taken from references 115 and 116 respectively, lead us to believe that a too rapid cooling of the melt produced the compound in some cases by a non-equilibrium process. Fig. 31a shows a line corresponding to K_2ThCl_6. Figure 31b shows a peritectic mixture at 406°C. This diagram was obtained by Ionov et al. (116) who obtained the phase diagram by slow cooling. If, on the other hand, the melt is rapidly cooled from 700°C, K_2ThCl_6 could form by a non-equilibrium process.

X-ray Diffraction Studies

It was mentioned in Chapter 4 that $KThCl_5$ and K_3ThCl_7 were prepared in a similar way to K_2ThCl_6. There are several

reports that the former two compounds melt congruently (114,116,134). Debye-Scherrer patterns of each of the three solids so obtained were distinct from one another. The X-ray diffraction reflections of K_2ThCl_6, $KThCl_5$ and K_3ThCl_7 are given in Tables 21-23, respectively. The pattern of K_2ThCl_6 (Table 21) was indexed as tetragonal. A line with $\sin^2\theta = 0.0149$ appeared strongly in the patterns of $KThCl_5$ and K_3ThCl_7 and weakly in the pattern of K_2ThCl_6. It is therefore likely that a small quantity of the 1:1 and/or the 3:1 compound occurred in the preparation of K_2ThCl_6. The heat of solution of an equimolar mixture of $KThCl_5$ and K_3ThCl_7 would differ from the heat of solution of $2K_2ThCl_6$ by the enthalpy of the process [52]:

$$2K_2ThCl_6 = KThCl_5 + K_3ThCl_7 \qquad [52]$$

This may be a small quantity as in the case of the analogous process: $3CaB_2O_4 = CaB_4O_7 + Ca_2B_2O_5$ for which $\Delta H_{reaction}$ is -2.1 KJ mol^{-1} (135). If the K_2ThCl_6 contained as much as 10 mole percent impurities and the enthalpy of reaction [52] were as much as ±20 KJ, the error in the measured value of ΔH_3 (Table 19) would be only ±1 KJ mol^{-1}. The thermal data for K_2ThCl_6 presented in Tables 19 and 20 are thus the subject of some uncertainty in this way, but it will be seen later that the data for the various salts are satisfactorily self-consistent.

Table 21. X-ray diffraction data for K_2ThCl_6.

$\sin^2\theta$ (obs.)	d (A°) (obs.)	hKℓ	$\sin^2\theta$ (calcd.)	Relative Intensity
0.0121	7.00	101	0.0123	vs
0.0149	6.31			w
0.0184	5.68	111	0.0178	vs
0.0327	4.26	102	0.0327	ms
0.0383	3.94	112	0.0382	ms
0.0440	3.67	220	0.0440	vs
0.0492	3.47	202	0.0492	w
0.0820	2.69	312	0.0822	s
0.0835	2.66	203	0.0832	s
0.0936	2.52	410	0.0935	s
0.1049	2.38	223	0.1052	w
0.1265	2.16	332	0.1262	w
0.1373	2.08	422	0.1372	w
0.1550	1.96	413	0.1547	w

Table 22. X-ray diffraction data for $KThCl_5$.

$\sin^2\theta$ (obs.)	d (A°) (obs.)	Relative Intensity
0.0149	6.31	S
0.0162	6.05	w
0.0283	4.58	ms
0.0349	4.12	w
0.0416	3.78	ms
0.0474	3.54	w
0.0527	3.35	S,br
0.0793	2.73	ms
0.0910	2.55	w
0.1014	2.42	w
0.1102	2.32	w
0.1498	1.99	S
0.1996	1.72	w

Table 23. X-ray diffraction data for K_3ThCl_7.

$\sin^2\theta$ (obs.)	d (A°) (obs.)	Relative Intensity
0.0149	6.31	vs
0.0199	5.46	vs
0.0401	3.85	vs
0.0545	3.30	w
0.0576	3.21	w
0.0763	2.79	S
0.0869	2.61	ms
0.0958	2.49	w
0.0995	2.44	w
0.1074	2.35	w
0.1341	2.10	w,br.
0.1518	1.98	w
0.1638	1.90	w

Cs_2ThCl_6 is trigonal and the lattice parameters are taken from the literature (119-120).

Debye-Scherrer patterns of K_2ThBr_6 (Table 24) and Cs_2ThBr_6 (Table 25) were indexed and had tetragonal and trigonal symmetries respectively. X-ray diffraction patterns of these two salts gave no indication of the presence of starting materials and all the lines were indexed. The X-ray densities of K_2ThBr_6 and Cs_2ThBr_6 (Table 26) obtained by Yatsimirskii's method (Eqn. 54) agree with those of the picnometer measurements. This provides further assurance of the correctness of the indexing. Although the phase diagrams of these two compounds have not been reported, the phase diagrams of the analogous uranium compounds viz., K_2UBr_6 and Cs_2UBr_6 are known and are both congruently melting compounds (118). In addition, attempts were made to prepare $KThBr_5$ and K_3ThBr_7 from the component halides as described in Chapter 4.

The Debye-Scherrer pattern of the expected complex $KThBr_5$ was identical to that of a mixture of $ThBr_4$ + KBr and that of expected K_3ThBr_7 was similar to that of K_2ThBr_6 +KBr implying that the $KThBr_5$ and K_3ThBr_7 complexes were not formed. These findings strongly indicate that K_2ThBr_6 is a congruently melting compound.

The lattice parameters of K_2ThCl_6, K_2ThBr_6 and Cs_2ThBr_6 were obtained from extrapolated Nelson-Riely plots, and are listed in Table 27.

Table 24. X-ray diffraction data for K_2ThBr_6.

$\sin^2\theta$ (obs.)	d (A°) (obs.)	hKℓ	$\sin^2\theta$ (calcd.)	Relative Intensity
0.0139	6.53	101	0.0139	vs
0.0188	5.62	111	0.0184	vs
0.0376	3.97	002	0.0376	w
0.0421	3.75	102	0.0421	ms
0.0501	3.44	301	0.0499	S
0.0557	3.26	202	0.0556	ms
0.0680	2.95	321	0.0679	w
0.0736	2.84	222	0.0736	w
0.0824	2.68	312	0.0826	w
0.0900	2.57	420	0.0900	w
0.0992	2.44	421	0.0994	w
0.1096	2.33	402	0.1096	w
0.1267	2.16	511	0.1264	w
0.1439	2.03	440	0.1440	w
0.1545	1.96	512	0.1546	w
0.1656	1.89	333	0.1656	w

Table 25. X-ray diffraction data for Cs_2ThBr_6.

$\sin^2\theta$ (obs.)	d (A°) (obs.)	hKℓ	$\sin^2\theta$ (calcd.)	Relative Intensity
0.0176	5.80	101	0.0177	vs
0.0349	4.12	111	0.0351	ms
0.0438	3.68	201	0.0438	vs
0.0605	3.13	210	0.0609	ms
0.0702	2.91	211	0.0699	w
0.0810	2.71	003	0.0810	s
0.0873	2.61	301	0.0873	ms
0.0968	2.47	212	0.0969	w
0.1158	2.26	203	0.0158	w
0.1222	2.20	311	0.1221	ms
0.1526	1.97	104	0.1527	w

Table 26. Densities of K_2ThBr_6 and Cs_2ThBr_6.

COMPOUND	DENSITY BY X-RAY MEASUREMENTS ($g\ cm^{-3}$)	DENSITY BY PICNOMETER MEASUREMENTS ($g\ cm^{-3}$)
K_2ThBr_6	5.01	4.74
Cs_2ThBr_6	5.08	4.99

Table 27. Calculated enthalpies of formation at 298K.

COMPOUND	SYMMETRY	LATTICE CONSTANT A°	r,A°*	U KJ mol^{-1}	$\Delta H_f^\circ(A_2MX_6,c)$ KJ mol^{-1}	$\Delta H_f^\circ(MX_6^{2-},g)$ KJ mol^{-1}	MEAN $\Delta H_f^\circ(MX_6^{2-},g)$
K_2ThCl_6	Tetragonal	a 10.36 c 9.32	4.372	1582.0	-2108.0	-1555.0	
Cs_2ThCl_6	Trigonal	a 7.629 c 6.050	4.670	1492.0	-2151.0	-1563.0	-1559.0
K_2ThBr_6	Tetragonal	a 11.478 c 7.94	4.437	1561.0	-1774.0	-1241.0	
Cs_2ThBr_6	Trigonal	a 9.537 c 8.10	4.741	1473.0	-1826.0	-1257.0	-1249.0
Cs_2UCl_6	Trigonal	a 7.507 c 6.050	4.620	1507.0	-2005.0	-1403.0	
K_2UBr_6	Tetragonal	a 10.94 c 10.67	4.742	1473.0	-1634.0	-1190.0	

* r is the effective cation-anion distance (= $r_+ + r_-$) as given by Yatsimirskii's method (121).

Lattice Energies

The values of the lattice energies of A_2MX_6 complexes (A=K and Cs; M=Th and U; X=Cl and Br) were estimated by use of the Kapustinskii-Yatsimirskii expression (Eqn. [32], Chapter 2). According to Yatsimirskii,

$$r(= r_+ + r_-) = \frac{11.85}{\sqrt[3]{J}} \qquad [53]$$

where J is the concentration (moles of ions in 1000 cm^3 of the solid salt). Further,

$$J = \frac{1000 \cdot d(\Sigma n)}{M} \qquad [54]$$

where d is the density of the substance, M is its molecular weight and (Σn) is the number of ions in the molecular formula of the complex salt.

It should be noted that the lattice energies calculated by the Kapustinskii and Yatsimirskii method are very approximate because the anionic groups are treated as mere point charges. A superior approach is that of Jenkins and Pratt but their procedure requires a knowledge of the basic radius of the MX_6^{2-} ion and the charge on the terminal halogen, i.e., q_x, as discussed in Chapter 2. The cruder calculations are presented here in the belief that they lead to valid comparisons in properties between closely related compounds. As we are interested in obtaining difference

values, the exercise appears to be justified.

Lattice energy data (Table 27) reveal that K_2ThCl_6 is 90 KJ mol^{-1} more stable than Cs_2ThCl_6 which compares well with bromo-system, where K_2ThBr_6 is 88 KJ mol^{-1} more stable than Cs_2ThBr_6. These differences arise from the differences in the size of the cations. Again, A_2ThCl_6 is 20±1 KJ mol^{-1} more stable than A_2ThBr_6. The lattice energies of the uranium compounds are also listed in Table 27.

Standard Enthalpies of Formation of A_2MX_6 Salts and MX_6^{2-} Ions

Scheme 6 embodies the cycles from which the relations for $\Delta H_f^\circ(A_2MX_{6,c})$ (Eqn. 55) and $\Delta H_f^\circ(MX_6^{2-},g)$ (Eqn. 56) were derived.

$$2A^+(g) + 2X^-(g) + MX_4(g) \xrightarrow{\overline{\Delta H}_g} 2A^+(g) + [MX_6]^{2-}(g)$$

$$\uparrow U_{AX} \qquad \uparrow \Delta H_{subl.} \qquad \uparrow U_{A_2MX_6}$$

$$2AX(c) + MX_4(c) \xrightarrow{\Delta H_c} A_2[MX_6](c)$$

Scheme 6

$$\Delta H_f^\circ(A_2MX_{6,c}) = \Delta H_c + 2\Delta H_f^\circ(AX,c) + \Delta H_f^\circ(MX_4,c) \qquad [55]$$

$$\Delta H_f^\circ(MX_6^{2-},g) = U_{(A_2MX_6)} - 2\Delta H_f^\circ(A^+,g) + \Delta H_f^\circ(A_2MX_{6,c}) \qquad [56]$$

The relations [55] and [56] were solved using the enthalpy of complexing values (Table 20), the lattice energies of the

complex salts (Table 27) and other ancillary data shown below. The values for $\Delta H_f^\circ(A_2MX_6,c)$ and $\Delta H_f^\circ(MX_6^{2-},g)$ are listed in Table 27.

The following standard thermodynamic data were used consistently throughout our study.

$$\Delta H_f^\circ(K^+)(g) = 514.2 \text{ KJ mol}^{-1} \quad (136) \qquad [57]$$

$$\Delta H_f^\circ Cs^+(g) = 452.3 \text{ KJ mol}^{-1} \quad (136) \qquad [58]$$

$$\Delta H_f^\circ KCl(c) = -436.7 \text{ KJ mol}^{-1} \quad (136) \qquad [59]$$

$$\Delta H_f^\circ CsCl(c) = -442.8 \text{ KJ mol}^{-1} \quad (136) \qquad [60]$$

$$\Delta H_f^\circ KBr(c) = -393.8 \text{ KJ mol}^{-1} \quad (136) \qquad [61]$$

$$\Delta H_f^\circ CsBr(c) = -394.5 \text{ KJ mol}^{-1} \quad (137) \qquad [62]$$

$$\Delta H_f^\circ ThCl_4(c) = -1184.4 \text{ KJ mol}^{-1} \quad (138) \qquad [63]$$

$$\Delta H_f^\circ ThBr_4(c) = -963.4 \text{ KJ mol}^{-1} \quad (138) \qquad [64]$$

$$\Delta H_f^\circ UCl_4(c) = -1018.4 \text{ KJ mol}^{-1} \quad (112) \qquad [65]$$

$$\Delta H_f^\circ UBr_4(c) = -802.5 \text{ KJ mol}^{-1} \quad (138) \qquad [66]$$

$$\Delta H_c(Cs_2UCl_6) = -100.8 \text{ KJ mol}^{-1} \quad (112) \qquad [67]$$

$$\Delta H_c(K_2UBr_6) = -43.5 \text{ KJ mol}^{-1} \quad (113) \qquad [68]$$

Halide Ion Affinities

The two-halide ion affinities, $\overline{\Delta H}_x(g)$, are of interest as they refer to the processes of forming the complex anion in the gas phase in which the effects of crystal forces do not play a role. This quantity reveals the acceptor property of $MX_4(g)$. The double-halide ion affinity ($\overline{\Delta H}_x(g)$) of gaseous tetrahalides MX_4 is defined as the enthalpy change for the process,

$$MX_4(g) + 2X^-(g) \rightarrow MX_6^{2-}(g) \qquad [69]$$

The values of $\overline{\Delta H}_x(g)$ are given by [70]:

$$\overline{\Delta H}_x(g) = \Delta H_f^\circ(MX_6^{2-},g) - 2\Delta H_f^\circ(X^-,g) - \Delta H_f^\circ(MX_4,g) \qquad [70]$$

The energy of reorganizing sp^3 hybridization of the gaseous MX_4 molecule to sp^3d^2 hybrids is involved in $\overline{\Delta H}_x(g)$ but it is difficult to evaluate this factor. Values of $\overline{\Delta H}_x(g)$ of thorium and uranium complexes are given in Table 28A.

The chloride ion affinity of $ThCl_4(g)$ is about 129 KJ mol^{-1} more negative than the bromide ion affinity of $ThBr_4(g)$ (comparisons were made from the mean values, Table 28A). In addition, the double chloride ion affinity of $ThCl_4(g)$ is about 52 KJ mol^{-1} more negative than that of $UCl_4(g)$. This clearly demonstrates class a behaviour of Th(IV) (139). However, the above situation is reversed for $UCl_4(g)$ and $UBr_4(g)$. The double bromide ion affinity of $UBr_4(g)$ is about

Table 28A. Double halide-ion affinities, $\overline{\Delta H}_x(g)$, for the process $MX_4(g) + 2X^-(g) = MX_6^{x2-}(g)$. Values in KJ mol^{-1}.

CONDENSED PHASE REACTION PRODUCT	$\overline{\Delta H}_x(g)$	MEAN
K_2ThCl_6	-147.5	
Cs_2ThCl_6	-155.8	-151.6
K_2ThBr_6	-15.0	
Cs_2ThBr_6	-31.0	-23.0
Cs_2UCl_6	-99.8	
K_2UBr_6	-108.7	

Table 28B. Double halide-ion affinities for related systems, KJ mol^{-1}.

	Cl	Br
Zr	-26	-9, -1
Hf	-37	-46
Sn	+39	+46
Nb	+3	+5
Ta	-35	+38

9 KJ mol^{-1} more negative than that of $UCl_4(g)$ and is also 86 KJ mol^{-1} more negative than the double bromide ion affinity of $ThBr_4(g)$. It can be concluded that U(IV) has incipient class b character, or in Pearson's terminology (140), U(IV) is a softer acid than Th(IV). We believe that the tendency toward class b character shown by certain high-valent elements may be attributed to their power to polarize atoms bonded to them. Indeed, U(IV) has a greater effective nuclear charge than has Th(IV) owing to the poor shielding of the 5f electrons. The uranium core thus has a stronger power to polarize electron densities from bromides and hence a stronger $p_\pi \rightarrow d_\pi$ bonding in UBr_6^{2-} moiety compared to $ThBr_6^{2-}$ ion.

The comparison of the halide ion affinities of $UCl_4(g)$ and $UBr_4(g)$ is reminiscent of those observed for $HfCl_4(g)$ and $HfBr_4(g)$ (130,132) (Table 28B). By referring to Table 28B, the double-halide ion affinities of MX_4 (M=Th and U) may be compared with those of MX_4 (M=Zr, Hf, Nb, Ta, and Sn), a group of compounds studied previously in this laboratory (111,130,132).

The chloride ion affinity of $ThCl_4(g)$ and the bromide ion affinity of $UBr_4(g)$ are the greatest of all the values listed. This is remarkable in view of the large size of the actinide ions for which $M^{4+}-X^-$ coulombic interaction is not strong. However, X^-X^- repulsions in the MX_6^{2-} groups would be smaller for the actinide ions also. The order of

the acceptor strength towards Cl^- is $ThCl_4 > UCl_4 > HfCl_4 > TaCl_4 > ZrCl_4 > NbCl_4 > SnCl_4$. The order of bromide affinities is similar except that the thorium compound follows that of halfnium, i.e., $UBr_4 > HfBr_4 > ThBr_4 > ZrBr_4 > NbBr_4 > TaBr_4 > SnBr_4$.

Jenkins and Pratt have shown that the chloride ion affinities of various other transition element tetrachlorides follow the same trend of diminishing in magnitude toward the right in a period (124-125). They found the same to be true for the homolytic M-Cl bond energies (see later) as well. Rather paradoxically, Brown et al. found that the stretching force constant increases in the series $HfCl_6^{2-}$ through $PtCl_6^{2-}$ and they related this to trends to σ- and π-bonding and optical electronegativities (141). They argued that since the increase of atomic number in a particular period increases the effective nuclear charge, optical electronegativity of the metal ion thereby increases, which causes increased σ- and π-bonding in the M-Cl system.

However, the two-halide ion affinities represent differences between the thermodynamic states of reactants and products and, therefore, may not relate in a simple fashion to the bond order and force constant of product species alone.

The calculations that led to the foregoing results made use of data taken from the literature. The enthalpies of sublimation at the indicated temperatures were,

$$\Delta H_{subl.}ThCl_4(1131K) = 247.0 \text{ KJ mol}^{-1} \text{ (142)} \quad [71]$$

$$\Delta H_{subl.}ThBr_4(1088K) = 184.0 \text{ KJ mol}^{-1} \text{ (142)} \quad [72]$$

$$\Delta H_{subl.}UCl_4(863K) = 193.7 \text{ KJ mol}^{-1} \text{ (137)} \quad [73]$$

$$\Delta H_{subl.}UBr_4(792K) = 175.3 \text{ KJ mol}^{-1} \text{ (137)} \quad [74]$$

Use of the heat capacities (143) gave the following room temperature values:

$$\Delta H^\circ_{subl.}ThCl_4(c) = 269.0 \text{ KJ mol}^{-1} \quad [75]$$

$$\Delta H^\circ_{subl.}ThBr_4(c) = 204.8 \text{ KJ mol}^{-1} \quad [76]$$

$$\Delta H^\circ_{subl.}UCl_4(c) = 207.4 \text{ KJ mol}^{-1} \quad [77]$$

$$\Delta H^\circ_{subl.}UBr_4(c) = 189.5 \text{ KJ mol}^{-1} \quad [78]$$

Using the above $\Delta H^\circ_{subl.}$ values of $MX_4(c)$, the $\Delta H^\circ_f MX_4(g)$ were obtained:

$$\Delta H^\circ_f ThCl_4(g) = -915.4 \text{ KJ mol}^{-1} \quad [79]$$

$$\Delta H^\circ_f ThBr_4(g) = -758.6 \text{ KJ mol}^{-1} \quad [80]$$

$$\Delta H_f^\circ UCl_4(g) = -811.0 \text{ KJ mol}^{-1} \quad [81]$$

$$\Delta H_f^\circ UBr_4(g) = -613.0 \text{ KJ mol}^{-1} \quad [82]$$

The standard enthalpies of formation of $Cl^-(g)$ and $Br^-(g)$ are given below,

$$\Delta H_f^\circ Cl^-(g) = -246.0 \text{ KJ mol}^{-1} \text{ (144)} \quad [83]$$

$$\Delta H_f^\circ Br^-(g) = -233.9 \text{ KJ mol}^{-1} \text{ (144)} \quad [84]$$

Bond-energies

Jenkins and Pratt (124) have defined M-X bond energies in the MX_6^{2-} moiety in two different ways that involve the quantities shown in Fig. 37. One definition refers to the homolytic fission of the bond,

$$MX_6^{2-}(g) \xrightarrow{\Delta H_f^a(MX_6^{2-},g)} M(g) + 6X(g) + 2e \quad [85]$$

in which case, the average (homolytic) bond energy, $E(M\text{-}X)_{hom}$, is defined as,

$$E(M\text{-}X)_{hom} = -\frac{1}{6}\Delta H_f^a(MX_6^{2-},g) \quad [86]$$

Alternatively, by referring to the heterolytic fission of the bond [87]:

$$MX_6^{2-}(g) \xrightarrow{\Delta H_f^i(MX_6^{2-},g)} M^{4+}(g) + 6X^-(g) \quad [87]$$

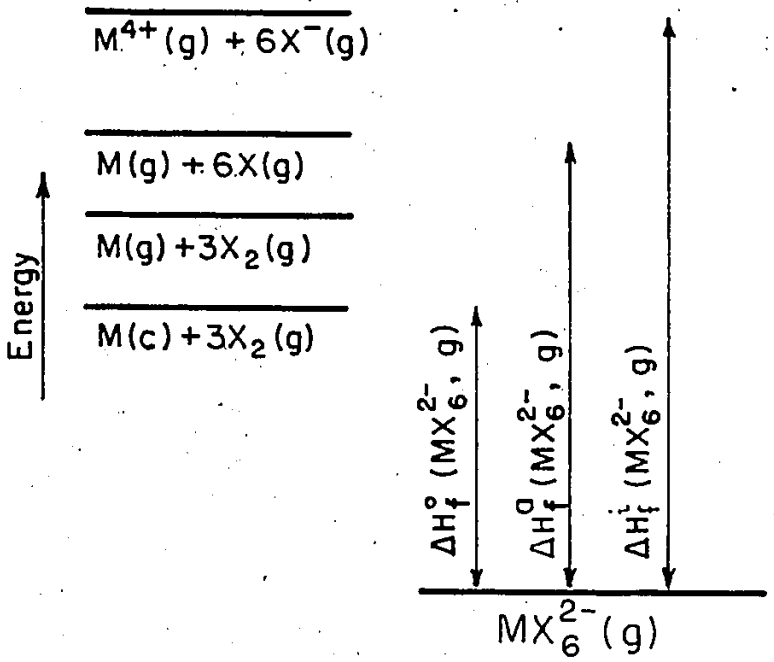

Fig. 37 Energy – Thermodynamic correlation for bond – energy definitions.

The average (heterolytic) bond energy, $E(M\text{-}X)_{het}$ is given as,

$$E(M\text{-}X)_{het} = -\frac{1}{6}\,\Delta H_f^i(MX_6^{2-},g) \qquad [88]$$

The quantities $\Delta H_f^a(MX_6^{2-},g)$ and $\Delta H_f^i(MX_6^{2-},g)$ are the change of enthalpies of the processes [85] and [87] respectively.

Pearson (145) has maintained that the heterolytic bond energy represents the coordinate bond energy and is more informative. From Fig. 37, it is evident that,

$$-\Delta H_f^a(MX_6^{2-},g) = \Delta H_f^\circ(M,g) + 6\Delta H_f^\circ(X,g) - \Delta H_f^\circ(MX_6^{2-},g) \qquad [89]$$

and

$$-\Delta H_f^i(MX_6^{2-},g) = \Delta H_f^\circ(M^{4+},g) + 6\Delta H_f^\circ(X^-,g) - \Delta H_f^\circ(MX_6^{2-},g) \qquad [90]$$

We used the following data from the sources cited:

$$\Delta H_f^\circ(Th,g) = 598.3 \text{ KJ mol}^{-1} \text{ (146)} \qquad [91]$$

$$\text{Ionization potential, } \sum_1^4 I_{Th} = 6.0 + 11.5 + 20 + 28.7 = 66 \text{ eV (147-150)} \qquad [92]$$

$$\Delta H_f^\circ(U,g) = 527.2 \text{ KJ mol}^{-1} \text{ (113,151)} \qquad [93]$$

$$\text{Ionization potential, } \sum_1^4 I_U = 68.0 \text{ eV (152)} \qquad [94]$$

$$\Delta H_{dissoc}^\circ(Cl_2) = 242.0 \text{ KJ mol}^{-1} \text{ (136)} \qquad [95]$$

$$\Delta H_{dissoc}^\circ(Br_2) = 192.9 \text{ KJ mol}^{-1} \text{ (136)} \qquad [96]$$

$$1 \text{ eV} = 96.49 \text{ KJ mol}^{-1} \qquad [97]$$

Bond energy data (Table 29) indicate that the energy of the Th-X bond is essentially the same in K_2ThX_6 and Cs_2ThX_6 despite the differences in structures and the attendant uncertainties in the calculation of lattice energies. This agreement affords some assurance about the validity of the methodology. The following periodic trends are evident in the metal-halogen homolytic bond strengths in $MX_6^{2-}(g)$ ions (Table 29):

Th-Cl > U-Cl > Th-Br > U-Br

The difference between the homolytic bond energies of Th-Cl and U-Cl is 38 KJ per bond, and this agrees well with the difference, 39 KJ per bond, between the values (Th-Cl=507 and U-Cl=468 KJ mol^{-1}) quoted by Jenkins and Pratt (153). The absolute values given by these authors differ from ours because of the different method of calculating lattice energies. The metal-halogen coordinate bond strengths are in the order:

Th-Cl > U-Cl > U-Br > Th-Br

The heterolytic bond energy is very meaningful as it supports our earlier view that thorium and uranium prefer chloro and bromo complexation, respectively.

In all cases, it is evident that $E(M\text{-}Cl)_{hom} > E(M\text{-}Br)_{hom}$ and also, $E(M\text{-}Cl)_{het} > E(M\text{-}Br)_{het}$.

Table 29. Homolytic, $E(M-X)_{hom}$ and heterolytic, $E(M-X)_{het}$ bond energies in $MX_6^{2-}(g)$ ions. Values in KJ mol^{-1}.

Compound	$-\Delta H_f^a(MX_6^{2-},g)$ KJ mol^{-1}	$E(M-X)_{hom}$ KJ mol^{-1}	Mean	$-\Delta H_f^i(MX_6^{2-},g)$ KJ mol^{-1}	$E(M-X)_{het}$ KJ mol^{-1}	Mean
K_2ThCl_6	2879.0	480.0		7148.0	1191.0	
Cs_2ThCl_6	2888.0	481.0	481.0	7156.0	1193.0	1192.0
K_2ThBr_6	2418.0	403.0		6907.0	1151.0	
Cs_2ThBr_6	2434.0	406.0	404.0	6923.0	1154.0	1153.0
Cs_2UCl_6	2656.0	443.0		7098.0	1183.0	
K_2UBr_6	2295.0	383.0		6958.0	1160.0	

Solid state Raman spectra of $ThCl_4$, $ThBr_4$ and the alkali complexes were recorded from 800 to 100 cm^{-1} (Table 30). The very strong band at 300 cm^{-1} for $ThCl_4$ is assigned to the totally symmetric Th-Cl stretch (154-156). This is shifted to 282 cm^{-1} and 310 cm^{-1} in K_2ThCl_6 and Cs_2ThCl_6 respectively. The corresponding mode gives a band at 195 cm^{-1} in the spectrum of $ThBr_4$ (155) and this also is seen to be shifted upon complexation (Table 30). Woodward and Ware obtained spectra for $ThCl_6^{2-}$ and UCl_6^{2-} in acetonitrile solution and derived the stretching force constants (a_{1g} mode), 1.51 and 1.40 mdyn/A°, respectively (157). These values confirm our previous finding that for thermochemical bond energies

$$E(Th\text{-}Cl)_{hom/het} > E(U\text{-}Cl)_{hom/het}$$

Unfortunately, the vibrational spectra of the solid compounds do not reveal the various modes required for a force field calculation.

Table 30. Raman spectral data of ThX_4 and $(Alk)_2ThX_6$.

COMPOUND	Th-X STRETCHING FREQUENCY
$ThCl_4$	300s
K_2ThCl_6	282vs
Cs_2ThCl_6	310s
$ThBr_4$	195s
K_2ThBr_6	175s
Cs_2ThBr_6	198vs

s = strong; vs = very strong

Conclusion

One of the principal reasons for undertaking a study of transition metal peroxo complexes in this laboratory was our interest in the use of the peroxo group stability as an indicator of fundamental bonding character within the transition group. As it continues to be somewhat questionable what the peroxo group stability implies, it was decided to fall back on the more fundamental thermochemical approach to the energetics of bonding which has also been pursued in this laboratory for some years. The present results on Th(IV)- and U(IV)- complexing were compared with the acceptor properties of other M(IV) ions (M=Zr, Nb, Hf, Ta and Sn) that were studied earlier by Westland et al. (111,130,132). This work has examined thermochemical bonding properties of M-X systems (M=Th and U; X=Cl and Br).

Our measurements of the enthalpies of formation of chloro complexes of thorium cast doubt upon the early work of Chauvenet whose measurements did not exhibit internal consistency. An examination of the literature on phase equilibria suggested to us that Chauvenet may not have worked with the compounds that he claimed to have prepared. X-ray diffraction results reported in this thesis establish the integrity of our preparations.

The K_2ThCl_6 salt was indexed as tetragonal. K_2ThBr_6 and Cs_2ThBr_6 salts were indexed as tetragonal and trigonal, respectively.

We have used data published by Vdovenko et al. (112) for calculating standard heats of formation and other data for chlorouranates. It is worth mentioning that Fuger and Brown (110) reported slightly different data for Cs_2UCl_6. The Russian workers prepared their salts by fusing the stoichiometric mixtures of the component halides in a quartz tube under vacuum while Fuger and Brown obtained Cs_2UCl_6 by adding CsCl to a solution of quadrivalent uranium produced by reduction of uranyl ion with powdered silver. In general, we prefer preparations made in the dry way, so we have used the Russian workers data for Cs_2UCl_6. Moreover, the data provided by those workers are internally consistent for a series of A_2UCl_6 compounds. We have used the data for K_2UBr_6 provided by the same group of Russian workers (113).

The double halide ion affinity of $MX_4(g)$ is of interest as it demonstrates the acceptor properties of these actinides in their +4 states. We have found that Th(IV) and U(IV) behave as class a and class b acceptors, respectively (139). This classification follows from the fact that $ThCl_4(g)$ has a greater chloride ion affinity than $UCl_4(g)$. On the other hand, $UBr_4(g)$ has a greater bromide ion affinity than $ThBr_4(g)$. It is interesting to note that the double halide ion affinities obtained in this work are by far the greatest compared to group 4B and 5B metal halides (Tables 28A and 28B). It is suggested that $X^- - X^-$ repulsions are very

important in the stability of $MX_6^{2-}(g)$ ions and are much stronger when the central atoms are smaller.

The values of the Th-X bond energy (Table 29) in K_2ThX_6 and Cs_2ThX_6 compounds remain the same despite the differences in structures of the above two sets of compounds and the attendant uncertainties in the calculation of lattice energies by the Kapustinskii-Yatsimirskii method. The Th-X bond energy values in K_2ThX_6 and Cs_2ThX_6 complexes signify that the energy of the inner-sphere bonds is almost independent of the atomic number of the outer-sphere cation. It is conclusive from the bond energy data (Table 29) that E(Th-Cl) > E(U-Cl), (E=bond energy). The coordinate bond energy values indicate that thorium and uranium prefer chloro and bromo complexation respectively.

SUGGESTIONS FOR FUTURE RESEARCH

Our understanding of the subjects discussed in this thesis could be furthered by extending the present work.

There have been no reports on the coordination chemistry of the adducts of $ThCl_4$ or UCl_4 containing bidentate, neutral, tridentate, neutral, quadridentate ligands, etc. One could synthesize series of heteroligand organoperoxo complexes of thorium and uranium from the above type of adducts and study their coordination chemistry as well as oxygen transfer reactions towards a number of organic substrates. This idea could be extended to other elements, e.g., Mo, W, Ti, Zr, Hf and other lighter transition elements. One could continue his whole research career perhaps by engaging himself in the synthesis and characterization of new organo peroxo complexes of thorium and uranium and studying their oxidizing properties.

The present thermochemical results on thorium and uranium could be significant for the preparative metallurgy of these elements as well as in giving insight into the bonding properties of actinides.

One could undertake a programme to isolate different adducts of the type $MCl_4 \cdot 2L$ (M=Th and U; L=O-, N- and S-donor monodentate organic ligands) and determine their enthalpies of complexing, ΔH_c, by solution calorimetry.

Since thorium and uranium appear to be class a and class b acids, respectively, there may be different trends in the stabilities of $ThCl_4$ and UCl_4 adducts. Thorium may exhibit the coordination preference trend O>N>S, while uranium may prefer the reverse order, i.e., S>N>O.

One might expect the class b property to increase toward the right in the period. This could be investigated by thermochemical studies on ternary complexes of NpX_4 and PuX_4 (X=Cl and Br). Such a study would certainly extend our present understanding of the subject.

CLAIMS TO ORIGINAL RESEARCH

1. The use of chelating ligands to stabilize novel coordination compounds of Th(IV) and U(VI) containing the coordinated peroxo group. A series of such compounds were prepared and their physical and chemical properties were examined. In particular, the peroxo group stretching frequency, (ν_1(0-0) of the MO_2 grouping), was shown to vary with the choice of ancillary ligands used and with the atomic number of the central atom.
2. Oxygen transfer reactions of some organoperoxo complexes of thorium and uranium towards trans-stilbene and allyl alcohol were investigated. The results have been rationalized through mechanistic pathways.
3. The existence of the complexes, K_2ThCl_6, K_2ThBr_6 and Cs_2ThBr_6 have been established.
4. The Debye-Scherrer pattern of K_2ThCl_6, K_2ThBr_6 and Cs_2ThBr_6 were indexed and hence the crystal symmetries and the lattice parameters of the above complexes were determined.
5. Comparative stabilities of A_2ThX_6 (A=K and Cs; X=Cl and Br) complexes were determined by solution calorimetry.

6. The present work describes for the first time the gas phase acceptor properties of Th(IV) and U(IV) and hence classification of these into class a and class b acids, respectively. A rationalization of this was provided. The results suggest that Cl^--Cl^- repulsion is much diminished in hexachlorothorates and - uranates relative to the other halometallates previously studied.
7. Quantitative comparisons of the energies of M-X bonds in $MX_6^{2-}(g)$ ions were obtained.
8. Raman spectra of A_2ThX_6 complexes were recorded to show M-X stretching.

REFERENCES

1. C. Frondel, "Systematic Mineralogy of Uranium and Thorium", U.S. Govt. Print. Off., Washington, 1958.

2. L. Pauling, Inaugural speech, C.I.C., Conference, Ottawa, Canada, 1980.

3. L.G. Berry and B. Mason, "Mineralogy", W.H. Freeman and Co., San Francisco, Charles E. Tuttle Co., Tokyo, 1961.

4. M.H. Staatz, "Geology and description of the thorium-bearing veins", U.S. Govt. Print. Off., Washington, 1972-1973.

5. N.J. Theis, Doctoral Thesis, Queens University, Kingston, 1976.

6. R.M. Williams and H.W. Little, "Uranium and Thorium in Canada - Resources, Production and Potential", International conference on the peaceful uses of Atomic Energy, 4th Geneva, N.Y. Vol. 8, 1971, United Nations, 1972, p. 37-58.

7. C.R. Phillips and Y.C. Poon, Minerals Sci. Engng., 12, 53 (1980).

8. R.D. Nininger, Proceedings of a Pannel on Uranium Exploration Geology held in Vienna, International Atomic Energy Agency, Vienna, 1970, p. 1.

9. A.J. Eardley, W.L. Stokes, F.W. Christiansen, N.C. Willams and C.L. Ashton, "Uranium, The World's Expanding Frontier", S. Wilhelm, E.F. Lingle & W.A. Steinmann, Texas, 1955.

10. "Uranium: Resources, Production, and Demand", A Joint Report by the OECD Nuclear Energy Agency and the International Atomic Energy Agency, France, 1973.

11. S.M. Roscoe, "Huronian rocks and uniferous conglomerates in the Canadian shield", Ottawa, Geological Survey of Canada, Geology branch, Paper 68-40, 1969.

12. J.W. Griffith and S.M. Roscoe, "Canadian Resources of Uranium and Thorium", Ottawa, Department of Mines and Technical Surveys. Mineral Resources, Division of Mines MR77, 1964.

13. L.H. Vogt, Jr., H.M. Faigenbuam and S.E. Wiberley, Chem. Rev. 63, 269 (1963).

14. J.A. Connor and E.A.V. Ebsworth, Adv. Inorg. Chem. Radiochem., 6, 279 (1964).

15. A.G. Sykes and J.A. Weil, Prog. Inorg. Chem., 13, 1 (1970).

16. H. Mimoun and I. Seree de Roch and L. Sajus, Tetrahedron, 26, 37 (1970).

17. L. Klevan, J. Peone, Jr. and S.K. Madan, J. Chem. Educ., 50, 670 (1973).

18. J.S. Valentine, Chem. Rev., 73, 235 (1973).

19. G. Henrici-Olive and S. Olive, Angew. Chem. Int. Ed. Engl. 13, 29 (1974).

20. L. Vaska, Acc. Chem. Res., 9, 175 (1976).

21. D.A. Muccigrosso, S.E. Jacobson, P.A. Apgar, and F. Mares, J. Am. Chem. Soc. 100, 7063 (1978).

22. G.A. Olah and J. Welch, J. Org. Chem., 43, 2830 (1978).

23. A.D. Westland, F. Haque and J.M. Bouchard, Inorg. Chem., 19, 2255 (1980).

24. H. Mimoun, J. Mol. Catal. 7, 1 (1980).

25. A.D. Westland and M.T.H. Tarafder, Inorg. Chem., 20, 3992 (1981).

26. H. Mimoun, M. Postal, F. Casabianca, J. Fischer and A. Mitschler, Inorg. Chem., 21, 1303 (1982).

27. A.D. Westland and M.T.H. Tarafder, Inorg. Chem., 21, 3228 (1982).

28. G. McLendon and A.E. Martell, Coord. Chem. Rev., 19, 1 (1976).

29. V.J. Choy and C.J. O'Connor, Coord. Chem. Rev. 9, 145 (1972/73).

30. E. Fremy, Liebigs Ann. Chem. 83, 227, 289 (1852).

31. P. Pfeiffer, E. Breith, E. Lubbe and T. Tsumaki, Liebigs Ann. Chem. 503, 84 (1933).

32. T. Tsumaki, Bull. Chem. Soc. Japan, 13, 252 (1938).

33. E. Bayer and P. Schretzmann, Struct. Bonding, 2, 181 (1967).

34. R.G. Wilkins, Advan. Chem. Ser. 100, 111 (1971).

35. R.F. Stewart, P.A. Estep, and J.J.S. Sebastian, U.S. Bur. Mines Inform. Circ. No. 7906 (1959).

36. H. Mimoun, Rev. Inst. Fr. Pet., 33, 259 (1978).

37. H. Taube, J. Gen. Physiol., 49, 29 (1965).

38. J.S. Griffith, Proc. Roy. Soc. A, 235, 23 (1956).

39. A.A. Vlcek, Trans. Faraday Soc. 56, 1137 (1970).

40. L. Pauling, Nature (London), 203, 182 (1964).

41. J.B. Wittenburg, B.A. Wittenburg, J. Peisach and W. Blumberg, Proc. Nat. Acad. Sci. U.S.A. 67, 1846 (1970).

42. J.J. Weiss, Nature (London), 202, 83 (1964).

43. L. Vaska, Acc. Chem. Res. 1, 335 (1968).

44. M.M. Taqui Khan and A.E. Martell, "Homogeneous Catalysis by Metal Complexes", Vol. 1, Academic Press, New York, 1974.

45. R. Guilard, Jean-Marc Latour, C. Lecomte, Jean-Claude Marchon, J. Protas and D. Ripoll, Inorg. Chem. 17, 1228 (1978).

46. S.E. Jacobson, R. Tang and F. Mares, Inorg. Chem. 17, 3055 (1978).

47. B. Bosnich, H. Boucher and C. Marshall, Inorg. Chem. 15, 634 (1976).

48. I.I. Volnov, Russ. Chem. Rev. 41, 314 (1972).

49. S. Muto, H. Ogata and Y. Kamiya, Chem. Lett., 809 (1975).

50. B. Gorewitt and M. Tsutsui, Adv. Catal. 27, 227 (1978).

51. R. Ugo, F. Conti, S. Cenini, R. Mason and G. Robertson, J. Chem. Soc. Chem. Commun. 1498 (1968); G.M. Zanderighi, R. Ugo, A. Fusi and Y. Ben Taarit, Inorg. Nucl. Chem. Lett., 12, 729 (1976).

52. R.A. Sheldon and J.A. Van Doorn, J. Organomet. Chem., 94, 115 (1975).

53. W.B. Beaulieu, G.D. Mercer and D.M. Roundhill, J. Am. Chem. Soc. 100, 1147 (1978).

54. A.O. Chong, K. Oshima and K.B. Sharpless, J. Am. Chem. Soc. 99, 3420 (1977).

55. T.G. Traylor and A.W. Baker, J. Am. Chem. Soc., 85, 2746 (1963).

56. P.M. Henry, Adv. Organomet. Chem. 13, 363 (1975).

57. H. Mimoun, I. Seree de Roch and L. Sajus, Bull. Soc. Chim. Fr., 1481 (1969).

58. H.B. Kagan, H. Mimoun, C. Mark and V. Schurig, Angew. Chem. Int. Ed. Engl. 18, 485 (1979).

59. S.E. Jacobson, R. Tang and F. Mares, J. Chem. Soc. Chem. Commun., 888 (1978).

60. S.E. Jacobson, D.A. Muccigrosso, and F. Mares, J. Org. Chem. 44, 921 (1979).

61. T. Katsuki and K.B. Sharpless, J. Am. Chem. Soc. 102, 5974 (1980).

62. B.E. Rossiter, T. Katsuki and K.B. Sharpless, J. Am. Chem. Soc. 103, 464 (1981).

63. G. Fritz, D. Habel, D. Kumer and G. Teichmann, Z. anorg. allgem. Chem. 302, 60 (1959).

64. K.W. Bagnall, D. Brown, P.J. Jones and J.A.H. du Preez, J. Chem. Soc. A, 737 (1968).

65. K.W. Bagnall, D. Brown, D.H. Holah and F. Lux, J. Chem. Soc. A, 465 (1968).

66. A.I. Vogel, "A Textbook of Quantitative Inorganic Analysis", 3rd ed., Longmans, Green and Co., London, 1961, p. 77.

67. D.A. Skoog and D.M. West, "Fundamentals of Analytical Chemistry", 3rd ed., Holt, Rinehart and Winston, New York, 1976, p. 180.

68. Ref. 66, p. 325.

69. "Dictionary of Organic Compounds", Eyre and Spottiswoode, London, 1965.

70. W.J. Geary, Coord. Chem. Rev. 7, 113 (1971).

71. P.C. Kundu, P.S. Roy and R.K. Banerjee, J. Inorg. Nucl. Chem. 42, 851 (1980).

72. H. Faraglia, B. Zarli, L. Sindellari, and G. Dall'Olio, Inorg. Chim. Acta. 19, 39 (1976).

73. K.W. Bagnall, J.G.H. du Preez, J. Bajorek, L. Bonner, H. Cooper and G. Segal, J. Chem. Soc., Dalton Trans., 2682 (1973).

74. D. Brown, MTP Int. Rev. Sci.: Inorg. Chem. Ser. One 7, 87 (1972).

75. G.R. Burns, Inorg. Chem. 7, 277 (1968).

76. M.A. Ali and S.G. Teoh, J. Inorg. Nucl. Chem. 40, 451 (1978).

77. M.A. Ali, Can. J. Chem., 58, 727 (1980).

78. J.E. Kovacic, Spectrochim. Acta, Part A, 23A, 183 (1967).

79. N.M. Karayannis, C.M. Mikulski, M.J. Stroko, L.L. Pytlewski and M.M. Labes, Inorg. Chim. Acta. 4, 455 (1970).

80. R.K. Agarwal, M. Srivastava and A.K. Srivastava, J. Inorg. Nucl. Chem., 43, 204 (1981).

81. R.K. Agarwal, A.K. Srivastava, M. Srivastava, N. Bhakru and T.N. Srivastava, J. Inorg. Nucl. Chem., 42, 1778 (1980).

82. D.K. Lavalle, M.D. Banghman and M.P. Phillips, J. Am. Chem. Soc. 99, 718 (1977).

83. I.G.G. Moore and A.R. Kirk, J. Heterocyl. Chem., 16, 789 (1979).

84. R.J. Pugmire and D.M. Grant, J. Am. Chem. Soc. 90, 697 (1968).

85. H.L. Retcofsky and R.A. Friedel, J. Phy. Chem. 72, 2619 (1968).

86. R.R. Fraser, Personal communication.

87. G.V. Jere and M.T. Santhamma, Inorg. Chim. Acta. 24, 57 (1977).

88. R. Guilard, M. Fontesse, P. Fournari, C. Lecompte and J. Protas, J. Chem. Soc., Chem. Commun. 161 (1976).

89. E. Wendling, Bull. Soc. Chim. Fr., 16 (1967).

90. U.M. Dzhemilev, V.P. Yur'ev, G.A. Tolstikov, F.B. Gersharov and S.R. Rafikov, Dokl. Chem. (Engl. Transl.) 196, 79 (1971). See also: R.A. Sheldon, Recl. Trav. Chim. Pays-Bas, 92, 370 (1973).

91. M.R. Barusch and J.Q. Payne, J. Am. Chem. Soc., 75, 1987 (1953).

92. J.P. Day and L.M. Venanzi, J. Chem. Soc. A, 197 (1966).

93. B.C. Lane and L.M. Venanzi, Inorg. Chim. Acta, 3, 239 (1969).

94. P.V. Balakrisnan, S.K. Patil, and H.V. Venkatesetty, J. Inorg. Nucl. Chem., 28, 540 (1966).

95. D. Brown, J. Hill and C.E.F. Rickard, J. Chem. Soc. A, 499 (1970).

96. M. Goldstein, Spectrosc. Prop. Inorg. Organomet. Compd. 7, 372 (1973).

97. S.P. McGlynn, J.K. Smith, and W.C. Neely, J. Chem. Phys., 35, 105 (1961).

98. R.L. Lintvedt and N. Ahmad, Inorg. Chem., 21, 2356 (1982).

99. J. Bernstein, M. Halman, S. Pinchas, and D. Samuel, J. Chem. Soc., 821 (1964).

100. W.P. Griffith, J. Chem. Soc. 5248 (1964).

101. F.A. Cotton and G. Wilkinson, "Advanced Inorganic Chemistry", 3rd ed., John Wiley and Sons, New York, 1972, p. 115.

102. C.R. Reynolds and D.W. Meek, Inorg. Chem., 13, 1741 (1974).

103. T. Moeller, "Inorganic Chemistry", John Wiley and Sons, New York, 1955, p. 135.

104. B.N. Laskorin, V.V. Yakshin, and L.I. Sokolskaya, Dokl. Akad. Nauk. SSSR, 223, 1405 (1975).

105. H. Tomioka, K. Takai, K. Oshima, H. Nazaki, and K. Toriumi, Tetrahedron Lett. 4843 (1980).

106. A.M. Matucci, E. Perolti, and A. Santambrogio, J. Chem. Soc., Chem. Commun. 1198 (1970).

107. R.A. Sheldon and J.K. Kochi, Oxidation and Combustion Revs., 5, 135 (1973).

108. N.V. Sidgwick, "The Chemical Elements and Their Compounds", Oxford University Press, London, Vol. 1, 1951, p. 637.

109. E. Chauvenet, Ann. Chim. Phys. 23, 425 (1911).

110. J. Fuger and D. Brown, J. Chem. Soc. A, 841 (1971).

111. D. Lal and A.D. Westland, J. Chem. Soc., Dalton Trans., 2505 (1974).

112. V.M. Vdovenko, V.A. Volkov, and I.G. Suglobova, Radiokhimiya, 16, 363 (1974).

113. V.M. Vdovenko, I.G. Suglobova, and D.E. Chirkst, Radiokhimiya, 16, 203 (1974).

114. R. Oyamada, Denki Kagaku, 39, 2 (1971).

115. V.N. Diesyatnik, V.A. Dubinin, I.F. Nitchkov, and S.P. Raspopin, Tsvetnaia Metallurgia, 87 (1966(4)).

116. V.I. Ionov, B.G. Korshunov, V.V. Kokoriev, and I.S. Morozov, Tsvetnaia Metallurgia, 102 (1960(3)).

117. A.N. Vokhmyakov, V.N. Desyatnik, and N.N. Kurbatov, USSR At. Energy, 35, 424 (1973).

118. V.M. Vdovenko, I.I. Kozhina, I.G. Suglobova and D.E. Chirkst, Radiokhimya, 15, 172 (1973).

119. J.R. Ferraro, J. Inorg. Nucl. Chem., 4, 283 (1957).

120. R.W.G. Wyckoff, "Crystal Structures", 2nd ed., Interscience, New York, 1965, p. 350.

121. K.B. Yatsimirskii, Zh. Neorgan. Khim. 6, 518 (1961).

122. H.D.B. Jenkins and K.F. Pratt, Proc. Roy. Soc. Lond. A, 356, 115 (1977).

123. H.D.B. Jenkins and K.F. Pratt, J. Chem. Soc., Faraday Transactions II, 74, 968 (1978).

124. H.D.B. Jenkins and K.F. Pratt, Adv. Inorg. Chem. Radio Chem., 22, 1 (1979).

125. H.D.B. Jenkins and K.F. Pratt, Prog. Solid St. Chem. 12, 125 (1979).

126. J.B. Nelson and D.P. Riley, Proc. Phys. Soc. (London), 57, 160 (1945).

127. N.N. Greenwood and P.G. Perkins, J. Inorg. Nucl. Chem., 4, 291 (1957).

128. O. Kubaschewski, E. Ll. Evans, and C.B. Alcock, "Metallurgical Thermochemistry", 4th ed., Pergamon, Oxford, 1967, p. 90.

129. R.J. Irving and I. Wadsoe, Acta Chem. Scand., 18, 195 (1964).

130. R. Makhija and A.D. Westland, J. Chem. Soc. Dalton Trans., 1707 (1977).

131. Z.M.S. Al-Kazzaz and R.A. Louis, Z. anorg. allgem. Chem., 440, 286 (1978).

132. P. Gelbman and A.D. Westland, J. Chem. Soc. Dalton Trans., 1598 (1975).

133. L. Eyring and E.F. Westrum, jun., J. Am. Chem. Soc. 72, 5555 (1950).

134. R. Oyamada and S. Yoshida, J. Phys. Soc. Japan 38, 1786 (1975).

135. Reference 128, p. 312.

136. JANAF Thermochemical Tables, Ed. by D.A. Stull, Dow Chemical Co., Midland, Michigan, 1960-1966.

137. Selected Values of Chemical Thermodynamic Properties. Ed. by F. Rossini, National Bur. Standards, Washington, Circular 500, 1952.

138. J. Fuger and D. Brown, J. Chem. Soc. Dalton Trans. 428 (1973).

139. S. Ahrland, J. Chatt, and N.R. Davis, Quart. Rev. 12, 265 (1958).

140. R.G. Pearson, J. Am. Chem. Soc., 85, 3533 (1963); Chem. Brit., 3, 103 (1967); J. Chem. Educ., 45, 581 643 (1968); Surv. Progr. Chem. 1, 1 (1969).

141. T.L. Brown, W.G. McDougle, and L.G. Kent, J. Am. Chem. Soc., 92, 3645 (1970).

142. W. Fischer, R. Gewehr, and M. Wingchen, Z. anorg. allgem. Chem. 242, 182 (1939).

143. I. Barin, O. Knacke, and O. Kubaschewski, in "Thermo-Chemical Properties of Inorganic Substances", Springer Verlag, New York, 1973.

144. CATCH Tables, "Computer Analysis of Thermochemical Data", Ed. by J.D. Cox, University of Sussex (1974).

145. R.G. Pearson and R.J. Mawby, Halogen Chem., 3, 55 (1967).

146. P.D. Zavitsanos, U.S. Nat. Tech. Inform. Serv., AD Rep. 1973, No. 762917 and No. 773197/9GA.

147. D.L. Hildenbrand and E. Murad, J. Chem. Phys., 61, 5466 (1974).

148. J. Sugar, J. Chem. Phys., 59, 788 (1973); 60, 4103 (1974).

149. E.G. Rauh and R.J. Ackermann, J. Chem. Phys., 60, 1396 (1974).

150. G.V. Samsonov, in "Handbook of the Physiocochemical Properties of the Elements", Plenum Press, N.Y., 1968.

151. A. Pattoret, J. Drowart, and S. Smoes, in "Thermodynamics of Nuclear Materials", Symposium Proceedings, Vienna, 1968, p. 613.

152. L.A. Maij, Latv. PSR Zinat Akad. Vestis. Kim. Ser., 1976, 51, 337.

153. H.D.B. Jenkins and K.F. Pratt, Inorg. Chim. Acta., 32, 25 (1979).

154. E.W. Bohres, W. Krasser, H.J. Schenk, and K. Schwochau, J. Inorg. Nucl. Chem., 36, 812 (1974).

155. J. Goffart, J. Fuger, B. Gilbert, L. Hocks, and G. Duyckaerts, Inorg. Nucl. Chem. Letters, 11, 581 (1975).

156. R. Oyamada and S. Yoshida, J. Phys. Soc. Japan, 38, 1786 (1975).

157. L.A. Woodware and M.J. Ware, Spectrochim. Acta, 24A, 924 (1968).